

UNIVERSITY OF TRENTO

DOCTORAL THESIS IN MATHEMATICS, XXIX CYCLE

**The importance of climatic and
ecological factors for vector-borne
infections: *Culex pipiens* and West
Nile virus**

PhD candidate:
Giovanni Marini

Supervisors:
Prof. Andrea Pugliese
Dr. Roberto Rosá



April 2017

Contents

| | |
|--|-----------|
| Introduction | 1 |
| 1 Early warning of West Nile virus mosquito vector: climate and land use models successfully explain phenology and abundance of <i>Culex pipiens</i> mosquitoes in Northwestern Italy | 7 |
| 1.1 Introduction | 7 |
| 1.2 Methods | 9 |
| 1.2.1 Mosquito data | 10 |
| 1.2.2 Environmental predictors | 10 |
| 1.2.3 Temporal windows | 11 |
| 1.2.4 Data analysis | 12 |
| 1.3 Results | 13 |
| 1.3.1 Mosquito indices | 13 |
| 1.3.2 Model results | 14 |
| 1.4 Discussion | 19 |
| 1.5 Conclusions | 20 |
| 1.A Supporting information | 21 |
| 1.A.1 Aggregation of environmental data over a range of time windows: preliminary analyses | 21 |
| 1.A.2 Selection of the optimum 12 week time window using variation in AIC (Δ AIC) | 24 |
| 1.A.3 Model selection tables | 25 |
| 2 The role of climatic and density dependent factors in shaping mosquito population dynamics: the case of <i>Culex pipiens</i> in Northwestern Italy | 27 |
| 2.1 Introduction | 27 |
| 2.2 Methods | 29 |
| 2.2.1 Data | 29 |
| 2.2.2 Modelling mosquito dynamics | 30 |
| 2.2.3 Model calibration | 31 |
| 2.3 Results and discussion | 32 |
| 2.4 Conclusions | 38 |
| 2.A Supporting Information | 40 |
| 2.A.1 Materials and methods | 40 |
| 2.A.2 Additional results | 43 |

| | | |
|----------|---|-----------|
| 3 | The effect of interspecific competition on the temporal dynamics of <i>Aedes albopictus</i> and <i>Culex pipiens</i> | 47 |
| 3.1 | Introduction | 47 |
| 3.2 | Methods | 49 |
| 3.2.1 | Study area and mosquito data | 49 |
| 3.2.2 | Delay analysis | 50 |
| 3.2.3 | Environmental data | 50 |
| 3.2.4 | Population model | 51 |
| 3.3 | Results | 52 |
| 3.4 | Discussion | 55 |
| 3.5 | Conclusions | 57 |
| 3.A | Supporting Information | 59 |
| 3.A.1 | Model calibration | 59 |
| 3.A.2 | Model output | 60 |
| 3.A.3 | Model fit | 61 |
| 3.A.4 | DIC and AIC analysis | 62 |
| 3.A.5 | Estimates of the competition-dependent additional mortality | 62 |
| 4 | Exploring vector-borne infection ecology in multi-host communities: a case study of West Nile virus | 67 |
| 4.1 | Introduction | 67 |
| 4.2 | The model | 68 |
| 4.2.1 | Infections without horizontal transmission | 70 |
| 4.2.2 | Horizontal transmission | 71 |
| 4.3 | Numerical example | 72 |
| 4.3.1 | Effect of vector and host ecology on \mathcal{R}_0 | 72 |
| 4.3.2 | Effect of competition and shifting mosquito feeding preference on infection seasonal dynamics | 75 |
| 4.4 | Conclusions | 84 |
| 4.A | Supporting Information | 86 |
| | Conclusions | 89 |
| | Acknowledgments | 91 |
| | Bibliography | 93 |

Introduction

More than 10% of the human deaths occurring worldwide are caused by infectious and parasitic diseases (World Health Organization, 2016). There exists a large variety of pathogens, responsible for such diseases, many of which are not directly transmitted from host to host but need a vector to be spread, such as ticks or mosquitoes. Through their bite, vectors might acquire the pathogen from infected hosts, and once infected they can transmit it to a susceptible host. These infections might affect several animal species, and those that can naturally be transmitted from animals to humans are called zoonosis. Direct zoonosis, such as influenza or rabies, are directly transmitted from animals to humans, through air or bites and saliva, while for vector-borne zoonosis transmission can take place through a vector that acts as a bridge for pathogen transmission. About three quarters of human emerging infectious diseases are caused by zoonotic pathogens, and many of them are spread by vectors such as mosquitoes (Taylor *et al.*, 2001). The possibilities for emergence and spread of new zoonoses in the next future are likely to rise as world population, urbanization and human movement are constantly increasing.

Mathematical models nowadays represent very powerful tools to make investigations and predictions for biological dynamical systems, providing helpful insights that can be extremely valuable for several aims. For instance, they can assess the efficacy of a vaccination strategy, they can help to design vector control treatments in a specific location and more generally they allow exploring what-if scenarios. As such systems evolve under stochastic forces, computational tools that include random influences are crucial to understand infections dynamics, including the underlying vector (if any) population features.

In this thesis, I will focus on a particular mosquito-borne zoonosis, West Nile virus (WNV), a flavivirus of emerging public health relevance in Europe and North America, and its main European vector, *Culex pipiens* mosquitoes (Zeller & Schuffenecker, 2004). Discovered originally in Uganda in 1937 (Smithburn *et al.*, 1940), WNV is now spread on every continent except Antarctica (Reisen, 2013). WNV is mainly transmitted through the bite of infected mosquitoes, that acquire the virus by feeding on infected birds. In nature it is maintained by bird-mosquito cycle while humans, horses and other mammals are considered as dead-end hosts for the virus (i.e. they do not develop a sufficiently high viremia to reinfect a mosquito) (see Figure 1). Most human WNV infections are asymptomatic and the majority of clinical cases are mild and present with flu-like symptoms. No specific therapy is available at the moment and severe cases with

signs of encephalitis, meningo-encephalitis or meningitis, are often observed among elderly people; for instance, about 220 cases were recorded in Italy between 2013 and 2016 (European Centre for Disease Prevention and Control, 2016). Several WNV epidemics have been documented in European countries in recent years (European Centre for Disease Prevention and Control, 2014), and such outbreaks, as well as the quick spread of the virus throughout North America since 1999, have led to increasing health concerns (Campbell *et al.*, 2002).

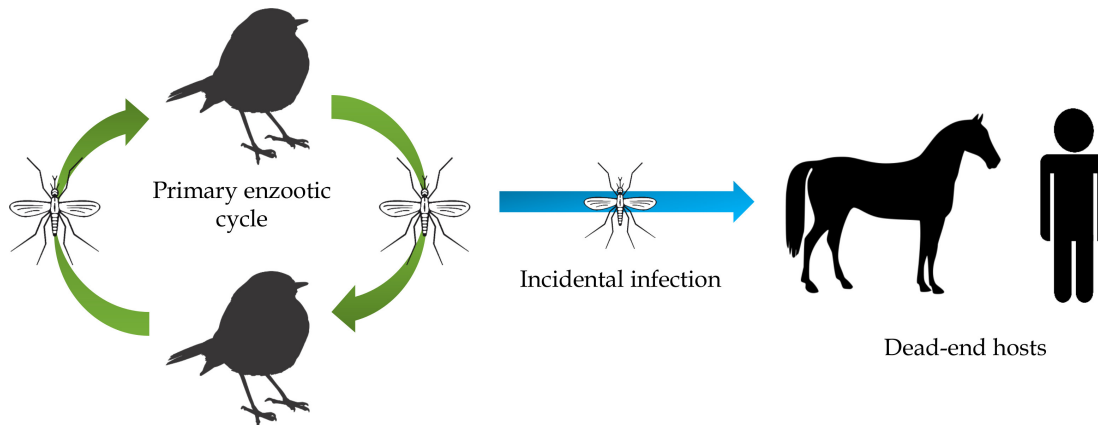


Figure 1: **WNV cycle.** Scheme of WNV routes of transmissions.

Mosquitoes belonging to the *Cx. pipiens* complex are thought to be the most efficient vectors for spreading WNV among birds, and from birds to humans and other mammals in North America (Bernard *et al.*, 2001; Kilpatrick *et al.*, 2005) as well as in Europe (Zeller & Schuffenecker, 2004). *Cx. pipiens* is an indigenous species which can be found in almost every European country (Farajollahi *et al.*, 2011). Its life cycle, similar to any other mosquito species, includes several stages, as illustrated in Figure 2. Female adults lay new eggs on water surfaces and, after hatching, larvae develop in the water and then enter a pupal stage, after which new adults will emerge. Only adult females need to have a blood meal on a host in order to lay eggs.

Beside WNV, *Cx. pipiens* is also involved in the transmission of other human and animal pathogens such as Usutu virus, whose first case outside Africa was recorded in Italy in 2009, St. Louis encephalitis, which caused about a hundred human cases in North America during the last decade, Rift Valley fever, Sindbis virus, avian malaria and filarial worms.

As the transmission of mosquito-borne diseases is largely driven by the abundance of the vector, to design appropriate control strategies it is crucial to understand the population dynamics of existing vector populations and evaluate how it depends on biotic and environmental factors. First, many laboratory studies (Loetti *et al.*, 2011; Ciota *et al.*, 2014; Spielman & Wong, 1973) show that demographic parameters are strongly influenced by environmental factors, such as temperature and daylight duration. Furthermore, published laboratory studies (Carrieri *et al.*, 2003; Costanzo *et al.*, 2005) pointed out that its abundance and dynamics might be strongly influenced by another mosquito species, namely *Aedes albopictus*, as they compete for resources at the larval stage when they share the same breeding site. Commonly known as "tiger mosquito", *Ae. albopictus* is an invasive alien species native to Asia and introduced in several European countries

at the end of the last century; since then, *Ae. albopictus* rapidly spread in urban and suburban environments, occupying a habitat already exploited by *Cx. pipiens*. It is now present in every Italian region and it is a great health concern as it is a vector for several pathogens (e.g. Zika, dengue, Chikungunya). Finally, it has been shown that *Cx. pipiens* mosquitoes do not bite avian hosts randomly but there are some highly preferred species, and such feeding preferences can vary during the season also depending on host availability (Kilpatrick *et al.*, 2006a; Rizzoli *et al.*, 2015). Clearly, biting habits might strongly affect pathogens, in particular WNV, transmission.

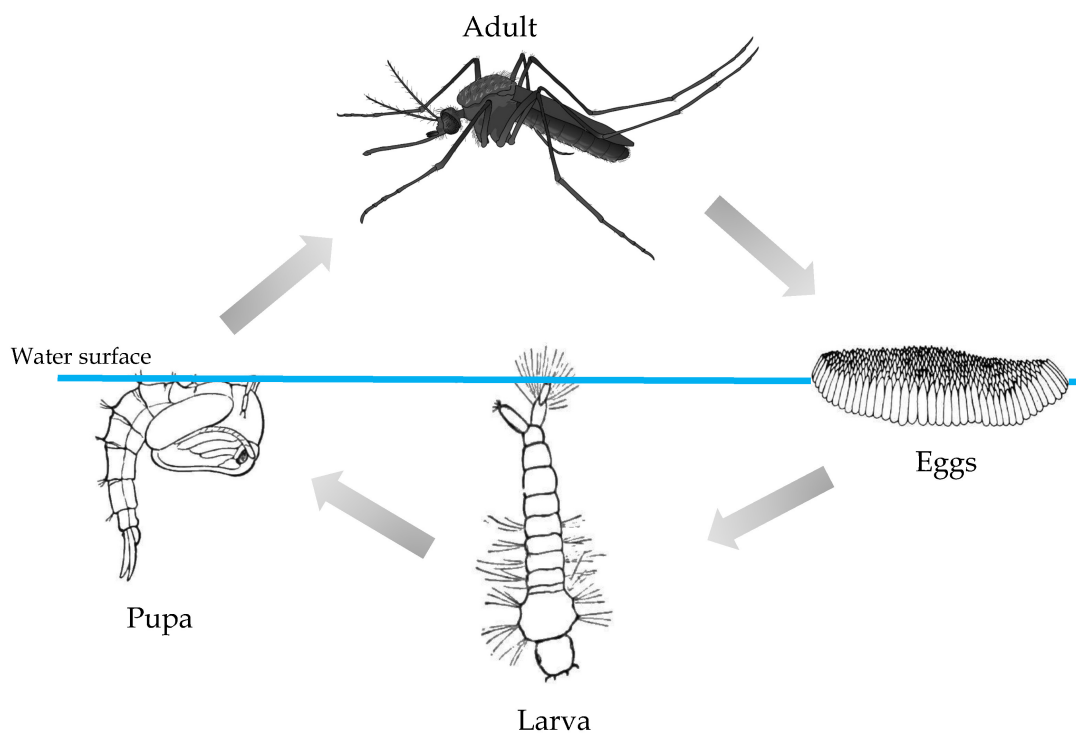


Figure 2: **Mosquito life cycle.** Adults lay eggs on the water surface; the larval and pupal stages are aquatic.

In this thesis I present some mathematical models that provide insights on several aspects of mosquito population dynamics. Specifically, I will investigate the effect of biotic and abiotic factors on *Cx. pipiens* dynamics by using adult mosquito trapping data, gathered over several years in Northern Italy, to feed theoretical models.

Interspecific competition might occur not only at the vector level but also between hosts; Roberts & Heesterbeek (2013) addressed systemically for the first time the interaction of ecological processes, such as consumer-resource relationships and competition, and the consequences for the epidemiology of infectious diseases spreading in ecosystems from a mathematical perspective. Following their study, I will investigate the effect of host competition on the dynamics of a vector-borne infection (such as WNV), taking into account vector feeding preferences too. While only theoretical, this model may be a useful representation of the dynamics of WNV that allows a better understanding of how competition between different bird species and feeding preferences might affect the circulation of the virus; thus, this model may be an extension of the important works by, for instance, Simpson *et al.* (2012), Bowman *et al.* (2005) and Fan *et al.* (2010).

In this thesis I will make a large use of two different kinds of model, namely statistical and mechanistic. The former are based on a hypothesized relationship between the variables in an observed dataset, where the relationship seeks to best describe the data. On the other hand, in mechanistic models the nature of the relationship is specified in terms of the biological processes that are thought to have given rise to the observed data, thus the parameters in such models all have biological definitions. Throughout the thesis I will answer several ecological questions by using different statistical and computational approaches, including for instance Generalized Linear Models (GLM) and Markov chain Monte Carlo (MCMC) technique. Finally, I would like to remark that developing a useful model does not require broad mathematical skills only but also a good knowledge of all biological aspects involved in the observed data, and that interaction with biologists is essential for that.

Below I am presenting a brief description of each chapter of my thesis.

Thesis outline

The main body of my thesis is a collection of four published scientific articles, so each chapter has its own introduction, methods, results and discussion sections.

In Chapter 1 we analyze the population dynamics of *Cx. pipiens* in Piedmont region (Northwestern Italy) using capture data gathered in about forty different locations during years 2000-2011. Specifically, several statistical models are developed aiming to determine early warning predictors of between year variations in mosquito population dynamics. We found that climate data collected early in the year, in conjunction with local land use, can be used to provide early warning of both the timing and magnitude of mosquito outbreaks.

Chapter 2 presents a density-dependent stochastic model that describes temporal variations of *Cx. pipiens* population dynamics including the effect of temperature and daylight duration on the abundance of both adults and immature stages of *Cx. pipiens*. The model is tailored to fit the temporal pattern of spatially averaged captures presented in Chapter 1; the results provide quantitative estimates on the effect of temperature and density-dependence on *Cx. pipiens* abundance.

Chapter 3 presents one of the first modeling effort aiming to quantify the effect of larval interspecific competition between *Ae. albopictus* and *Cx. pipiens*. Such interaction is investigated through a mechanistic model that integrate the *Cx. pipiens* model presented in Chapter 2 and the *Ae. albopictus* model already present in literature (Poletti *et al.*, 2011; Guzzetta *et al.*, 2016a,b), using capture data of both species collected in Trentino and Veneto regions (Northeastern Italy) in 2014-2015.

Chapter 4 presents a theoretical model to investigate how ecological factors might affect the dynamics of a vector-borne pathogen in a population composed by different hosts which interact with each other. Specifically, we consider the case when different host species compete with each other and the vector might have different feeding preference, which can also be time dependent. As a prototypical example, we apply our model to study the invasion and spread, during a typical season, of WNV in an ecosystem composed of two competent avian host species and possibly of dead end host species.

Finally, the last chapter summarizes the main results of the thesis and present a brief discussion on possible future directions.

1 Early warning of West Nile virus mosquito vector: climate and land use models successfully explain phenology and abundance of *Culex pipiens* mosquitoes in Northwestern Italy

Roberto Rosá^a, Giovanni Marini^{a,b}, Luca Bolzoni^{a,c}, Markus Neteler^a, Markus Metz^a, Luca Delucchi^a, Elizabeth Chadwick^d, Luca Balbo^e, Andrea Mosca^e, Mario Giacobini^f, Luigi Bertolotti^f, Annapaola Rizzoli^a

a: Department of Biodiversity and Molecular Ecology, Research and Innovation Centre, Fondazione Edmund Mach, San Michele all'Adige (TN), Italy

b: Department of Mathematics, University of Trento, Trento, Italy

c: Istituto Zooprofilattico Sperimentale della Lombardia e dell'Emilia Romagna, Parma, Italy

d: Cardiff University, School of Biosciences, The Sir Martin Evans Building, Museum Avenue, CF10 3AX Cardiff, Wales

e: Istituto per le Piante da Legno e l'Ambiente - IPLA S.p.a., Torino, Italy

f: Dipartimento di Scienze Veterinarie, Università degli Studi di Torino, Torino, Italy

Parasites & Vectors 2014; 7: 269

1.1 Introduction

West Nile virus (WNV) is a flavivirus of emerging public health relevance in Europe (European Centre for Disease Prevention and Control, 2013). In nature it is maintained in enzootic cycles between avian reservoir hosts and mosquitoes. Humans are dead-end hosts in which infection can induce symptoms from mild flu-like fever to severe neurological syndromes such as meningitis, encephalitis, and acute flaccid paralysis (Sambri *et al.*, 2013).

Prevention by vaccination has been possible for horses since 2003, but a human vaccine is not yet available (Iyer & Kousoulas, 2013). Discovered originally in Uganda in 1937 (Smithburn *et al.*, 1940), WNV is now found on every continent except Antarctica (Reisen, 2013). Several epidemics have been documented in European countries during the last 4 years (European Centre for Disease Prevention and Control, 2013), and this recent upsurge in outbreaks within endemic areas, as well as the spread of the virus throughout the New World since 1999, have led to increasing health concerns (Campbell *et al.*, 2002). Effective prevention and control policies are dependent on both a clearer understanding of the risk factors associated with infection, and advance warning of likely outbreaks.

Adequate mosquito density is critical for effective WNV transmission, and has a strong correlation with the number of human cases (Colborn *et al.*, 2013; Kilpatrick & Pape,

2013). However, implementing mosquito control measures in response to reports of human cases typically is ineffectual because most humans have been infected by this time and cases appear at the end of the mosquito season, when populations are already in decline (European Centre for Disease Prevention and Control, 2013; Winters *et al.*, 2008). Early warnings of mosquito outbreaks would provide a much needed prediction of spill-over risk (Yang *et al.*, 2009; Cleckner *et al.*, 2011; Deichmeister & Telang, 2011), enabling more timely control measures to be implemented, especially within WNV circulation areas.

Mosquitoes belonging to the *Cx. pipiens* complex are thought to be the most efficient vectors for spreading WNV among birds, and from birds to humans and other mammals in North America (Bernard *et al.*, 2001; Kilpatrick *et al.*, 2005) as well as in Europe (Zeller & Schuffenecker, 2004). They are also involved in the transmission of other human and animal pathogens such as Usutu virus (Gaibani *et al.*, 2013), avian malaria and filarial worms (Farajollahi *et al.*, 2011).

Cx. pipiens mosquitoes lay their eggs in water, and larval stages are aquatic. Aquatic habitats are therefore a prerequisite for mosquito populations, and rainfall is important in creating and maintaining suitable larval habitats (Becker *et al.*, 2010), thus strongly affecting the abundance of adult mosquitoes (Degaetano, 2005). Temperature also strongly influences distribution, flight behaviour and dispersal, and abundance of mosquitoes (Becker *et al.*, 2010). Specifically, temperature impacts on several aspects of the *Cx. pipiens* life cycle including development rates (Loetti *et al.*, 2011; Geery & Holub, 1989), gonotrophic cycle length (Clements, 1992) and diapause duration (Spielman, 2001) as well as the duration of the extrinsic incubation period of the virus (Kilpatrick *et al.*, 2008). Urban infrastructure often provides key habitats for *Cx. pipiens*, reflecting its affinity for stagnant water and urban areas where artificial containers of water are numerous (Deichmeister & Telang, 2011; Trawinski & Mackay, 2010). Vegetation density is also important, due both to a positive correlation with abundance of preferred avian host species (Brown *et al.*, 2008), and because trees and shrubs may offer resting habitats and sugar sources to adults (Gardner *et al.*, 2013). Mosquito population density therefore reflects a complex interaction among climate, land use and vegetation coverage.

In order to develop robust statistical models to predict mosquito population dynamics, detailed data are needed describing the phenology and abundance of mosquito populations, and associated environmental data at a suitable spatial and temporal resolution to act as predictor variables. Both the spatial and temporal range and resolution will determine the accuracy and range over which resulting model predictions can be made. In the Piedmont area of northern Italy, an extensive mosquito trapping programme has been in place since 1997, run by the Municipality of Casale Monferrato until 2006, and then by the Istituto per le Piante da Legno e l'Ambiente (IPLA). The area is at risk from WNV, having suitable vector and reservoir host populations, and increasing numbers of human cases of WNV in adjacent areas (Barzon *et al.*, 2013; Monaco *et al.*, 2010; Calistri *et al.*, 2010).

Detailed environmental data are available at suitable spatial and temporal resolution across the area, thus providing an excellent system to test predictors of mosquito population dynamics. Similarities of climate and land use (Rizzoli *et al.*, 2009) allow model predictions to be cautiously applied across northern Italy, where WNV has been circulating since 2008 (Calistri *et al.*, 2010).

Previously, part of this dataset (years 2000 to 2006) was used to test associations be-

tween weekly mosquito abundance (various species) and a range of environmental data, including land use and weekly averaged climate, during the time period 10-17 days prior to measures of mosquito populations (Bisanzio *et al.*, 2011). This approach tested for predictors that immediately preceded short term variation in weekly mosquito abundance. Here we followed a different approach, aiming to determine early warning predictors of between year variation in mosquito population dynamics. We focused on *Cx. pipiens* and we extended the dataset for analysis until 2011. The objective was to identify the best early warning predictors of annual variation in *Cx. pipiens* abundance and phenology, with the ultimate goal to guide entomological surveillance and thereby facilitate monitoring of WNV transmission risk.

1.2 Methods

The study area encompassed 987 km² of the eastern Piedmont Region of north-western Italy (centroid: 45.07°N, 8.39°E) (see Figure 1.1). There are highly suitable habitats for avian hosts of WNV, and breeding sites for mosquitoes, in close conjunction to human habitation. The landscape is primarily agricultural (mixed agriculture 72%, rice fields 14%), with areas of deciduous forest on the southern hills, and riverine habitat in the north (for further details see (Bisanzio *et al.*, 2011)). The climate is characterised by cold winters and warm summers (0.4 and 24°C respectively), and abundant precipitation (about 600 mm/yr) primarily falling in spring and autumn (Bisanzio *et al.*, 2011).

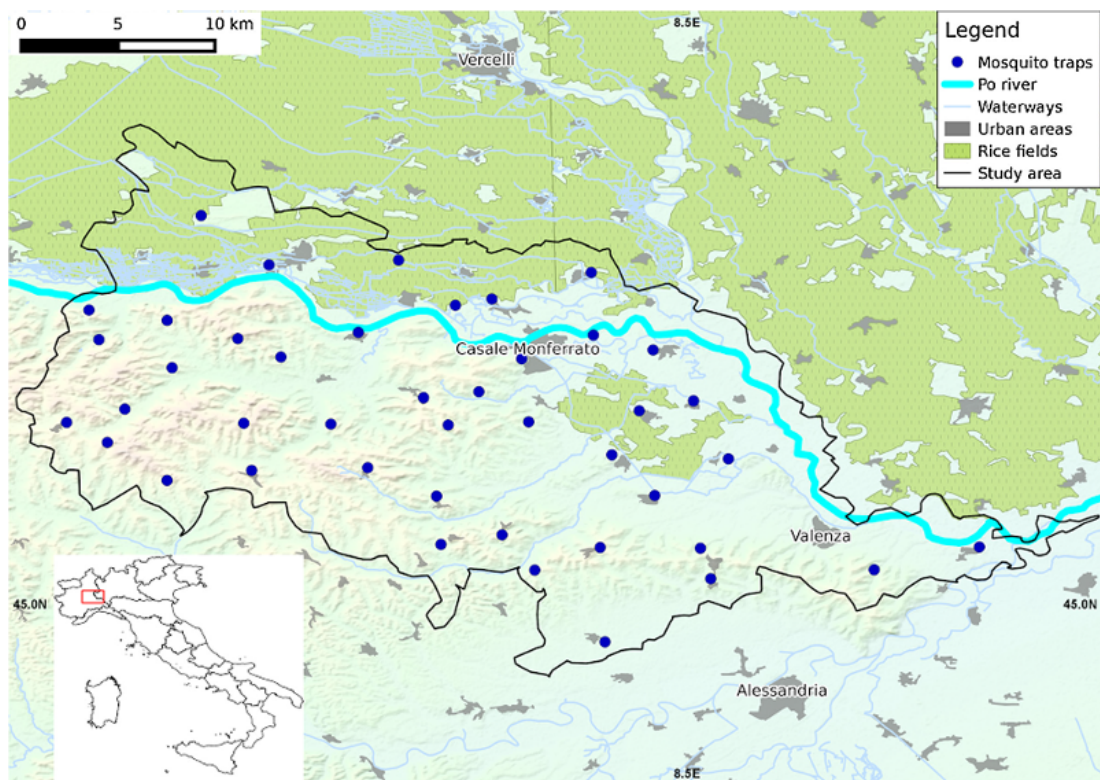


Figure 1.1: **Map of the study area.** Trap locations and land use are indicated. The map of Italy (inset) shows the location of the study area in the north west of the country.

1.2.1 Mosquito data

Mosquitoes were collected using CO₂ baited traps, operated by Municipality of Casale Monferrato and the Istituto per le Piante da Legno e l'Ambiente (IPLA) (Bisanzio *et al.*, 2011). Trapping sites were dispersed throughout the study area, with a minimum distance of 5 km between traps. Specific placement was based on coverage of all habitats deemed suitable for mosquitoes, in all participating municipalities, while enabling estimation of urban nuisance, and avoiding external disturbing factors (e.g. lighting, CO₂ sources). Further details are provided in (Bisanzio *et al.*, 2011). The current study includes data from 2001 to 2011, collected at 44 different sites (including 28-40 sites and an average of 37 sites activated each year) (see Figure 1.1). Although most traps were run throughout, variation in activation at some sites occurred depending on the participation of individual municipalities in the scheme. Alongside monitoring efforts, mosquito control strategies have been implemented in the study area since 1998 (Bisanzio *et al.*, 2011). However, the target of all treatments was *Ochlerotatus caspius*, and analyses (not presented here) showed that *Cx. pipiens* mosquitoes were not affected by interventions. Traps were set one night every week, for a twenty-week period starting at the beginning of May and ending in mid-September, thus encompassing the main period of mosquito activity. Traps were collected the following day, and the catch counted, sexed and identified. Each year since 2009, mosquitoes captured during a 6-7 night period at several sites (an average of 5 sites per year) have been pooled and tested for WNV. Until now no positive results have been found. For each trap, in every year, we (i) summed the total number of *Cx. pipiens* captured during the twenty-week survey period (TOTAL), (ii) calculated the week by which 5% and 95% of the population were captured, these being designated the start (ON) and end (OFF) of the mosquito season, respectively, and (iii) calculated the number of weeks between the arrival of 5% and 95% of the trapped population, this designated as season length (SEASL). As in (Jouda *et al.*, 2004), our definitions of ON and OFF are threshold values for population abundance, and do not necessarily reflect the cessation or initiation of diapause. Peak abundance within years was considered in preliminary analyses as a fourth measure of population dynamics, but was illdefined and unpredictable, therefore results are not presented here.

1.2.2 Environmental predictors

Environmental predictors were selected based on published evidence of their importance to mosquito populations (Degaetano, 2005; Gardner *et al.*, 2013; Bisanzio *et al.*, 2011; Chuang *et al.*, 2012). All environmental data were processed in GRASS GIS (Neteler *et al.*, 2012), and extracted from the spatial database at the point corresponding with trap location. *Cx. pipiens* have a very limited dispersal (a few hundred metres (Becker, 1997)), which is within the pixel size for most spatial data (below), so data averaging over a wider area was not considered appropriate.

Climate

Precipitation was measured as total precipitation (TOT_PREC) and number of days of precipitation (DAY_PREC) from the gridded ECA&D (European Climate Assessment & Dataset, Version 8) (ECA&D project, 2013; Haylock *et al.*, 2008) at approximately 25 km pixel resolution. Land surface temperature (LST) data were collated from the Moderate Resolution Imaging Spectroradiometer (MODIS) products MOD11A1 and MYD11A1,

recorded twice daily. The original MODIS LST products were reconstructed at 250 m resolution, i.e. gap-filled to remove void pixels due to clouds (Neteler, 2010; Metz *et al.*, 2014). For analyses, LST data were used to derive two values: (i) weekly mean LST, and (ii) a cumulative measure of temperature named here “growing degree weeks” (GDW) (see (Ruiz *et al.*, 2010)). This was derived by taking the positive difference in each week between mean LST and a threshold of 9°C (mosquitoes fail to develop below this threshold, see (Loetti *et al.*, 2011)). Weekly differences were summed cumulatively from the first week of the year, so that the n -th GDW was obtained by summing the n consecutive differences (negative differences were assigned a value of zero).

Vegetation and water indices

Normalized Difference Vegetation Index (NDVI) was obtained from the MODIS product MOD13Q1, recorded every 16 days, and the Normalized Difference Water Index (NDWI) derived from the MODIS product MOD09A1, recorded every 8 days, both at 500 m resolution. For both the NDVI and the NDWI data, gaps were filled and outliers removed using a harmonic analysis of each time series (Roerink *et al.*, 2000). These data were used as proxies for vegetation coverage (NDVI) (Estallo *et al.*, 2012) and for environmental water (NDWI), which includes surface water (McFeeters, 2013) as well as vegetation water content (Estallo *et al.*, 2012).

Land use

The distance from every sampling site to the nearest urban centre (DIST_URBAN) and rice field (DIST_RICE) was calculated using the Corine Land Cover raster dataset (using the CORINE classes 111 and 112 to map the urban settlements and 213 for the rice fields (European Environment Agency, 2014) both at 100 m resolution).

1.2.3 Temporal windows

We built 22 temporal windows by grouping periods of 12 consecutive weeks, starting from the first week of the year (weeks 1-12) and ending with weeks 22-33 (approximately the end of May to mid-August). The 22 windows were divided into two groups: the first ten windows (1-12, 2-13, etc., to 10-21) were designated the “early period” and latter twelve windows (11-22, 12-23, etc., to 22-33) were designated the “late period”. The start of the mosquito season, “ON”, occurred on average during week 25, so our definition of early period predictors were those that were completed at least four weeks prior to this (i.e. ending weeks 10-21).

For each 12-week window, mean values were calculated for land surface temperature and vegetation indices (LST, NDVI and NDWI), whereas precipitation data were summed (TOT_PREC and DAY_PREC). For GDW, the cumulative value achieved by the end of the given window was used. Where these data are described in the text, the relevant temporal window is denoted in subscript, e.g. LST_{1-12} for mean land surface temperature during weeks 1-12.

The aggregation of 12 weeks was selected in order to test the effect of variations at a seasonal timescale and to avoid errors due to short term variation in mosquito collections. Comparisons with aggregation windows of alternative duration (1, 2, 4 and 8 weeks) proved this approach to be successful; twelve week windows produced more robust models and higher goodness-of-fit values, when compared to results obtained by aggregating

data over shorter windows (see section 1.A.1).

1.2.4 Data analysis

We investigated the association between *Cx. pipiens* abundance (TOTAL) and seasonality (the start of the mosquito season, ON, and season length, SEASL, as defined above), and a range of environmental predictors. All statistical analyses were performed using R version 3.0.2 (R Development Core Team, 2008). Dependent variables were transformed prior to analysis in order to normalize their distribution, following the Box-Cox method (Box & Cox, 1964). Transformations applied were $x^{1.3}$ for ON and $x^{0.2}$ for TOTAL while data for season length were normally distributed.

Preliminary analyses

Linear mixed effect models were used to ascertain, for each climatic variable, vegetation index and water index in turn, (i) which of the early period windows proved to be the best predictor of the start of the season (ON), and (ii) which of all the time windows (early and late) proved to be the best predictor of mosquito abundance (TOTAL) and season length (SEASL). In all models, trap identification number was included as a random variable. Models were ranked using the Akaike Information Criterion (AIC) (Akaike, 1974), and for each climatic variable and vegetation/water index, the time window producing the lowest AIC was selected for inclusion in subsequent full models. For NDWI the first eight time windows were not included in preliminary analyses due to the potential presence of snow cover, which can dramatically alter the reliability of satellite acquisition of this parameter (Xiao *et al.*, 2002; Delbart *et al.*, 2005). Terms that were not significant for any of the early or late time periods were not included in the full model. Variance Inflation Factor (VIF) (Pan & Jackson, 2008) was used to test for collinearity between all explanatory variables. Where collinearity was significant (VIF values > 4, (Pan & Jackson, 2008)), the variable producing the higher AIC was excluded. This led to the exclusion of GDW and total precipitation from further analyses. Vegetation and water indices were not correlated; however, NDVI was not significant in any of preliminary models, thus it was excluded from further analyses.

Full models

Following exclusion of collinear and non-significant variables, we developed linear mixed models including the remaining environmental variables, each measured over the optimum time window as selected through preliminary analyses. All two-way interaction terms were included in full models. In addition, we included distance to urban areas and to rice fields, and again included trap identification number as a random variable. Models were fitted in turn to predict (i) the start of the mosquito season (using early period predictors only), (ii) season length and (iii) mosquito abundance (modelled initially using only early period predictors, and then again using both early and late period predictors, in order to assess the additional variance explained by inclusion of the latter period).

Multi-model inference (Burnham & Anderson, 2002) was used to compare all possible models using the R package "MuMIn" (Barton, 2013). Models were ranked using AIC, and differences in AIC (Δ AIC) between consecutively ranked models were used to calculate weights and relative evidence ratios for each variable. The best models were selected using a threshold of Δ AIC \leq 4 (Burnham & Anderson, 2002). All variables included in

the best models were ranked according to their importance (weight), i.e. the cumulative Akaike weight (wAIC) of the models that include that explanatory variable (Barton, 2013; Whittingham *et al.*, 2006). This provides an idea of the frequency with which the predictor was included in the most likely models, and not directly the importance of its effect on the predicted variable. Average coefficient for each variable was calculated following modelling average procedure (Burnham & Anderson, 2002).

In order to quantify the effect size of each predictor variable, predictions were made from the best models for each significant predictor variable in turn. For predictive models, all variables but one were fixed at their average values, and predictions made across the full range of the selected variable. For example, to test the association between temperature and the start of the mosquito season (ON), in a model where temperature, precipitation and NDWI were significant predictors, precipitation and NDWI were entered into the model as constants (fixed at their average measured value), while values for temperature were allowed to vary within their observed range. Models and plots were created using transformed data (for ON and TOTAL); predictions described in the text use back-transformed values to aid interpretability.

1.3 Results

1.3.1 Mosquito indices

The start of the mosquito season (ON) typically occurred during weeks 24-27 of the year (see Figure 1.2a), and the main capture period (SEASL) lasted for 56-70 days (see Figure 1.2b). The number of individuals captured (TOTAL) varied between 44 and 4648 per trap per year; more precisely, for one third of the traps the observed abundances varied between 44 and 500, for another third between 500 and 1000 and the remainder between 1000 and 4648 individuals (see Figure 1.2c).

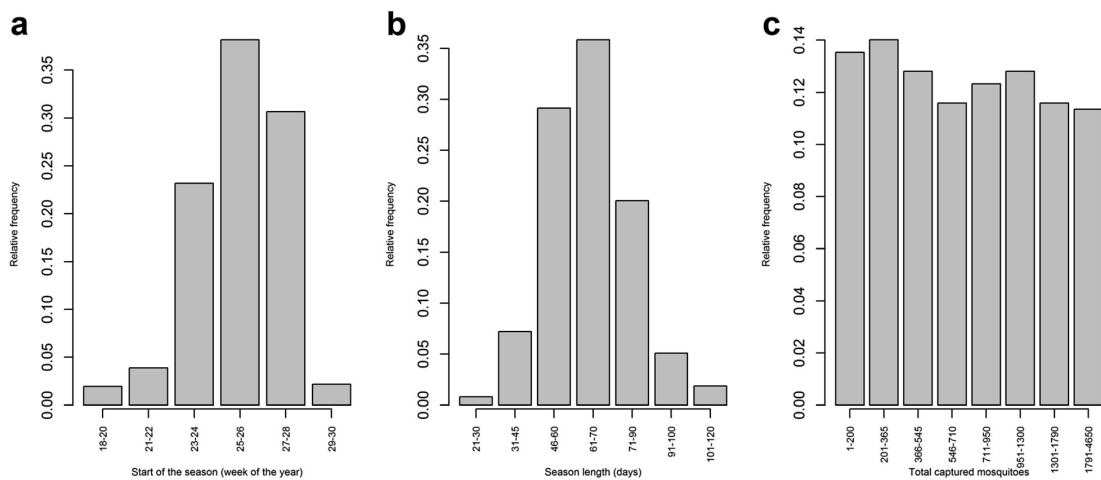


Figure 1.2: **Timing and abundance of the mosquito season.** Frequency distributions for (a) the start of mosquito season (the date by which 5% of total captures were made), (b) season length (the period in days between the collection of 5% and 95% of the captured population) and (c) the total number of *Cx. pipiens* captured.

1.3.2 Model results

Preliminary analyses

For prediction of the start of the season (ON), the optimum time windows selected for inclusion in the model were weeks 8-19, 6-17, and 10-21 for temperature (LST), precipitation (DAY_PREC) and NDWI respectively (determined by comparison of AICs, see Figure 1.6). For prediction of season length (SEASL) using only early period predictors, the optimum windows for temperature and NDWI were the same as for prediction of ON (8-19; 10-21) but the optimum window for precipitation was earlier, weeks 2-13. Late period predictors were weeks 16-27 for temperature, 20-31 for precipitation and 11-22 for NDWI (see Figure 1.6). For prediction of mosquito abundance (TOTAL) using only early period predictors, the optimum windows for temperature and precipitation were weeks 10-21 and 1-12, respectively; NDWI was not significant for any time window. Additional late period predictors were weeks 21-32, 15-26 and 22-33 for temperature, precipitation and NDWI respectively (see Figure 1.6).

Full models

For the start of the season (ON) 32 full models were produced and a single best model was selected, explaining 26% ($R^2 = 0.258$, Akaike weight = 0.96) of the variance; remaining models had $\Delta AIC > 4$ and were disregarded (see section 1.A.3). Model outputs (see Table 1.1) are therefore based on a single model, rather than averages from multiple models as elsewhere. Within the measured range of environmental data, temperature had the greatest effect on the start of the season. Higher spring temperatures were associated with an earlier start to the season, such that an increase of 5°C in LST_{8-19} (from 11 to 16°C) predicts the start of the season some 14 days earlier (a shift in the average ON from day 187 to 173) (see Figure 1.3a). Increasing NDWI also predicts an earlier start to the season, such that a shift in $NDWI_{10-21}$ from -0.1 to +0.06 led to a start of the season 10 days earlier (see Figure 1.3b), while more days of precipitation delayed the start of the season such that an increase in DAY_PREC_{6-17} from 14 to 37 days of precipitation during the 12 week period led to a delay in the start of the season of 10 days (see Figure 1.3c). All terms selected in the best models (LST_{8-19} , $NDWI_{10-21}$ and DAY_PREC_{6-17}) were highly important with a predictor weight equal to or very close to 1 (see Table 1.1). Neither distance to urban area or rice fields were significant predictors.

When considering only the early period, two models, out of 32 models produced, were selected to predict season length, explaining between 13 and 14% ($R^2 = 0.135$, $R^2 = 0.141$) of the variance, and differed in their inclusion/exclusion of temperature (Akaike weights were 0.21 and 0.77). From model averaging, the early period variables associated with earlier start of the season (ON, above) also predict increased season length, so higher NDWI and temperature predict a longer season (although note that following averaging procedures temperature is significant only at a 92% threshold, with $p = 0.079$), and more days of precipitation predict a shorter season. Again, distance to urban areas and rice fields were not significant predictors, for either of the two best models. For early period predictors only, an increase in $NDWI_{10-21}$ from -0.1 to +0.06 predicts an increase of 14 days in season length (from 56 to 70 days), while an increase in days of precipitation from 7 to 30 days during the 12 week period (DAY_PREC_{2-13}) predicts an eleven day decrease in season length (from 71 to 60 days) (see Figure 1.4a). An increase of 5°C in LST_{8-19} (from 11 to 16°C) predicts an extension of 7 days in season length (from 65 to

72 days).

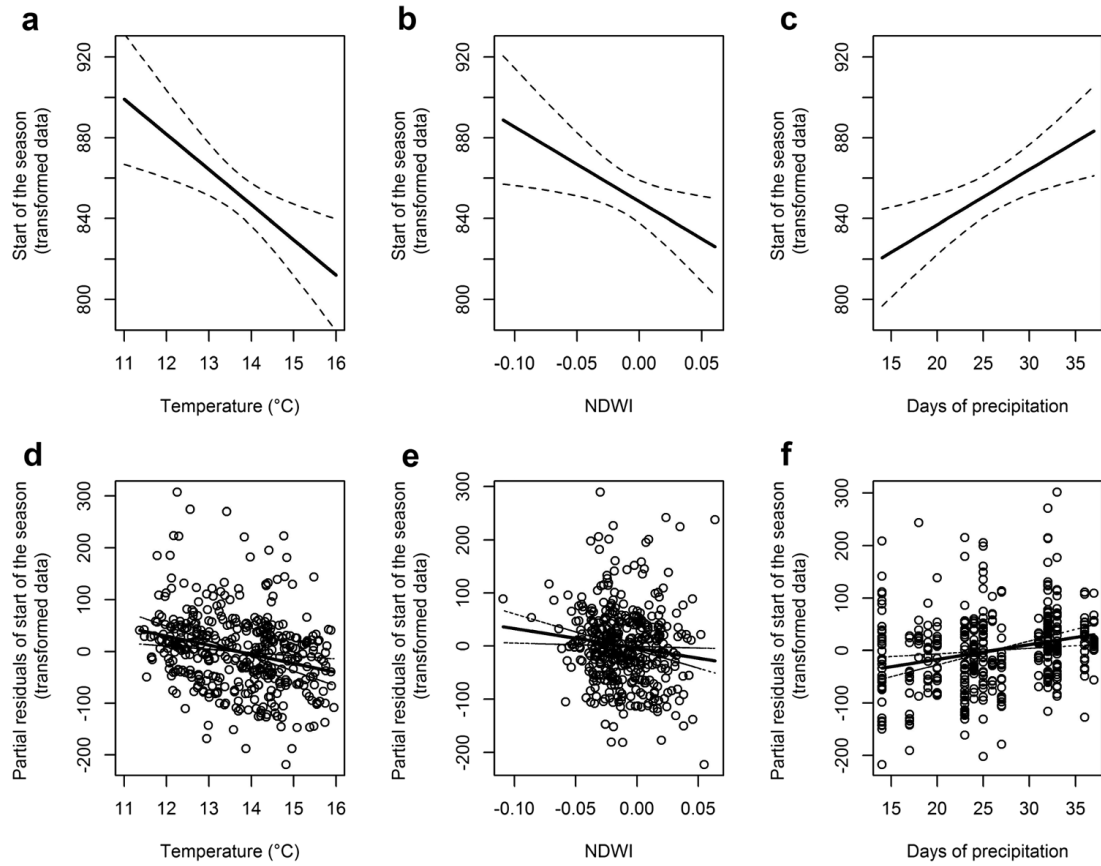


Figure 1.3: **Association between the start of the mosquito season and environmental variables.** Panels a-c show model predictions; panels d-f show partial residuals. The first column (a,d) shows the association between the start of the season and temperature (LST_{8-19}), the second (b,e) shows the association with $NDWI_{10-21}$ and the third (c,f) shows the association with precipitation (DAY_PREC_{6-17}). Note that all plots show transformed data on the y axis (i.e. $x^{1.3}$); back transformed values are presented in the text to assist interpretation.

| Variable | Weight | Coeff. | Std. error | z-value | Pr(> z) |
|--------------------|--------|---------|------------|---------|-----------|
| Intercept | | 1014.19 | 96.54 | 10.51 | <0.001 |
| LST_{8-19} | 1 | -17.3 | 5.6 | -3.09 | 0.002 |
| $NDWI_{10-21}$ | 1 | -369.07 | 155.43 | -2.37 | 0.018 |
| DAY_PREC_{6-17} | 0.99 | 2.76 | 0.88 | 3.12 | 0.002 |

Table 1.1: **Predicting the start of the mosquito season (ON).** The weight and significance of terms remaining in the best selected model.

When incorporating late period variables in addition to early period, 128 full models were produced and six of them were selected as best, with R^2 between 0.147 and 0.160 and Akaike weights between 0.28 and 0.06. Improvement to the model fit from inclusion of late period variables was therefore minimal, when compared to early period predictors alone (see above). Comparison of the model terms suggests, however, that precipitation

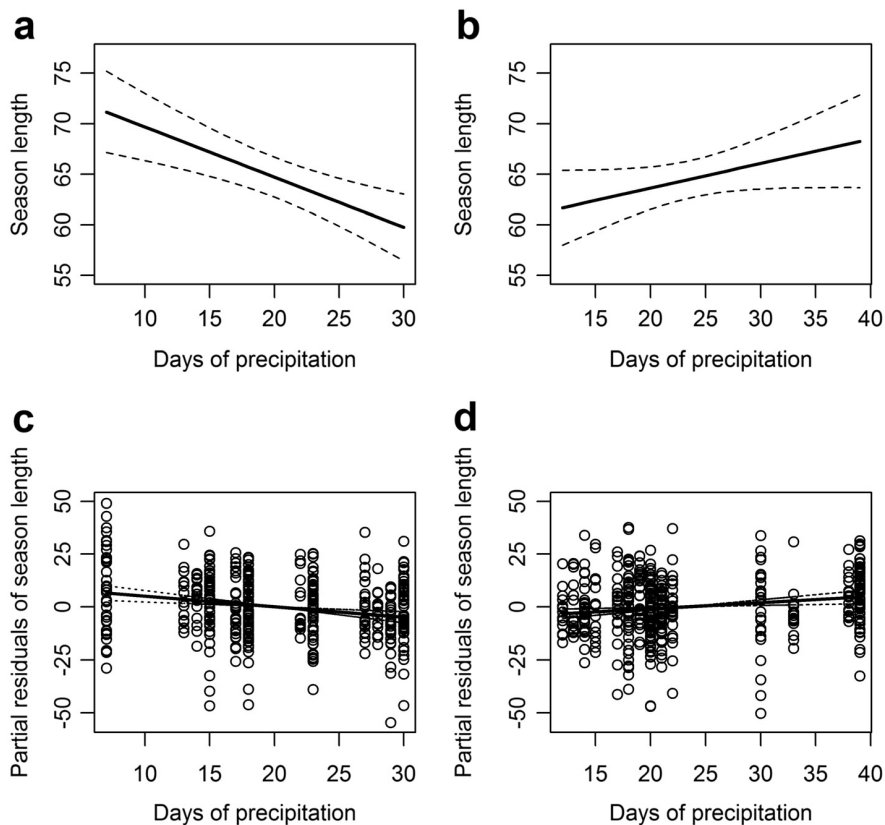


Figure 1.4: **Association between season length and days of precipitation.** Panels a-b show model predictions; panels c-d show partial residuals. The first column (a,c) shows the association with days of precipitation during the early period (DAY_PREC_{2-13}) while the second column (b,d) shows the association with precipitation in the late period (DAY_PREC_{20-31}).

during the late period (DAY_PREC_{20-31}) has the opposite effect of precipitation during the early period (DAY_PREC_{2-13}) (see Figure 1.4b). More days of precipitation during the late period predict a longer season, such that an increase from 12 to 39 days of precipitation (DAY_PREC_{20-31}) predicts a seven day increase in season length, whereas in the early period only model, more days of precipitation delay the season start and so shorten season length (as described above). The association with late period precipitation is stronger than that of early period precipitation, so that when both terms are included in the same model, early period precipitation becomes non-significant with a predictor weight of only 0.4, as compared to a high significance of $p = 0.004$ and a weight of 0.79 for late period precipitation (see Table 1.2). Late period temperatures (LST_{16-27}) have a marked impact on season length such that a shift of 6°C (from 19 to 25°C) predicts a lengthening of the season by 22 days (see Figure 1.5a). As for precipitation, the addition of late period temperature renders early period temperature non-significant, with predictor weight of only 0.53, as compared to late period temperature which is both highly significant ($p = 0.003$) and has a high predictor weight (0.98) (Table 1.2). The most important model term in terms of predictor weight was, however, NDWI measured during the early period (NDWI_{10-21}), which is positively associated with season length, and retains the same high predictor weight (1) in both groups of models (early only, early+late) (Table 1.2). An increase in NDWI_{10-21} from -0.1 to $+0.06$ predicts an increase in season

length of 14 or 17 days (the greater increase being predicted by the early+late models).

| Model | Variable | Weight | Coeff. | Std. error | z-value | Pr(> z) |
|-------------------|---------------------------|--------|--------|------------|---------|-----------|
| Early | Intercept | | 59.57 | 15.42 | 3.86 | < 0.001 |
| | NDWI ₁₀₋₂₁ | 1 | 85.23 | 31.52 | 2.7 | 0.007 |
| | DAY_PREC ₂₋₁₃ | 0.99 | -0.5 | 0.14 | 3.65 | < 0.001 |
| | LST ₈₋₁₉ | 0.78 | 1.5 | 0.85 | 1.76 | 0.079 |
| Early+Late | Intercept | | -19.11 | 28.45 | 0.67 | 0.501 |
| | NDWI ₁₀₋₂₁ | 1 | 104.26 | 31.36 | 3.32 | 0.001 |
| | LST ₁₆₋₂₇ | 0.98 | 3.78 | 1.26 | 2.98 | 0.003 |
| | DAY_PREC ₂₀₋₃₁ | 0.79 | 0.29 | 0.1 | 2.88 | 0.004 |
| | LST ₈₋₁₉ | 0.53 | 0.1 | 1.11 | 0.09 | 0.926 |
| | DAY_PREC ₂₋₁₃ | 0.4 | -0.28 | 0.16 | 1.73 | 0.083 |

Table 1.2: **Predicting season length (SEASL)**. The average weight and significance of variables remaining in the two best 'Early predictors only' and six best 'Early + Late predictors' models. Note that terms in italics are significant in some of the selected best models but not in others, and that overall, weighted model averaging procedures suggest that they are not significant.

Of the 16 full models produced, two were selected to predict mosquito abundance (TOTAL) from early period predictors, explaining between 46 and 49% of the variance ($R^2 = 0.464$, $R^2 = 0.488$) with Akaike weights of 0.12 and 0.79 respectively. Abundance was best predicted by early period models including days of precipitation at the start of the year (DAY_PREC₁₋₁₂), and distance to rice fields. An increase in precipitation predicts an increase in abundance (e.g. an increase from 7 to 30 days rain predicts an increase from approximately 400 to 1000 mosquitoes per trap). Traps closer to rice fields captured more mosquitoes than those 13 km away (average 680 mosquitoes per trap year, compared to 560). The very different prediction weights of the two terms selected in the early period models (Table 1.3), however, indicate that while days of precipitation play an important role, distance to rice fields has a very limited effect on early period model predictions. Incorporation of additional late period predictors did not greatly improve the model fit; again, two models were selected, out of 128 models produced, and explained 52% of the variance ($R^2 = 0.523$, $R^2 = 0.524$) with Akaike weights of 0.35 and 0.49 respectively. Days of precipitation at the start of the year (DAY_PREC₁₋₁₂) remained a highly significant predictor, and predicted a similar effect (an increase from 7 to 30 days of rain predicts an increase in total abundance from 420 to 860 mosquitoes per trap year). Distance to rice fields was not a significant predictor in early+late period models, while average temperature during the late period (LST₂₁₋₃₂) exerted a significant negative effect on predictions, such that an increase in temperature from 21 to 30°C led to a marked decrease in abundance from approximately 1150 to only 150 mosquitoes per trap year (Figure 1.5b). The days of precipitation measured during the early period (DAY_PREC₁₋₁₂) is the most important term predicting TOTAL in both groups of models (early only, early+late) while temperature has a strong impact on model prediction for the early+late model only (Table 1.3). Late period NDWI (NDWI₂₂₋₃₃) was selected only in one of the best models and following model averaging was not significant.

| Model | Variable | Weight | Coeff. | Std. error | z-value | Pr(> z) |
|-------------------|--------------------------|--------|----------|------------|---------|-----------|
| Early | Intercept | | 1.27 | 8.4e-03 | 152.83 | < 0.001 |
| | DAY_PREC ₁₋₁₂ | 1 | 2.8e-02 | 3.2e-03 | 8.75 | < 0.001 |
| | DIST_RICE | 0.13 | -7.8e-05 | 1.6e-05 | 4.78 | < 0.001 |
| Early+Late | Intercept | | 6.96 | 0.53 | 12.97 | < 0.001 |
| | LST ₂₁₋₃₂ | 1 | -0.15 | 0.021 | 7.24 | < 0.001 |
| | DAY_PREC ₁₋₁₂ | 1 | 1.7e-02 | 3.1e-03 | 5.04 | < 0.001 |
| | NDWI ₂₂₋₃₃ | 0.6 | -0.886 | 1.150 | 0.77 | 0.441 |

Table 1.3: **Predicting mosquito abundance (TOTAL)**. The average weight and significance of variables remaining in the two best 'Early predictors only' and two best 'Early + Late predictors' models. Note that terms in italics are significant in some of the selected best models but not in others, and that overall, weighted model averaging procedures suggest that they are not significant.

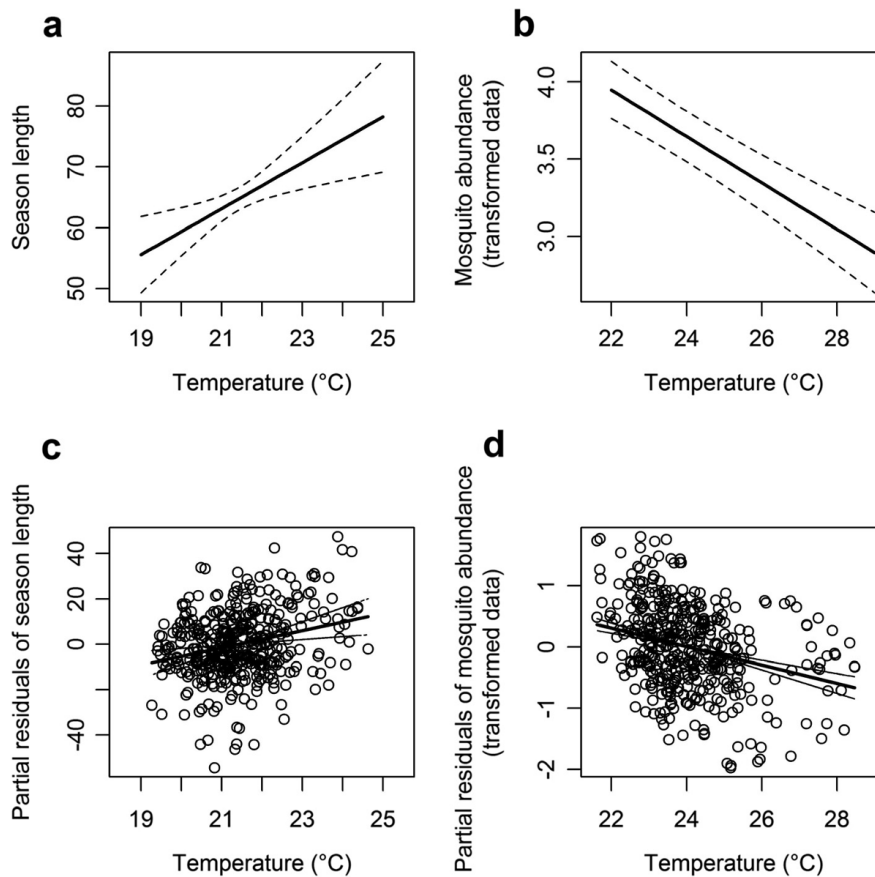


Figure 1.5: **Association between season length, total abundance and late season temperatures**. Panels a-b show model predictions; panels c-d show partial residuals. The first column (a,c) shows the association between late season temperature (LST₁₆₋₂₇) and season length; the second column (b,d) shows the association between late season temperature (LST₂₁₋₃₂) and mosquito abundance. Note that plots in the second column show transformed data on the y axis.

1.4 Discussion

The transmission of WNV is strongly linked to the abundance of the *Culex* mosquito vector (Colborn *et al.*, 2013; Kilpatrick & Pape, 2013), and many studies have focused on describing and quantifying habitat associations and spatio-temporal distributions of the vector species to guide implementation of effective control strategies (Winters *et al.*, 2008; Diuk-Wasser *et al.*, 2006). In particular, early predictions of both the timing and intensity of future mosquito abundance will help to enable decision makers to apply effective prevention and control plans (Yang *et al.*, 2009).

The current study aimed to identify early warning predictors of *Cx. pipiens* abundance and phenology, with the ultimate goal of improving entomological surveillance and focussing interventions to enable early detection of virus circulation in mosquitoes. To achieve this, we modelled the association between annual measures of mosquito abundance and phenology (start of the season and season length) and a set of environmental predictors.

Environmental predictors were selected based on published evidence of their importance to mosquito populations, and were averaged across twelve week periods in order to test the effect of variation at a seasonal scale, rather than focusing on daily or weekly fluctuations (e.g. (Bisanzio *et al.*, 2011)).

Our results indicate that warm temperatures during the early period (prior to the main mosquito season) lead to an earlier start, and extend the duration of the mosquito season (SEASL), but are not associated with a significant increase in abundance. This is likely to result from the acceleration of mosquito development rates driven by higher temperatures (Loetti *et al.*, 2011). Higher temperatures during the late period (encompassing the main period of mosquito host seeking activity) are similarly associated with increased season length, but also with a decrease in total abundance. This latter result is opposite to the one found by Bisanzio *et al.* (2011) but is coherent with the observed captures: for instance 2003 was the hottest summer during the current study, and also the year with the least captures. This is also consistent with results obtained from laboratory experiments where adult survival and longevity of *Cx. pipiens* were negatively affected by high temperatures (Ciota *et al.*, 2014). In addition, when high temperatures during summer are associated with low precipitation, as was the case in 2003, the combined effects of very hot and dry conditions are likely to cause rapid drying of aquatic breeding sites, with a consequent negative impact on mosquito populations. Recent observations in north-eastern Italy corroborate the negative impact of high summer temperatures, revealing a significant decline in populations when temperatures approached the maximum tolerance for *Cx. pipiens* over a prolonged period (Mulatti *et al.*, 2014).

Early period precipitation postponed and shortened the activity of host-seeking mosquitoes, but at the same time was associated with greater abundance. Conversely, precipitation during the late period was associated with an extension of the season. An association between increased abundance and early period precipitation is probably associated with the increase in formation and persistence of mosquito breeding sites while more days of precipitation during the late period would prolong the existence of breeding pools, thus sustaining mosquito populations later in the year (Degaetano, 2005).

Higher values for environmental water (NDWI) during the early period were associated with an earlier start to the season and an increase in season length. These results highlight the importance of suitable breeding habitat, including surface water as well as vegetation water content (Brown *et al.*, 2008; Estallo *et al.*, 2012; McFeeters, 2013).

Good levels of moisture, especially in the soil, are a fundamental requirement for the formation and persistence of mosquito breeding sites (Estallo *et al.*, 2012).

Although the two physical distances (to rice fields, and to urban areas) do not seem to be very important for *Cx. pipiens* in the current study, the negative association between abundance and distance from rice fields suggests that this land use provides important habitat in north-western Italy. This result was confirmed by larval collection of *Cx. pipiens* in rice-fields. Distances to urban areas were never selected in any of our models, suggesting that in this region of Italy urban settlements are not an important breeding habitat for *Cx. pipiens*, although it is possible that habitat type causes a bias in trap attractiveness. This is different to a number of other studies, carried out in North America and Europe, where it has been shown that *Cx. pipiens* prefers urban settlements (Deichmeister & Telang, 2011; Trawinski & Mackay, 2010; Becker, 1997). These preferences in North America may reflect differences in the ecology of *Cx. pipiens* in the Old, versus the New World, or may reflect differences in the biogeography of the two regions. Alternatively, such differences may reflect the presence of different forms of the species. Form *pipiens* prefers a more rural habitat, while *molestus* is more urban (Osório *et al.*, 2014). The form present in the eastern Piedmont area has not been definitively identified, but the relatively infrequent bites to humans (pers. obs) makes *pipiens* (which are predominantly bird-feeding) the more likely. Although Bisanzio *et al.* (2011) present spatial analyses (based on the same area as the current study) in which the highest abundances of *Cx. pipiens* were close to urban areas, the term was not significant in their final model. The equivocal nature of the results suggested by Bisanzio *et al.* (2011), and the lack of support for urban preference in the current study, using a longer timeseries, supports a view that urban areas are of limited importance to *Cx. pipiens* in north western Italy.

1.5 Conclusions

Although a wide range of environmental and non-environmental factors are involved in West Nile Virus outbreaks (Reisen, 2013), the current study indicates that basic climatic monitoring data collected early in the year, in conjunction with local land use, can be used to provide early warning vector population dynamics, and therefore potential transmission risk. Overall, our analysis suggests that the early period of the year (prior to the start of the mosquito season) is very important to *Cx. pipiens* population dynamics: improvements to model accuracy by inclusion of the late period (during the main period of host seeking activity) were minimal. This result is particularly important in view of the need for timely implementation of mosquito control actions. The models developed are suitable for application in other areas where climate and land use are similar, while the principles used in model design can be applied across any area where mosquito population data and environmental data can be obtained. This has implications not only for West Nile Virus, but also for a wide range of other diseases that could be limited by mosquito control.

1.A Supporting information

1.A.1 Aggregation of environmental data over a range of time windows: preliminary analyses

In order to select an appropriate period of time for aggregation of environmental data, we ran preliminary analyses comparing single model predictions of mosquito indices (ON, SEASL and TOTAL). Explanatory variables were the environmental predictors (DAY_PREC, LST or NDWI), and data for each environmental predictor were summed (DAY_PREC) or averaged (LST and NDWI) within each temporal window, using a range of aggregation periods: 1, 2, 4, 8, 12 weeks.

Comparisons were therefore made between:

- 1 week aggregation, producing 33 temporal windows from week 1 until week 33;
- 2 week aggregation, producing 32 temporal windows from weeks 1-2 until weeks 32-33;
- 4 week aggregation, producing 30 temporal windows from weeks 1-4 until weeks 30-33;
- 8 week aggregation, producing 26 temporal windows from weeks 1-8 until weeks 26-33;
- 12 week aggregation, producing 22 temporal windows from weeks 1-12 until weeks 22-33.

To make comparisons between models we looked at:

- The percentage of models with significant coefficients (Table 1.4).
- Consistency - estimated by how many times the coefficients from models using two consecutive temporal windows changed their sign (Table 1.5).
- Minimum and Mean values of model AIC (Tables 1.6 and 1.7).

The 12-week aggregation performed better than all other choices, across all of the given parameters. The 12 week period gave on average the highest percentage of significant coefficients (76%), the lowest number of changes of coefficient sign (6), and the lowest values of MIN and MEAN AIC (3385.24 and 3420.02 respectively).

| | | Aggregation period (weeks) | | | | |
|------------|----------|----------------------------|------|------|------|------|
| | | 1 | 2 | 4 | 8 | 12 |
| ON | DAY_PREC | 0.95 | 0.75 | 0.78 | 0.93 | 1.00 |
| | LST | 0.67 | 0.70 | 0.94 | 1.00 | 1.00 |
| | NDWI | 0.38 | 0.42 | 0.40 | 0.83 | 1.00 |
| SEASL | DAY_PREC | 0.70 | 0.63 | 0.77 | 0.77 | 0.86 |
| | LST | 0.61 | 0.59 | 0.77 | 0.88 | 1.00 |
| | NDWI | 0.20 | 0.29 | 0.18 | 0.28 | 0.29 |
| TOTAL | DAY_PREC | 0.58 | 0.63 | 0.63 | 0.81 | 0.95 |
| | LST | 0.70 | 0.75 | 0.73 | 0.65 | 0.64 |
| | NDWI | 0.20 | 0.25 | 0.27 | 0.28 | 0.07 |
| All models | | 0.55 | 0.56 | 0.61 | 0.71 | 0.76 |

Table 1.4: Significance of coefficients (%).

| | | Aggregation period (weeks) | | | | |
|------------|----------|----------------------------|----|----|---|----|
| | | 1 | 2 | 4 | 8 | 12 |
| ON | DAY_PREC | 7 | 5 | 3 | 0 | 0 |
| | LST | 3 | 3 | 0 | 0 | 0 |
| | NDWI | 0 | 2 | 0 | 0 | 0 |
| SEASL | DAY_PREC | 12 | 8 | 4 | 2 | 1 |
| | LST | 9 | 7 | 2 | 0 | 0 |
| | NDWI | 4 | 4 | 2 | 2 | 2 |
| TOTAL | DAY_PREC | 16 | 6 | 4 | 0 | 0 |
| | LST | 6 | 6 | 4 | 2 | 2 |
| | NDWI | 6 | 2 | 1 | 1 | 1 |
| All models | | 63 | 43 | 20 | 7 | 6 |

Table 1.5: Number of changes of coefficient sign.

| | | Aggregation period (weeks) | | | | |
|------------|----------|----------------------------|---------|---------|---------|---------|
| | | 1 | 2 | 4 | 8 | 12 |
| ON | DAY_PREC | 4860.36 | 4729.09 | 4733.10 | 4726.25 | 4733.78 |
| | LST | 4862.16 | 4744.36 | 4750.51 | 4748.47 | 4730.55 |
| | NDWI | 4438.35 | 4781.76 | 4786.31 | 4796.04 | 4801.20 |
| SEASL | DAY_PREC | 4865.77 | 4731.22 | 4734.31 | 4731.77 | 4724.15 |
| | LST | 4866.80 | 4749.80 | 4751.50 | 4751.80 | 4719.20 |
| | NDWI | 4438.79 | 4779.01 | 4783.42 | 4792.01 | 4780.82 |
| TOTAL | DAY_PREC | 763.36 | 618.80 | 634.67 | 637.49 | 651.26 |
| | LST | 764.49 | 656.40 | 624.28 | 610.83 | 623.34 |
| | NDWI | 688.14 | 700.33 | 700.12 | 695.43 | 702.88 |
| All models | | 3394.25 | 3387.86 | 3388.69 | 3387.79 | 3385.24 |

Table 1.6: Minimum values of model AIC.

| | | Aggregation period (weeks) | | | | |
|------------|----------|----------------------------|---------|---------|---------|---------|
| | | 1 | 2 | 4 | 8 | 12 |
| ON | DAY_PREC | 4912.25 | 4786.94 | 4778.19 | 4759.43 | 4759.40 |
| | LST | 4909.12 | 4785.25 | 4781.99 | 4771.03 | 4767.06 |
| | NDWI | 4777.65 | 4793.08 | 4797.79 | 4799.93 | 4801.62 |
| SEASL | DAY_PREC | 4912.70 | 4788.84 | 4786.97 | 4780.72 | 4774.71 |
| | LST | 4927.64 | 4807.04 | 4811.70 | 4812.60 | 4797.89 |
| | NDWI | 4777.19 | 4793.76 | 4798.80 | 4801.72 | 4792.06 |
| TOTAL | DAY_PREC | 809.38 | 699.33 | 703.82 | 694.19 | 697.41 |
| | LST | 804.86 | 691.83 | 692.36 | 678.22 | 682.99 |
| | NDWI | 805.29 | 712.60 | 716.84 | 698.18 | 707.00 |
| All models | | 3515.12 | 3428.74 | 3429.83 | 3421.78 | 3420.02 |

Table 1.7: Average values of model AIC.

1.A.2 Selection of the optimum 12 week time window using variation in AIC (Δ AIC)

The time window producing the lowest AIC was selected for inclusion in full models.

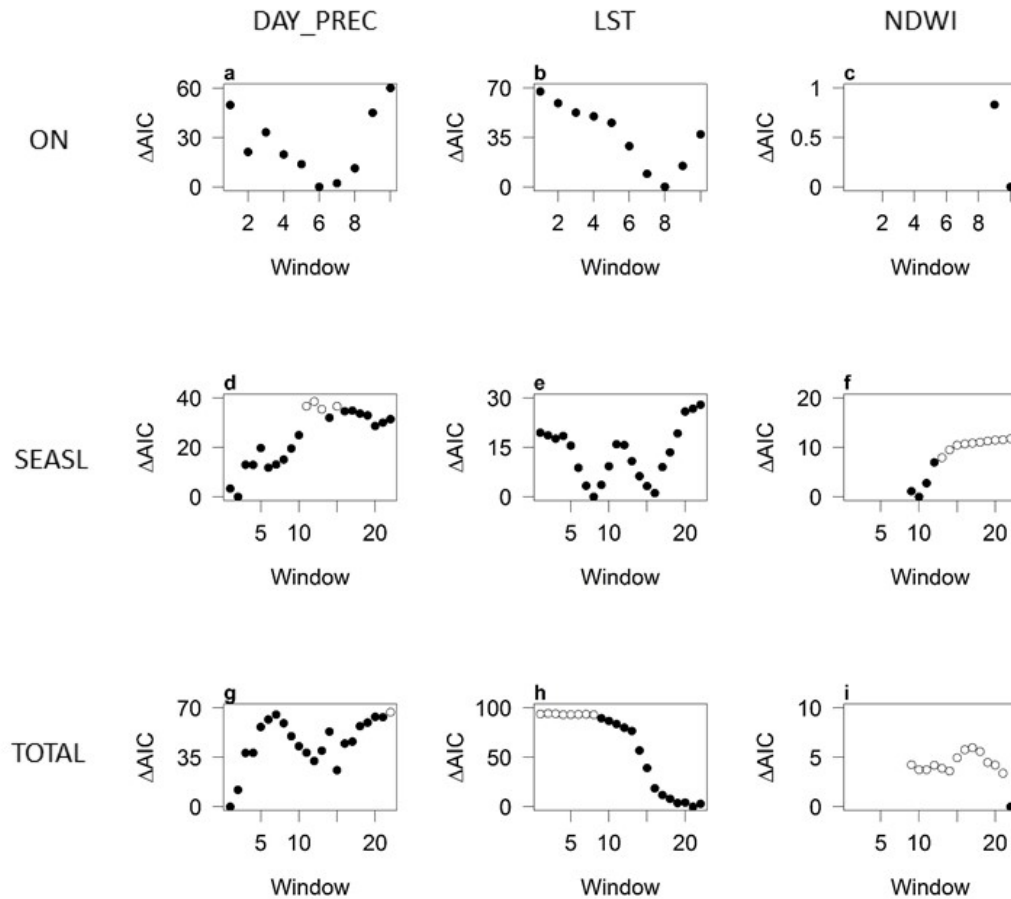


Figure 1.6: Variation in AIC (Δ AIC) of preliminary models using 12 week aggregation period. Comparisons are made between different temporal windows for DAY_PREC (left column), LST (central column) and NDWI (right column) as predictors of the start of mosquito season ON (upper row), season length SEASL (central row) and mosquito abundance TOTAL (lower row). Temporal windows are labelled according to the starting week, i.e. 1 (weeks 1-12), 2 (weeks 2-13), etc., to 21 (weeks 21-33). Filled dots indicate significant coefficients ($p < 0.05$).

1.A.3 Model selection tables

| Models | AIC | Δ AIC | wAIC | R^2 |
|--|---------|--------------|----------|-------|
| ON ~ LST ₈₋₁₉ + DAY_PREC ₆₋₁₇ + NDWI ₁₀₋₂₁ | 4687.93 | 0.00 | 0.962207 | 0.258 |
| ON ~ DIST_URBAN + LST ₈₋₁₉ + DAY_PREC ₆₋₁₇ + NDWI ₁₀₋₂₁ | 4695.29 | 7.36 | 0.024327 | 0.266 |
| ON ~ LST ₈₋₁₉ + NDWI ₁₀₋₂₁ | 4697.15 | 9.22 | 9.59E-03 | 0.240 |
| ON ~ DAY_PREC ₆₋₁₇ + NDWI ₁₀₋₂₁ | 4700.45 | 12.52 | 1.84E-03 | 0.241 |
| ON ~ DIST_RICE + LST ₈₋₁₉ + DAY_PREC ₆₋₁₇ + NDWI ₁₀₋₂₁ | 4701.11 | 13.17 | 1.33E-03 | 0.258 |
| ON ~ LST ₈₋₁₉ + DAY_PREC ₆₋₁₇ | 4703.46 | 15.52 | 4.10E-04 | 0.247 |
| ON ~ DIST_URBAN + DAY_PREC ₆₋₁₇ + NDWI ₁₀₋₂₁ | 4706.06 | 18.12 | 1.12E-04 | 0.252 |
| ON ~ DIST_URBAN + LST ₈₋₁₉ + NDWI ₁₀₋₂₁ | 4706.28 | 18.35 | 9.99E-05 | 0.245 |
| ON ~ DIST_RICE + LST ₈₋₁₉ + NDWI ₁₀₋₂₁ | 4708.90 | 20.97 | 2.69E-05 | 0.243 |
| ON ~ DIST_URBAN + LST ₈₋₁₉ + DAY_PREC ₆₋₁₇ | 4710.08 | 22.14 | 1.49E-05 | 0.257 |

Table 1.8: The ten “best” full models predicting start of the mosquito season (ON) - those with lowest AIC values obtained from model selection. For each model we report AIC, the difference in AIC with respect to the best model (Δ AIC), the Akaike weight (wAIC) and R^2 .

| Models | AIC | Δ AIC | wAIC | R^2 |
|---|---------|--------------|----------|-------|
| SEASL ~ LST ₈₋₁₉ + DAY_PREC ₂₋₁₃ + NDWI ₁₀₋₂₁ | 3380.28 | 0.00 | 0.767278 | 0.141 |
| SEASL ~ DAY_PREC ₂₋₁₃ + NDWI ₁₀₋₂₁ | 3382.85 | 2.57 | 0.212613 | 0.135 |
| SEASL ~ LST ₈₋₁₉ + NDWI ₁₀₋₂₁ | 3388.97 | 8.69 | 9.95E-03 | 0.114 |
| SEASL ~ DIST_URBAN + LST ₈₋₁₉ + DAY_PREC ₂₋₁₃ + NDWI ₁₀₋₂₁ | 3389.89 | 9.61 | 6.28E-03 | 0.153 |
| SEASL ~ DIST_URBAN + DAY_PREC ₂₋₁₃ + NDWI ₁₀₋₂₁ | 3391.68 | 11.39 | 2.57E-03 | 0.148 |
| SEASL ~ LST ₈₋₁₉ + DAY_PREC ₂₋₁₃ | 3394.00 | 13.72 | 8.05E-04 | 0.127 |
| SEASL ~ DIST_RICE + LST ₈₋₁₉ + DAY_PREC ₂₋₁₃ + NDWI ₁₀₋₂₁ | 3396.14 | 15.86 | 2.76E-04 | 0.143 |
| SEASL ~ DAY_PREC ₂₋₁₃ | 3398.28 | 17.99 | 9.49E-05 | 0.116 |
| SEASL ~ DIST_RICE + DAY_PREC ₂₋₁₃ + NDWI ₁₀₋₂₁ | 3399.48 | 19.20 | 5.2E-05 | 0.135 |
| SEASL ~ DIST_URBAN + LST ₈₋₁₉ + NDWI ₁₀₋₂₁ | 3400.02 | 19.73 | 3.98E-05 | 0.123 |

Table 1.9: The ten “best” full models predicting length of the mosquito season (SEASL) using early period data only - those with lowest AIC values obtained from model selection. For each model we report AIC, the difference in AIC with respect to the best model (Δ AIC), the Akaike weight (wAIC) and R^2 .

| Models | AIC | Δ AIC | wAIC | R^2 |
|---|---------|--------------|----------|-------|
| SEASL ~ NDWI ₁₀₋₂₁ + LST ₁₆₋₂₇ + DAY_PREC _{20.31} | 3374.32 | 0.00 | 0.283167 | 0.156 |
| SEASL ~ LST _{8.19} + NDWI ₁₀₋₂₁ + LST ₁₆₋₂₇ + DAY_PREC _{20.31} | 3374.41 | 0.09 | 0.27071 | 0.156 |
| SEASL ~ LST _{8.19} + DAY_PREC ₂₋₁₃ + NDWI ₁₀₋₂₁ + LST ₁₆₋₂₇ + DAY_PREC _{20.31} | 3376.08 | 1.76 | 0.117533 | 0.16 |
| SEASL ~ DAY_PREC ₂₋₁₃ + NDWI ₁₀₋₂₁ + LST ₁₆₋₂₇ + DAY_PREC _{20.31} | 3376.08 | 1.76 | 0.117364 | 0.16 |
| SEASL ~ LST _{8.19} + DAY_PREC ₂₋₁₃ + NDWI ₁₀₋₂₁ + LST ₁₆₋₂₇ | 3376.58 | 2.26 | 0.091288 | 0.15 |
| SEASL ~ DAY_PREC ₂₋₁₃ + NDWI ₁₀₋₂₁ + LST ₁₆₋₂₇ | 3377.55 | 3.23 | 0.056259 | 0.147 |
| SEASL ~ LST _{8.19} + NDWI ₁₀₋₂₁ + LST ₁₆₋₂₇ | 3378.36 | 4.04 | 0.03753 | 0.138 |
| SEASL ~ LST _{8.19} + DAY_PREC ₂₋₁₃ + NDWI ₁₀₋₂₁ | 3380.28 | 5.96 | 0.014372 | 0.141 |
| SEASL ~ DAY_PREC ₂₋₁₃ + NDWI ₁₀₋₂₁ | 3382.85 | 8.53 | 3.98E-03 | 0.135 |
| SEASL ~ NDWI ₁₀₋₂₁ + LST ₁₆₋₂₇ | 3383.76 | 9.44 | 2.52E-03 | 0.125 |

Table 1.10: of the ten “best” full models predicting season length (SEASL) using early and late period data - those with lowest AIC values obtained from model selection. For each model we report AIC, the difference in AIC with respect to the best model (Δ AIC), the Akaike weight (wAIC) and R^2 .

| Models | AIC | Δ AIC | wAIC | R^2 |
|--|--------|--------------|----------|-------|
| TOTAL ~ DAY_PREC ₁₋₁₂ | 634.19 | 0.00 | 0.79395 | 0.464 |
| TOTAL ~ DIST_RICE + DAY_PREC ₁₋₁₂ | 637.92 | 3.73 | 0.12304 | 0.488 |
| TOTAL ~ LST ₁₀₋₂₁ + DAY_PREC ₁₋₁₂ | 638.90 | 4.71 | 0.075289 | 0.467 |
| TOTAL ~ DIST_RICE + LST ₁₀₋₂₁ + DAY_PREC ₁₋₁₂ | 644.04 | 9.85 | 5.76E-03 | 0.489 |
| TOTAL ~ DIST_URBAN + DAY_PREC ₁₋₁₂ | 647.14 | 12.95 | 1.22E-03 | 0.473 |
| TOTAL ~ DIST_URBAN + DIST_RICE + DAY_PREC ₁₋₁₂ | 648.49 | 14.30 | 6.22E-04 | 0.501 |
| TOTAL ~ DIST_URBAN + LST ₁₀₋₂₁ + DAY_PREC ₁₋₁₂ | 652.21 | 18.03 | 9.67E-05 | 0.476 |
| TOTAL ~ DIST_URBAN + DIST_RICE + LST ₁₀₋₂₁ + DAY_PREC ₁₋₁₂ | 655.10 | 20.92 | 2.28E-05 | 0.501 |
| TOTAL ~ 1 | 692.45 | 58.27 | 1.77E-13 | 0.365 |
| TOTAL ~ LST ₁₀₋₂₁ | 693.21 | 59.03 | 1.21E-13 | 0.375 |

Table 1.11: The ten “best” full models predicting mosquito abundance (TOTAL) using early period data only - those with lowest AIC values obtained from model selection. For each model we report AIC, the difference in AIC with respect to the best model (Δ AIC), the Akaike weight (wAIC) and R^2 .

| Models | AIC | Δ AIC | wAIC | R^2 |
|---|--------|--------------|----------|-------|
| TOTAL ~ DAY_PREC ₁₋₁₂ + LST ₂₁₋₃₂ + NDWI ₂₂₋₃₃ | 592.74 | 0.00 | 0.494334 | 0.524 |
| TOTAL ~ DAY_PREC ₁₋₁₂ + LST ₂₁₋₃₂ | 593.42 | 0.68 | 0.351739 | 0.523 |
| TOTAL ~ DIST_RICE + DAY_PREC ₁₋₁₂ + LST ₂₁₋₃₂ + NDWI ₂₂₋₃₃ | 597.94 | 5.20 | 0.036789 | 0.543 |
| TOTAL ~ LST ₁₀₋₂₁ + DAY_PREC ₁₋₁₂ + LST ₂₁₋₃₂ + NDWI ₂₂₋₃₃ | 598.29 | 5.55 | 0.030896 | 0.526 |
| TOTAL ~ DAY_PREC ₁₋₁₂ + LST ₂₁₋₃₂ + DAY_PREC ₁₅₋₂₆ + NDWI ₂₂₋₃₃ | 598.88 | 6.14 | 0.022952 | 0.530 |
| TOTAL ~ LST ₁₀₋₂₁ + DAY_PREC ₁₋₁₂ + LST ₂₁₋₃₂ | 599.18 | 6.44 | 0.019778 | 0.525 |
| TOTAL ~ DAY_PREC ₁₋₁₂ + LST ₂₁₋₃₂ + DAY_PREC ₁₅₋₂₆ | 599.46 | 6.72 | 0.017162 | 0.529 |
| TOTAL ~ DIST_RICE + DAY_PREC ₁₋₁₂ + LST ₂₁₋₃₂ | 602.01 | 9.27 | 4.80E-03 | 0.539 |
| TOTAL ~ DIST_URBAN + DAY_PREC ₁₋₁₂ + LST ₂₁₋₃₂ + NDWI ₂₂₋₃₃ | 602.10 | 9.36 | 4.58E-03 | 0.537 |
| TOTAL ~ DIST_URBAN + DAY_PREC ₁₋₁₂ + LST ₂₁₋₃₂ | 602.48 | 9.73 | 3.80E-03 | 0.536 |

Table 1.12: The ten “best” full models predicting mosquito abundance (TOTAL) using early and late period data - those with lowest AIC values obtained from model selection. For each model we report AIC, the difference in AIC with respect to the best model (Δ AIC), the Akaike weight (wAIC) and R^2 .

2 The role of climatic and density dependent factors in shaping mosquito population dynamics: the case of *Culex pipiens* in Northwestern Italy

Giovanni Marini^{a,b}, Piero Poletti^{c,d}, Mario Giacobini^e, Andrea Pugliese^b, Stefano Merler^c, Roberto Rosà^a

a: Department of Biodiversity and Molecular Ecology, Research and Innovation Centre, Fondazione Edmund Mach, San Michele all'Adige (TN), Italy

b: Department of Mathematics, University of Trento, Trento, Italy

c: Bruno Kessler Foundation, Trento, Italy

d: Dondena Centre for Research on Social Dynamics and Public Policy, Department of Policy Analysis and Public Management, Università Commerciale L. Bocconi, Milan, Italy

e: Dipartimento di Scienze Veterinarie, Università degli Studi di Torino, Torino, Italy

PLoS ONE 2016; 11(4): e0154018

2.1 Introduction

Zoonotic pathogens are believed to cause about three quarters of human emerging infectious diseases, many of which (22%) are spread by vectors such as mosquitoes (Taylor *et al.*, 2001). One of the most recent emerging mosquito-borne diseases in the Western Hemisphere is West Nile Virus (WNV), a flavivirus first isolated in Uganda in 1937 (Smithburn *et al.*, 1940). It is maintained in a bird-mosquito transmission cycle primarily involving *Culex* species mosquitoes of which the *Cx. pipiens* complex is thought to be one of the most important in Europe (Zeller & Schuffenecker, 2004). In recent years, WNV has been circulating in many European countries, including Italy, causing hundreds of human cases (European Centre for Disease Prevention and Control, 2014). *Cx. pipiens* is also involved in the transmission of other human and animal pathogens such as Usutu virus (Gaibani *et al.*, 2013), whose first case outside Africa was recorded in Italy in 2009 (Pecorari *et al.*, 2009), St. Louis encephalitis (Reisen *et al.*, 2008), which caused about a hundred human cases in North America during the last decade (ArboNET, 2014), Rift Valley fever (Turell *et al.*, 2014), Sindbis virus (Lundstrom *et al.*, 2001), avian malaria and filarial worms (Farajollahi *et al.*, 2011).

The transmission of mosquito-borne diseases is largely driven by the abundance of the vector (Colborn *et al.*, 2013; Kilpatrick & Pape, 2013). Thus, rigorous surveillance of mosquito density and control programs based on its reduction represent key components of disease containment and prevention. Therefore, in order to design appropriate control strategies it is crucial to understand the population dynamics of existing vector populations and evaluate how it depends on environmental factors.

In the Piedmont region of Northwestern Italy, an extensive program of monitoring adult

mosquitoes has been implemented, since 1997, by the Municipality of Casale Monferato and the Istituto per le Piante da Legno e l'Ambiente (IPLA). The area is at risk for WNV, because of the presence of suitable vector and reservoir host populations, and the increasing numbers of human cases of WNV in adjacent areas (Calistri *et al.*, 2010; Monaco *et al.*, 2010). Previous studies ((Bisanzio *et al.*, 2011) and Chapter 1) analyzed spatio-temporal variations of mosquito species collected in the area, detecting a very high heterogeneity in the temporal pattern of mosquito population dynamics both inter- and intra-annually. In particular, looking at *Cx. pipiens* population dynamics from 2001 to 2011, we detected a huge variation in total yearly mosquito abundance among different traps, ranging from 40 to more than 4000 individuals captured per year (see Chapter 1). Also the timing of mosquito seasonal dynamics varied significantly among traps and years. Specifically, for around 90% of the observations the start of mosquito season varied from the beginning of June to mid-July, while the length of mosquito season varied from 45 to 90 days (see Section 1.3).

The main goal of our work is to describe and interpret in a robust theoretical framework the high heterogeneity observed among different seasons for *Cx. pipiens* population dynamics in Northwestern Italy, by explicitly taking into account some important eco-climatic and biological factors.

In Chapter 1 we found that precipitation and temperatures during the early period of the year (spring and early summer) might remarkably influence *Cx. pipiens* population dynamics. In particular, warm temperatures early in the year were associated with an earlier start of the mosquito season and increased season length, while early precipitation delayed the start, and shortened the length of the mosquito season, but increased total abundance. Indeed, temperature is well known to affect several aspects of *Cx. pipiens* life cycle including development and survival rates (Ciota *et al.*, 2014; Loetti *et al.*, 2011).

Density-dependence in mosquito population growth is another important factor in regulating *Cx. pipiens* population dynamics (Mulatti *et al.*, 2014). In fact, it has been found that inclusion of density-dependence, in combination with key environmental factors, significantly improves model prediction of *Cx. pipiens* population expansion in Northern Italy (Mulatti *et al.*, 2014). By using a statistical model, the authors found that the most significant environmental drivers of *Cx. pipiens* population dynamics were the daylight duration and temperature conditions in the 15 day period prior to sampling while precipitation and humidity had only a minor influence on *Cx. pipiens* growth rates.

Diapause is a common mechanism adopted by mosquitoes to survive through winter. While other mosquitoes, for instance *Aedes albopictus*, overwinter through diapausing eggs (Denlinger & Armbruster, 2014), in the case of *Cx. pipiens*, only adult females undergo diapause halting blood feeding and therefore host-seeking behavior (Denlinger & Armbruster, 2014). More specifically, immature stages develop into diapausing adults according to the photoperiod they are exposed to (Spielman & Wong, 1973).

We therefore develop a density-dependent stochastic model that describes temporal variations of *Cx. pipiens* population dynamics including the effect of temperature and daylight duration on the abundance of both adults and immature stages of *Cx. pipiens*. Mechanistic models include, with more or less details, the biological processes driving mosquito population dynamics and provide a suitable framework to investigate the main determinants of dynamical patterns beyond the observed conditions (Bolker, 2008). Several mechanistic models have been proposed to explore mosquito population dynamics especially for *Anopheles* species (e.g. (Arifin *et al.*, 2014; Beck-Johnson *et al.*, 2013; Ya-

mana & Eltahir, 2013; Cailly *et al.*, 2012)) and *Ae. albopictus* (e.g. (Erickson *et al.*, 2010; Poletti *et al.*, 2011; Tran *et al.*, 2013)) while, to the best of our knowledge, fewer attempts have been carried out for modelling *Cx.* species population dynamics (Gong *et al.*, 2011; Loncaric & Hackenberger, 2013; Morin & Comrie, 2010; Pawelek *et al.*, 2014). Mathematical models represent a powerful tool to investigate the role played by different climatic factors on vector population dynamics and to evaluate the effectiveness of alternative mosquito control strategies, as suggested by recent works on *Cx. quinquefasciatus* (Morin & Comrie, 2010), *Anopheles* species (Cailly *et al.*, 2012) and *Ae. albopictus* (Tran *et al.*, 2013). We follow a stochastic approach as deterministic models ignore the contribution of demographic stochasticity which is especially relevant when the vector population is low, for instance at the beginning and at the end of mosquito activity season. The proposed model explicitly accounts for the temporal variation of all immature stages, i.e. eggs, four larval instars and the pupal stage; it is assumed that the lengths of all mosquito life stages depend on temperature and that developmental rates of larval stages are density-dependent; finally, a diapausing mechanism is included in response to the photoperiod.

The effect of precipitation on survival and development of mosquito life stages is not explicitly accounted for, as, to the best of our knowledge, no reliable data on *Cx. pipiens* are present in literature for modeling and calibrating such mechanism. In the Results Section, we discuss correlation of density dependence with precipitation, which could indirectly enter the model in this way.

Finally, extensive model simulations have been carried out in order to better understand the role played by different eco-climatic factors in shaping the seasonal specific vector dynamics and to forecast, under various illustrative scenarios, likely changes in *Cx. pipiens* seasonal dynamics if temperature or density-dependent inputs would change.

2.2 Methods

2.2.1 Data

Cx. pipiens mosquitoes were collected on public land using CO₂ dry ice baited traps operated by Municipality of Casale Monferrato and the Istituto per le Piante da Legno e l'Ambiente (IPLA), under the regional program for mosquito surveillance, authorized by Regione Piemonte. The traps were dispersed over an area of 987 km² in the Eastern Piedmont Region in North West of Italy (see Figure 1.1 and (Bisanzio *et al.*, 2011) for more details). The study region is characterized by cold winters and warm summers (average temperature of 0.4°C and 24°C, respectively), abundant precipitation (600 mm/yr) and by a mostly agricultural landscape (86%) with few urban settlements (3%). This makes the area a highly suitable habitat for *Cx. pipiens*. Traps were set up one night every week, for a twenty-week period starting at the beginning of May and ending in mid-September, for 12 consecutive years (2000-2011). Traps were collected the following day and all catches counted, sexed and identified. Since some locations were not deployed every year (see Section 1.2 and (Bisanzio *et al.*, 2011)), we consider in this study only data coming from traps sampled for all the 12 consecutive years (i.e., 24 out of 44). Trapping conditions including positioning, battery and trap type, and CO₂ source (0.5 kg placed in traps each evening before a capture session) were identical among different sites and years. Moreover, during the study period, no relevant activities were performed to control *Cx. pipiens* and no substantial changes have been observed in the land use of

the area and in the human population size.

The biotype present in the eastern Piedmont area has not been definitively identified. However, given the relatively infrequent bites to humans in the considered area, in Chapter 1 we suggested *Cx. pipiens pipiens* - which is predominantly bird-feeding - as the more likely biotype. It is possible that human exposure to mosquito bites may be lower in more agricultural areas. However, a recent study conducted in a region of Northern Italy showed that *Cx. pipiens* prefer to take blood meals from avian hosts both in rural and urban areas (Rizzoli *et al.*, 2015). For a more detailed description of the study area and the trapping conditions, see (Bisanzio *et al.*, 2011) and Section 1.2.

2.2.2 Modelling mosquito dynamics

The model for the dynamics of the abundance of the vector in seven life stages of *Cx. pipiens*, namely eggs (E), 4 larval instars (L_1, L_2, L_3, L_4), pupae (P) and non-diapausing female adults (A), is based on the following system of equations:

$$M = \begin{cases} E' &= \frac{n_E}{d_A} A - (\mu_E + \tau_E) E \\ L_1' &= \tau_E E - \left(\tau_{L_1} + \mu_{L_1} \left(1 + \frac{L_1 + L_2 + L_3 + L_4}{K} \right) \right) L_1 \\ L_2' &= \tau_{L_1} L_1 - \left(\tau_{L_2} + \mu_{L_2} \left(1 + \frac{L_1 + L_2 + L_3 + L_4}{K} \right) \right) L_2 \\ L_3' &= \tau_{L_2} L_2 - \left(\tau_{L_3} + \mu_{L_3} \left(1 + \frac{L_1 + L_2 + L_3 + L_4}{K} \right) \right) L_3 \\ L_4' &= \tau_{L_3} L_3 - \left(\tau_{L_4} + \mu_{L_4} \left(1 + \frac{L_1 + L_2 + L_3 + L_4}{K} \right) \right) L_4 \\ P' &= \tau_{L_4} L_4 - (\tau_P + \mu_P) P \\ A' &= \frac{1}{2} \tau_P (1 - p) P - \beta \mu_A A - \chi_C \alpha A \\ C' &= \chi_C \alpha A \end{cases}$$

where $\tau_E, \tau_{L_1}, \tau_{L_2}, \tau_{L_3}, \tau_{L_4}, \tau_P$ are the temperature dependent developmental rates driving the transitions of vectors across the different life stages considered; $\mu_E, \mu_{L_1}, \mu_{L_2}, \mu_{L_3}, \mu_{L_4}, \mu_P, \mu_A$ are the temperature dependent death rates associated with the different stages; n_E is the number of eggs laid in one oviposition; d_A is the length of the gonotrophic cycle; K is the density-dependent scaling factor driving the carrying capacity for the larval stages; p is the probability (depending on daylight duration) that a fully developed pupa becomes a diapausing adult; β gauges the possible increase in adult mortality rate due to wild conditions with respect to lab conditions; α is the capture rate; χ_C is a function of the time defined equal to 1 when the trap is open and 0 otherwise; C represents the cumulative number of captured female adult mosquitoes. Since only female adult mosquitoes are explicitly considered in the model, the term $\frac{1}{2}$ in the equation for the adults accounts for the sex ratio (Vinogradova, 2011). Note, moreover, that diapausing females do not take blood meals before overwintering (Denlinger & Armbruster, 2014) and they cannot be captured with the considered traps. For this reason, only non-diapausing female adults are considered in the model.

Daily mean temperature and precipitation records for the period and study area considered were obtained from ARPA Piedmont (Arpa Piemonte, 2014). Daylight durations for the centroid of the study region during the considered period were obtained from the US Naval Observatory (United States Naval Meteorology and Oceanography Command, 2013).

We actually adopted a discrete-time stochastic version of model M , with time-step $\Delta t = 1$ day, in order to account for the stochastic nature of the processes. Precisely, the model is a Markov chain whose states represent the number (an integer) of individuals in all

developmental stages, and whose transition probabilities are built according to binomial distributions whose means are obtained from the rate in system M . Details are specified in Section 2.A. The seasonal dynamics of the mosquito population is simulated for 12 years, from April 1 (corresponding to approximately one month before the first capture session) to October 1. Since, to the best of our knowledge, no data are available on the overwintering of *Cx. pipiens*, we simulate each year y separately by initializing the system with $A_0(y) > 0$ non-diapausing adults.

2.2.3 Model calibration

Mortality and developmental rates across different vector life stages have been modeled as a function of temperature following the approach already proposed in (Poletti *et al.*, 2011) on the basis of data collected in (Loetti *et al.*, 2011; Eirayah & Abugroun, 1983). Specifically, we modeled the developmental period and the mortality rate associated with different vector stages at each temperature by fitting a suitable set of functions of the temperature T - comprising exponential and parabolic functions - to durations and rates measured at different specific temperatures through laboratory experiments (Loetti *et al.*, 2011; Eirayah & Abugroun, 1983). For the egg developmental rate, we used the same function proposed in (Loncaric & Hackenberger, 2013). The same technique was used to estimate the probability p for a developed pupa to become a diapausing adult as a function of daylight duration using the data presented in (Spielman & Wong, 1973). The uncertainty of parameters' estimates was obtained by using a bootstrap procedure similar to that used in (Poletti *et al.*, 2011; Chowell *et al.*, 2007). More details on the technique employed are presented in Section 2.A.

To the best of our knowledge, data on adult mortality at different temperature are not available for *Cx. pipiens*. Therefore, the mortality rate of adult female mosquitoes has been taken as the function of temperature suggested in (Ciota *et al.*, 2014), also allowing for an increase in adult mortality rate in the wild relatively to lab conditions. The average number of laid eggs n_E per oviposition and the duration of the gonotrophic cycle d_A in our simulations were chosen uniformly in the intervals [150,240] and [2,8] days respectively, according to results presented in (Becker *et al.*, 2010; Faraj *et al.*, 2006).

Free model parameters to be estimated are the capture rate α , the increase of adult death rate in the wild β , the density-dependent factor K , and the number of initial adults A_0 . More specifically, we assumed α and β to be equal among all years considered, while the value of K and A_0 could be year-specific.

Model predictions for the dynamics of mosquito population during a specific season depend on the free parameters $\theta = (\alpha, \beta, K, A_0)$ but are also influenced by the intrinsic stochasticity of simulations and by the uncertainty on parameters defining the transition rates used in the model (e.g. the developmental and mortality rates for different mosquito life-stages). By denoting the latter set as ω we define as $\lambda_{\{m,y\}}(\theta, \omega)$ the number of captures at month m and year y predicted by the model with parameters θ and ω . In order to estimate the free parameters by taking into account both the stochasticity of the process and the uncertainty on parameter estimates defined by ω , for each year y , we define the expected number of captures at month m associated with θ , denoted hereafter by $\tilde{\lambda}_{\{m,y\}}(\theta)$, as the $\lambda_{\{m,y\}}(\theta, \omega)$ corresponding to the simulation producing the median cumulative number of yearly captures among the simulations obtained by employing the same parameter set θ and varying ω .

The posterior distributions of the free parameters θ were explored by Markov chain

Monte Carlo (MCMC) sampling applied to the likelihood of observing the monthly number of trapped adults, averaged among the 24 considered sites. Assuming that for each month the number of observed trapped adult mosquitoes follows a Poisson distribution with mean obtained from the model, the likelihood of the observed data over the twelve simulated years has been defined as

$$L = \prod_{y=2000}^{2011} \prod_{m=1}^5 e^{-\tilde{\lambda}_{\{m,y\}}(\theta)} \frac{\tilde{\lambda}_{\{m,y\}}(\theta)^{n_{\{m,y\}}}}{n_{\{m,y\}}!}$$

where y runs over the different considered years, m runs over months, $n_{\{m,y\}}$ is the observed average number of trapped adults over the 24 sites at month m and year y as reported in (Bisanzio *et al.*, 2011) and in Chapter 1, and $\tilde{\lambda}_{\{m,y\}}(\theta)$ is the predicted number of captures at month m and year y simulated by the model with parameters $\theta = (\alpha, \beta, K, A_0)$.

The posterior distribution of θ was obtained by using random-walk Metropolis-Hastings sampling approach (Gilks *et al.*, 1996) and normal jump distributions. A total of 100,000 iterations were performed and a burn-in period of 5,000 steps was chosen. Convergence was checked by considering chains associated with different starting points in the parameter space and by visual inspection on the trace plots of chains.

Model predictions associated with the estimated posterior distributions of model parameters for the different seasons (from 2000 to 2011) were analyzed in terms of i) the weekly number of *Cx. pipiens* captured during the twenty-week survey period; ii) the total number of captured mosquitoes at the end of each year; iii) the highest weekly capture during each year; iv) the week at which the highest capture was observed; v) the start and the end of the mosquito season, defined as in Section 1.2 to be the weeks by which respectively 5% and 95% of the cumulative captures in the simulated season occurred; for clarity, from now on, we will denote these values by onset and offset; vi) the season length, defined as the number of weeks between the onset and the offset of the season (as in Section 1.2). The uncertainty surrounding model predictions is generated by both the variability of the estimated posterior distribution of free model parameters and the intrinsic stochasticity characterizing model simulation.

Finally, we applied the model to assess the influence of the temperature on the population dynamics. To this aim, we simulated each year y with 10 different temperature patterns $T(y, t)$ ranging from $\overline{T(y, t)} - 2.5^\circ$ to $\overline{T(y, t)} + 2.5^\circ$, where $\overline{T(y, t)}$ is the observed temporal pattern of temperature associated with year y . Following a similar approach, we investigated the role played by the larval carrying capacity by simulating each year y with different density-dependent factors K , ranging from $0.5 \cdot \overline{K(y)}$ to $1.5 \cdot \overline{K(y)}$, where $\overline{K(y)}$ is the estimated density-dependent factor for year y .

2.3 Results and discussion

The proposed model can well reproduce the number of weekly captures of adult mosquitoes reported between May and September for all the twelve years of observation (2000-2011). In particular, more than 90% of the weekly trap records lie within the 2.5-97.5% quantile of model predictions. The model shows the ability of reproducing both the strong seasonality characterizing the adult population dynamics within different years and the high heterogeneity observed among different seasons in terms of mosquito density (see Figure 2.1).

In agreement with collected data (see Figure 2.2c), our results show that the average cumulative number of trapped adults can substantially change between seasons, ranging from 510 (2.5-97.5% quantile predictions: 100-1887) in 2003 to 2425 (2.5-97.5% quantile predictions: 1194-4677) in 2000.

The highest capture is predicted to occur, on average, between the 27th and 31st week of the year (corresponding to the month of July) in good agreement with observed values (see Figure 2.2b). On the opposite, the predictions on the maximum number of trapped adults in a single capture session during the entire season are extremely variable among different simulations and do not accurately reproduce observed values. This field measure is highly sensitive and reflects stochastic variations driven by site-specific factors such as rain and wind condition of the day. Indeed, strong wind and rainfalls might alter *Cx. pipiens* dispersal and host-seeking behavior, possibly reducing the probability of being captured. In fact, data collected show that captures of two consecutive trapping sessions can be remarkably different (with differences sometimes of an order of magnitude). In order to smooth the inherent variability in captures, we computed, for each trap, the 3-point moving average of weekly captures. The distribution of the maxima of moving averages, for each year, is shown in Figure 2.2d; it can be seen that the variability in model predictions is consistent (though a bit lower) with the observed variability among traps. In addition, years characterized by higher maximum number of trapped adults within a single capture are associated with higher peaks in model predictions.

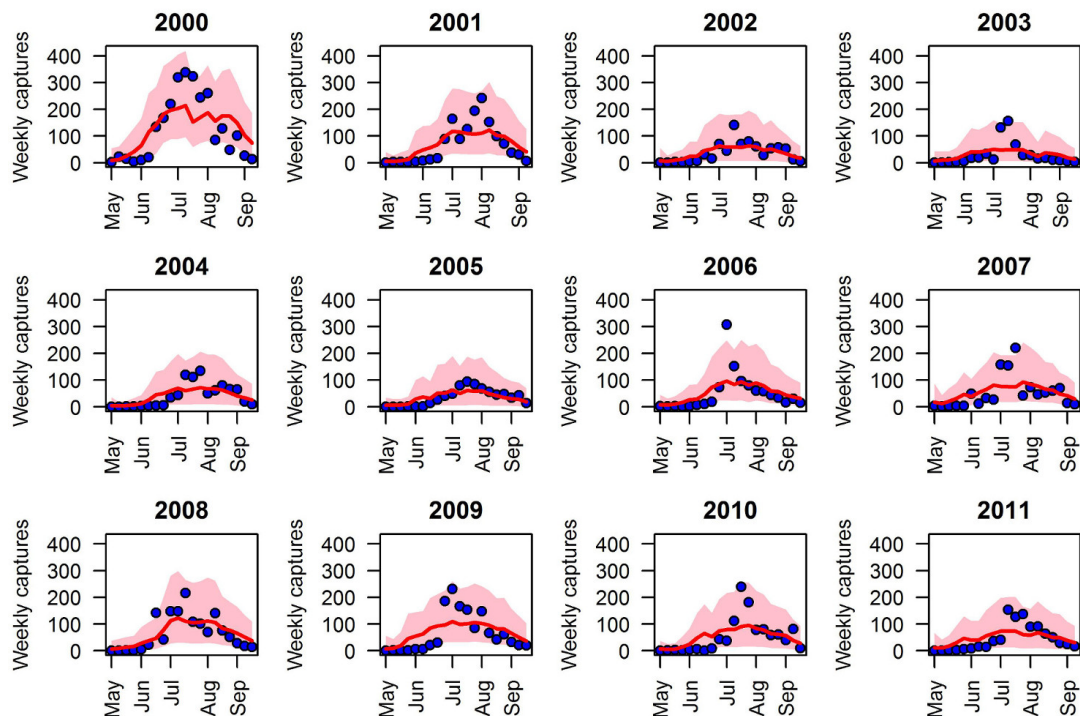


Figure 2.1: **Model fit.** Average number of weekly captured *Cx. pipiens* during the twenty-week survey period observed in Piedmont region from 2000 to 2011 (blue points) and predicted by model simulation based on the estimated posterior distribution of free parameters (median in red, pink region defines 2.5-97.5% quantile predictions).

The 2.5-97.5% quantile of the predicted offsets are between the 34th and 37th week (mid-

August - mid-September) in each year, like the observed captures (see Figure 2.2a). The predicted onsets are on the average between the 21st and the 23rd week (end of May - beginning of June), a few weeks earlier than what observed (median values between 24th-27th week, June).

In Chapter 1 we found that the starting time of the mosquito season (onset) was negatively correlated with the average temperature of weeks 8-19 (i.e., higher temperatures hasten the onset), and found that season length was positively correlated with mean temperature of weeks 16-27. Our analysis confirms such results suggesting that the median predicted onset, which defines the starting time of the season, is negatively correlated ($y = 27.81 - 0.52x$, $p\text{-value} < 0.01$) with the average temperature recorded between mid-February and the beginning of May, which ranges from 9.6°C in 2004 to 13.4°C in 2007. This is in line with the observed faster development of immature stages associated with higher temperatures.

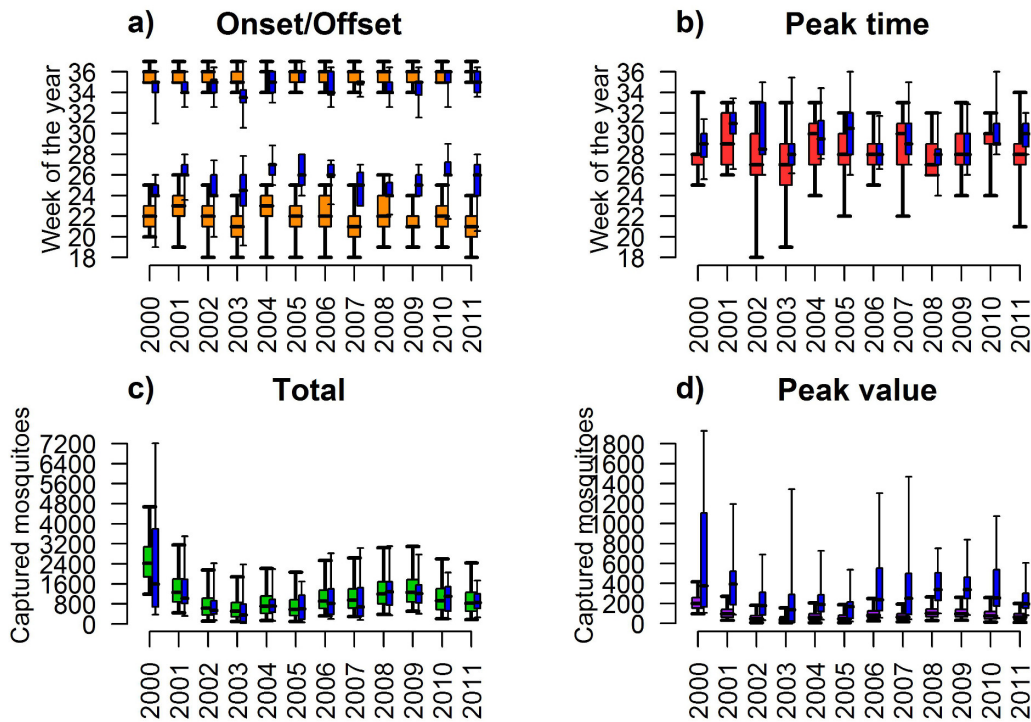


Figure 2.2: **Annual synthetic indexes.** Boxplot (2.5%, 25%, 75% and 97.5% quantile and median) of predicted onset (lower orange bars in panel a) and offset (higher orange bars in panel a), defined as the week of the year when the 5% and the 95% of the cumulative captures are reached respectively; week of the year associated with peak (highest) capture (red bars in panel b); total annual captures, i.e. the sum of the 20 weekly captures (green bars in panel c); peak capture, i.e. maximum number of trapped adults in a single capture session (purple bars in panel d). Blue boxplots represent the distributions of the observed site-specific values. Distributions of the observed peak capture were obtained by computing the maximum of 3-point moving average of weekly captures.

Furthermore, the median predicted season length is positively correlated ($y = -2.00 + 0.80x$, $p\text{-value} < 0.01$) with the average temperature recorded between mid-April and the end of June, which varies from 18.5°C in 2004 to 21.5°C in 2003.

The model accounts for the observed heterogeneous dynamics of the mosquito population

among different seasons thanks to the explicit inclusion of two seasonal factors. The first one is the dependence of developmental and mortality rates of different mosquito stages on temperature. The second one is represented by the assumption of a year specific density-dependent factor for larval stages, which may reflect possible differences in the availability of breeding sites in different years.

The estimated posterior distribution of the initial number of adults (namely A_0) spans a wide range, between approximately 1 and 1,000 in each season (see Figure 2.3a), with negligible differences among different years.

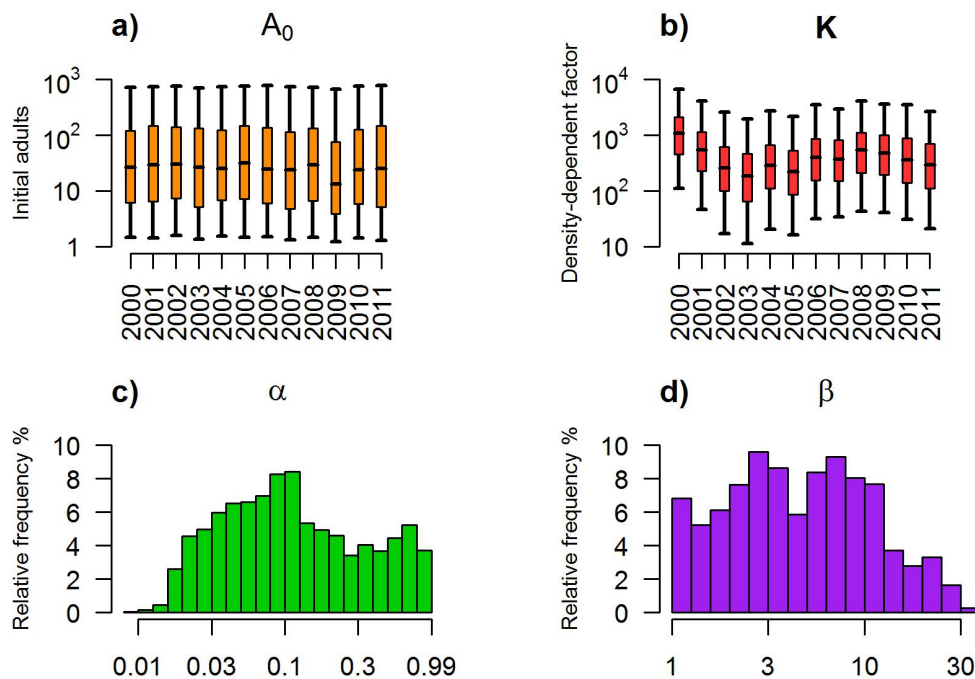


Figure 2.3: **Estimated parameters.** Boxplot (2.5%, 25%, 75% and 97.5% quantile and median) of posterior distributions of parameters A_0 (panel a) and K (panel b) estimated in different years. Histograms of relative frequencies for posterior distributions of parameters α (panel c) and β (panel d).

Conversely, estimated posterior distributions of the density-dependent factor are remarkably different among years (see Figure 2.3b). In Chapter 1 we found that *Cx. pipiens* population size in different years is positively correlated with the number of days of precipitation in the first three months of the year. Following the same approach presented in the previous chapter, we explored possible correlations between the estimated density-dependent factors and the number of rainy days among different temporal windows. We considered 22 temporal windows built by grouping periods of 12 consecutive weeks, starting from the first week of the year (weeks 1-12) and ending with weeks 22-33. For each window, number of days of precipitation was summed. We found that the median value of the estimated density-dependent factor is positively correlated ($y = -380.54 + 32.14x$, $p\text{-value} < 0.01$) with the number of rainy days in weeks 13-24 (end of March - mid-June), which encompass partially the first half of the simulated period. Therefore, although the model does not take precipitation explicitly into account, our

analysis highlights its likely influence on mosquito population dynamics. This positive correlation is biologically reasonable as more rain can create more breeding sites and therefore increase the carrying capacity of larval stages, which is proportional to the density-dependent factor.

The capture rate α is estimated to be on average 11.35% (10% median, see Figure 2.3c) in good agreement with values published in (Simpson *et al.*, 2009), where it was estimated to be 10.8% through a field experiment carried out using bird-baited traps placed outdoors in an open lawn area. However, it is worth noting that this experiment was carried out in a setting different from our study area, using different traps. Furthermore, the posterior distribution we obtained for α is very wide, and thus does not give strong support to any specific estimate.

The estimated posterior distribution of β , the increase in adult mortality rate in the wild relatively to lab conditions, is also very wide (95% CI 1.09,23.98, see Figure 2.3d) with an estimated average of 4.61 (4.52 median). This result is in good agreement to what has been observed in (Niebylski & Craig, 1994) for *Ae. albopictus*, for which adult survival is four times lower in the wild relatively to the survival observed under laboratory conditions.

Undoubtedly, independent estimates on a subset of our free parameters would allow providing more robust estimates of these specific biological quantities. However, the MCMC approach represents a suitable statistical technique to handle uncertainties about parameters, as it takes into account all possible parameters' configurations compliant with patterns observed in the data. Simulations were run also by assuming seasonal dependent α and β . The two different modeling assumptions result in qualitatively similar predictions about the abundance of the mosquito among different years (see Section 2.A). These results strongly suggest that the more parsimonious model with seasonal independent α and β should be preferred as associated with a lower value of the Deviance Information Criterion (DIC) (Spiegelhalter *et al.*, 2002).

Temperature plays a crucial role in shaping the population dynamics of *Cx. pipiens*. As already suggested by the statistical correlations presented above, higher temperatures can both hasten the occurrence of high adult densities (see Fig 2.4b) and lengthen the breeding season (see Figure 2.4a). On the other hand, either too high or too low temperatures during the season might be responsible of a noticeable decrease in peak mosquito abundance (see Figure 2.4c) as a consequence of the balance between two opposite phenomena; high temperatures increase mosquito mortality rates (especially in adults) while low temperatures can strongly reduce the developmental rates of mosquito immature stages. Our results suggest that a reduction of the temperature of 1.5°C decreases both the highest mosquito density during the season and the cumulative number of captured mosquitoes of about 20%, while in the extreme case of a decrease of 2.5°C a reduction of 40% of the total abundance and peak values is expected (see Figure 2.4d). This confirms that the inability of immature stages to cope with low temperature is a critical factor in shaping *Cx. pipiens* habitat suitability.

Hotter seasons might also reduce the maximal abundance of adult mosquitoes (about -25% for the +2.5°C scenario) but produce only negligible effects on the overall number of captured adults during the whole season. This apparent contradiction can be explained by the observation that higher temperatures increase mosquito populations during spring and decrease them during summer (see Figure 2.11).

On the other hand, changes in the larval carrying capacity produce proportional effects on mosquito abundance during the whole breeding season. For instance, our analysis

shows that a 30% reduction of the density-dependent factor K causes a decrease of about the same percentage on both the highest capture and the cumulative number of captured adult mosquitoes (see Figures 2.5c and 2.5d). Lower values of the larval carrying capacity prevent the development of a large number of larvae into pupae and, in turn, into adults. Consequently, under favorable conditions, an increase of this parameter increases the population size. However, the length of the breeding season and the time of the highest capture are not significantly influenced by the magnitude of larval carrying capacity. Indeed, the occurrence of favorable conditions, such as the increase of the developmental rates of aquatic stages into adults, is mainly driven by temperature. These results suggest that the carrying capacity, which correlates with the abundance of spring precipitations and is possibly linked to the availability of mosquito breeding sites, affects the reproduction number, and thus the growth rate, of the population but it does not influence the developmental and the mortality rates at the beginning and at the end of the season, which are the main determinants of season length.

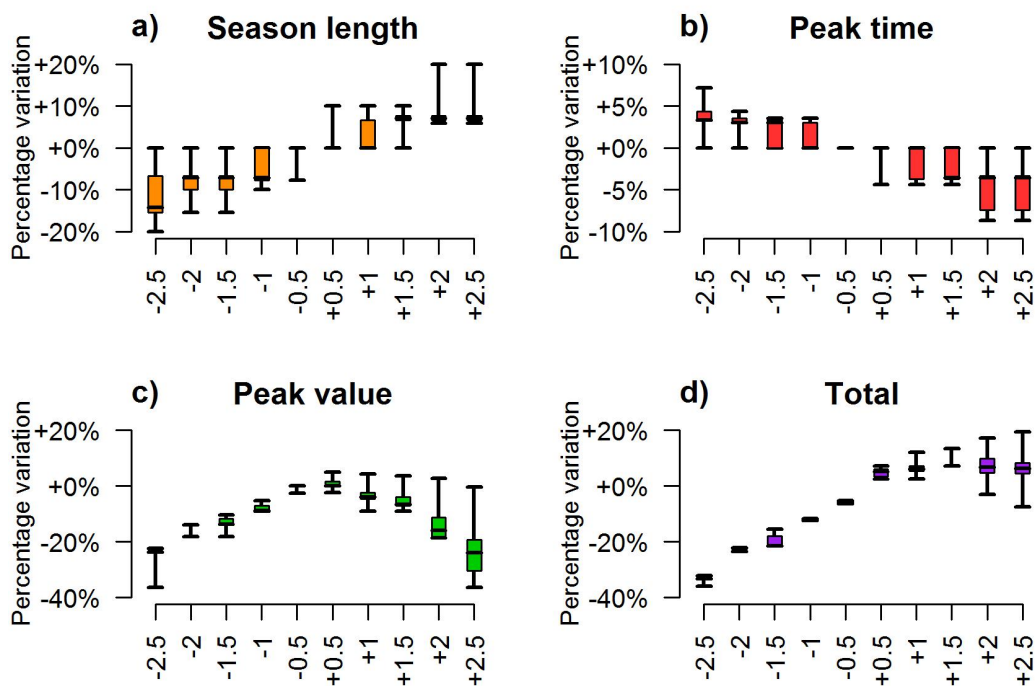


Figure 2.4: **Effect of temperature variations on *Cx. pipiens*.** Boxplots (2.5%, 25%, 75% and 97.5% quantile and median) of predicted annual synthetic indexes associated with different temperature inputs (x -axis, from -2.5°C to $+2.5^{\circ}\text{C}$ with respect to actual records). Panel (a) shows the effect on the duration of the breeding season, defined as the difference between the week of the year when the 95% and the 5% of the cumulative captures are reached; panels (b) and (c) show respectively the effect on the timing and the value of the peak capture; panel (d) shows the effect on the total annual captures.

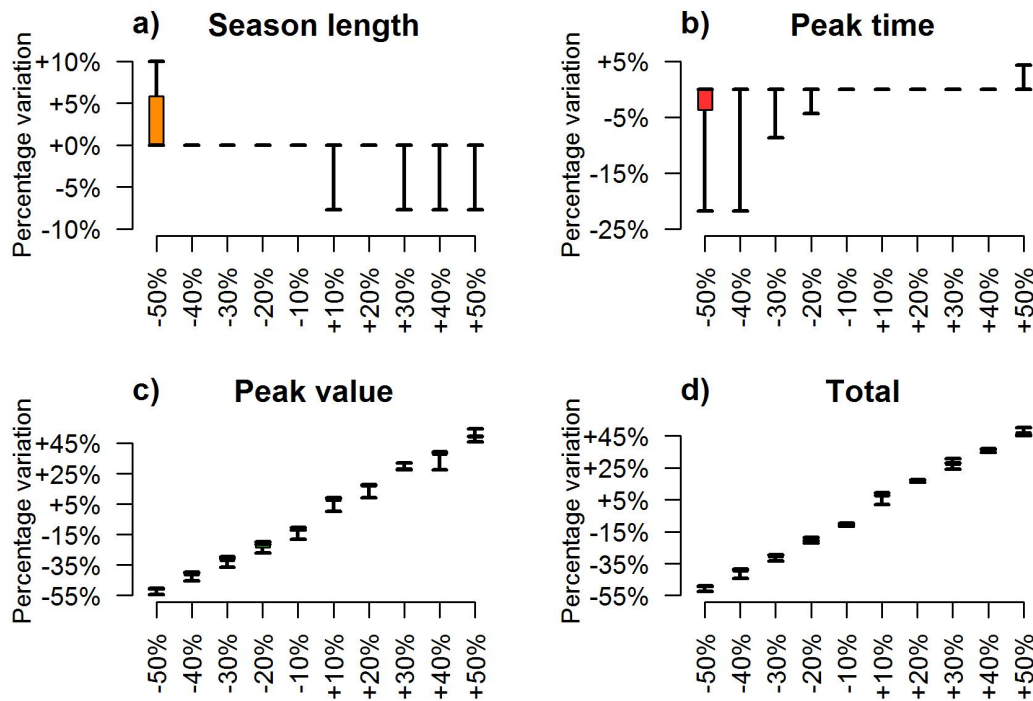


Figure 2.5: **Effects of density-dependent factor variations on *Cx. pipiens*.** Boxplots (2.5%, 25%, 75% and 97.5% quantile and median) of predicted annual synthetic indexes associated with different values of K (x-axis, from -50% to +50% with respect to fitted values). Panel (a) shows the effect on the duration of the breeding season; panels (b) and (c) show respectively the effect on the timing and the value of the peak capture; panel (d) shows the effect on the total annual captures.

2.4 Conclusions

In this paper, we investigated which are the main drivers of the observed high heterogeneity characterizing the *Cx. pipiens* population among different seasons in Northwestern Italy.

We found that inter-seasonal variability is determined by two main drivers: i) differences in larval carrying capacities, which in turn might depend on the cumulative number of rainy days from end of March to mid-June, potentially correlated to the availability of breeding sites, and ii) differences in average temperatures, which affect both developmental and survival rates.

Overall, this work provides useful indications about the dynamics of *Cx. pipiens* during a typical breeding season. Our results suggest that variations in the number of rainy days and temperature, like those observed in the study period, may give rise to substantially different seasonal mosquito abundances and provide interesting insights on how possible climatic changes could affect the future density of this vector in Piedmont and in similar areas.

The data also exhibit a large degree of spatial heterogeneity, as trap captures vary in abundance and temporal patterns. Investigating these patterns would require detailed information on habitat utilization and related mosquito movement, which are not available and are beyond the scope of the present work. Instead, data coming from different

traps were aggregated in order to strengthen the investigation of seasonal heterogeneity, by reducing the influence of climatic condition characterizing single specific days.

In this work, *Cx. pipiens* population dynamics has been modeled on the basis of the empirical relations found in laboratory experiments between demographic and developmental rates of the various life stages (eggs, larvae, pupae, female adults) on temperature and, as far as diapause is concerned, photoperiod. Use of statistical methods on population data have allowed us to use the model with field data, elucidating the role of density-dependence. Availability of data on survival and fertility rates in the wild - where for instance *Cx. pipiens* adults are expected to seek refuge from heat in summer and from cold in winter - could allow for refinements of the model and for using it beyond a single season.

Acknowledgments

The fieldwork was realized by the technicians of the "Istituto per le Piante da Legno e l'Ambiente" operative center of Casale Monferrato. The authors especially acknowledge Andrea Mosca for useful discussions on fieldwork data. We thank the anonymous reviewers for their helpful and constructive comments that contributed to improve the final version of the manuscript.

2.A Supporting Information

2.A.1 Materials and methods

Model calibration

In this chapter, we have introduced a model to investigate the vital dynamics of *Cx. pipiens* during a typical breeding season by considering temperature-dependent mortality and developmental rates both for immature and mature/adult stages of mosquito and by assuming that the diapause rate depends on daylight duration.

The lengths of the developmental periods associated to different mosquito life stages (i.e. for any $s \in S = \{L_1, L_2, L_3, L_4, P\}$) at different temperatures were calibrated according the following procedure. Given the length of developmental period L_s for temperatures $T \in \mathcal{T} = \{7^\circ C, 10^\circ C, 15^\circ C, 20^\circ C, 25^\circ C, 30^\circ C, 33^\circ C\}$ as observed in (Loetti *et al.*, 2011), we assume that $L_s(T) = f_s(T; \omega) + \varepsilon_T$ where $f_s(T; \omega)$ is a parametric function of the temperature T (ω indicates the set of free model parameters defining f) in a suitable set of functions, comprising exponential, parabolic and logistic functions, and ε_T is a random sample of a 0 mean normal distribution with unknown variance σ^2 . For each considered life stage, we calibrate the function $f_s(T; \omega)$ by minimizing the square error ψ between predicted and observed length of the period which is defined as $\psi = \sum_{T \in \mathcal{T}} (L_s(T) - f_s(T; \omega))^2$. Uncertainty of estimated parameters (i.e., ω) was computed following a bootstrap procedure similar to the one adopted in (Chowell *et al.*, 2007; Poletti *et al.*, 2011). In particular, we simulated 100 different $\{L_s(T)\}_{T \in \mathcal{T}}$ by adding an error sampled from a normal distributed $N(0, \sigma^2)$ to the best interpolation $f_s(T; \tilde{\omega})$ where the variance σ^2 was taken as the average of the estimated residuals associated to the best interpolation of the model i.e., the average of the quadratic differences $(L_s(T) - f_s(T; \tilde{\omega}))^2$. Finally, for each simulated $\{L_s(T)\}_{T \in \mathcal{T}}$ we repeated the optimization procedure described above. Obtained estimates of $l_s(T; \omega)$ were used to compute the rate of development as $\tau_s(T; \omega) = 1/l_s(T; \omega)$. The same technique was applied to estimate the probability p for a fully developed pupa to become a diapausing adult as function of the daylight duration using the data presented in (Spielman & Wong, 1973) and to estimate the mortality rates of all immature stages as functions of temperature.

However, since mortality data for different mosquito life-stages were available as survival probabilities, an additional step was required to estimate the associated mortality rates. The survival probability for different mosquito life-stages observed in (Loetti *et al.*, 2011; Eirayah & Abugroun, 1983) was obtained in lab conditions by following a cohort of n individuals until all of them would either die or develop in the subsequent life stage. In our analysis, we estimate the mortality rates associated to eggs, different larval instars and pupae by maximizing the likelihood of observing the number of surviving individuals k obtained in the lab experiments at fixed temperatures, given the initial number of individuals n and a known developmental rate for each temperature and each mosquito life-stage.

For instance, specializing model M to the case of a cohort of pupae kept at a fixed temperature \bar{T} and starting at time 0 with the initial value $n(\bar{T})$, one sees that, following the approach described in (Kemeny & Snell, 1976), the probability that a pupa will eventually develop into an adult (instead of dying) is $p(\bar{T}) = \frac{\tau_P(\bar{T})}{\mu_P(\bar{T}) + \tau_P(\bar{T})}$, so that the number of pupae developing into adults will be a binomial of parameters $n(\bar{T})$ and $p(\bar{T})$.

A simple computation shows then that the maximum likelihood estimate of $\mu_P(\bar{T})$ is

$$\mu_P(\bar{T}) = \frac{\tau_P(\bar{T})(1-p)}{p} \text{ with } p = k/n.$$

Estimates of developmental times and mortality rates at different temperatures and the diapause rate associated with different daylight durations are presented in Figure 2.6. Our analysis suggests that at higher temperatures, survival probabilities of all stages decrease and developmental times shorten, while longer daylight durations reduce the probability that a fully developed pupa becomes a diapausing adult. In the case of eggs and pupae, lower temperatures (i.e., below 15°C) can increase the death rate as well.

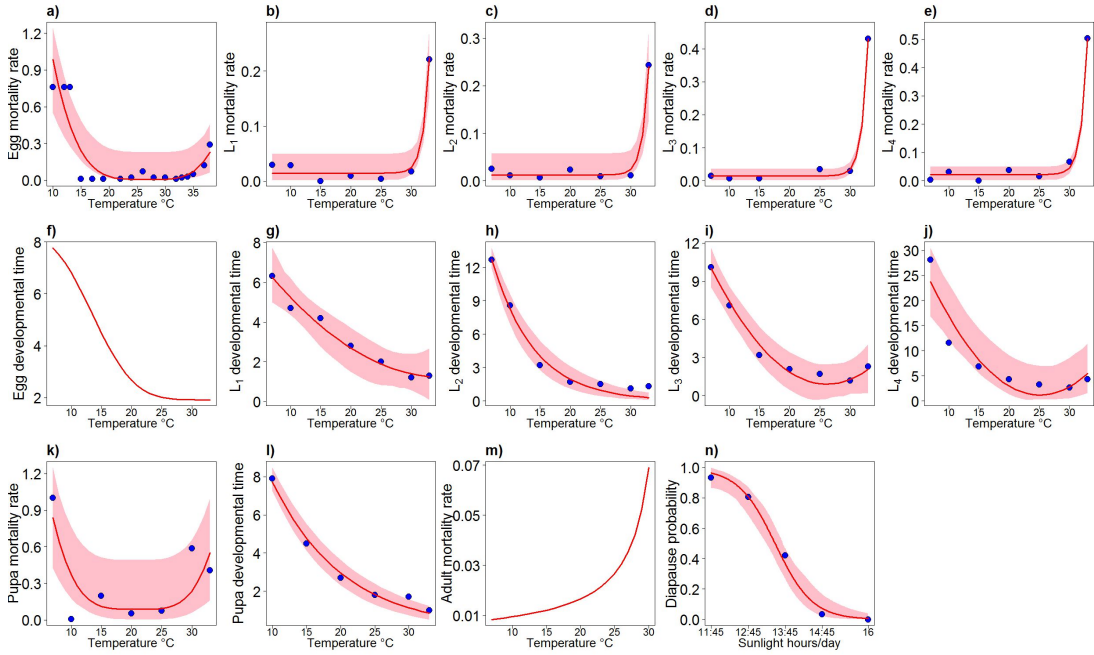


Figure 2.6: **Mortality and developmental rates at different temperatures.** Panels (a-l): estimated mortality rates (day^{-1}) and developmental times (in days) at different temperatures for the eggs, the larval stages and the pupal stage (i.e., E, L_1, L_2, L_3, L_4, P). Panel (m): adult mortality rate (day^{-1}) modeled as function of the temperature as published in (Ciota *et al.*, 2014). Panel (n): probability of a fully developed pupa to become a diapausing adult, modeled as function of the daylight duration. Data from experiments are shown with blue dots, red lines represent the best interpolation and pink region defines the 95% credible intervals obtained through the bootstrap procedure described in the text.

According to our model formulation, predictions of mosquito dynamics during each breeding season are driven by daylight duration (see Figure 2.7) and by observed seasonal temperatures (see Figure 2.8). The average temperature recorded from April 1 to September 30 during all the study period ranges from 19.3°C (2002) to 21.3°C (2003).

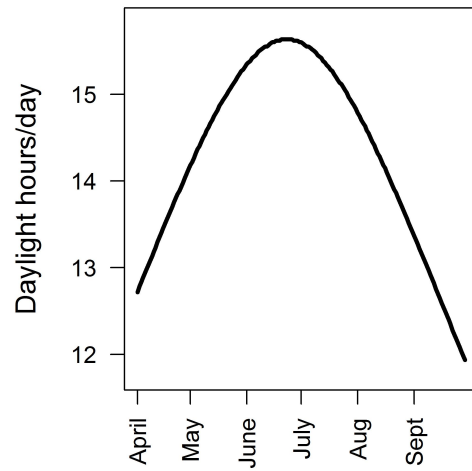


Figure 2.7: **Daylight duration during a typical breeding season.** Daylight duration defined as the difference between the time of the sunset and the time of the sunrise (in hours) from April 1 to September 30 obtained from the United States Naval Meteorology and Oceanography Command (2013).

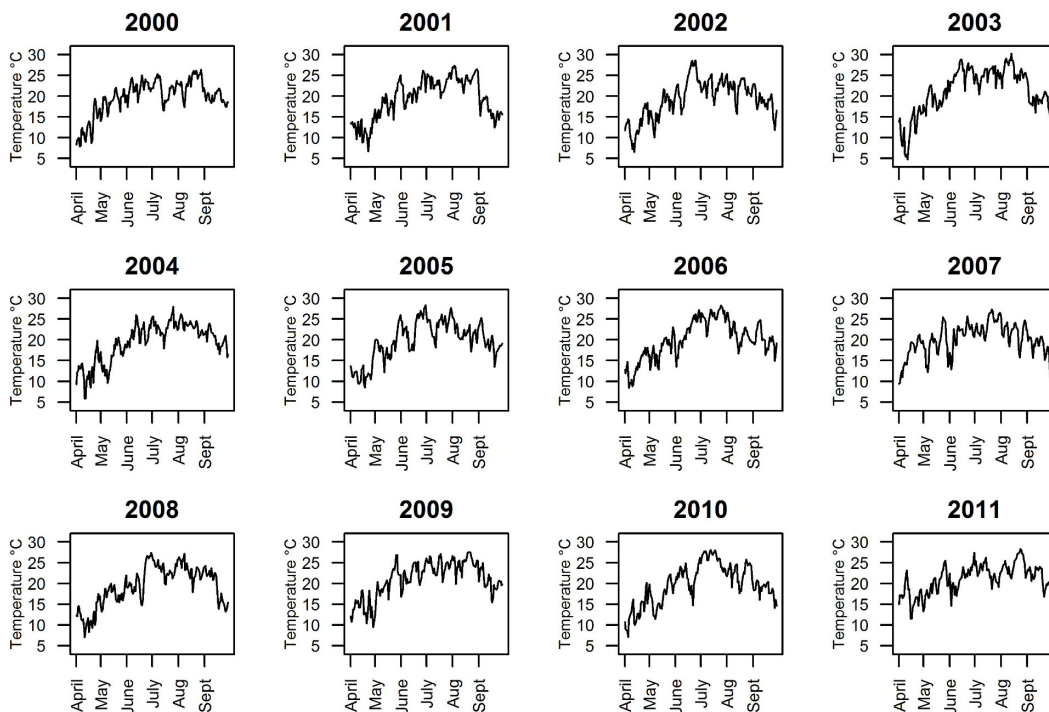


Figure 2.8: **Temperature patterns among different breeding seasons.** Air mean temperatures recorded from April 1 to September 30 during the twelve years considered in the model.

Transition probabilities

Different life-stages of mosquito population are updated from time t to time $t + 1$ according to the following procedure. Given a specific population class c we denote the set of possible transition from the class c to other population classes as \mathbb{T} where each specific transition $\tau \in \mathbb{T}$ occurs at a specific rate r_τ . In our simulations at each time step t the number of individuals k leaving the class c is drawn from a binomial distribution $\mathcal{B}(n, \sum_{\tau \in \mathbb{T}} r_\tau \Delta T)$, where n is the number of individuals in class c at time t . The number of individuals following the different transitions $\tilde{\tau} \in \mathbb{T}$ will then be computed from a multinomial with parameters k and $r_{\tilde{\tau}} / \sum_{\tau \in \mathbb{T}} r_\tau$.

For instance, in case of eggs, at each time t eggs can either develop into larval instar at a rate τ_E or die at a rate μ_E . If E is the number of eggs at time t , first one will obtain the total number of exits, k , by drawing a number from a binomial distribution $\mathcal{B}(E, \mu_E \Delta t + \tau_E \Delta t)$; then the number of new larvae will be drawn from a binomial of parameters k and $\tau_E / (\mu_E + \tau_E)$ (correspondingly the number of dead eggs will be a binomial of parameters k and $\mu_E / (\mu_E + \tau_E)$).

2.A.2 Additional results

The proposed model is able to well reproduce the annual variations and the high heterogeneity observed in mosquito population dynamics among different breeding seasons (see Figure 2.9).

Figure 2.10 shows the effects of the perturbation of the observed temperature on *Cx. pipiens* dynamics. In particular, for the hotter scenarios the abundance of mosquito population in spring is higher and begins to increase sooner while mosquito abundance during the summer is much lower.

The effects due to the perturbation of the density-dependent factor are shown in Figure 2.11. Obtained results suggest that an increase [decrease] of this parameter causes an upper [lower] shift of the entire curve.

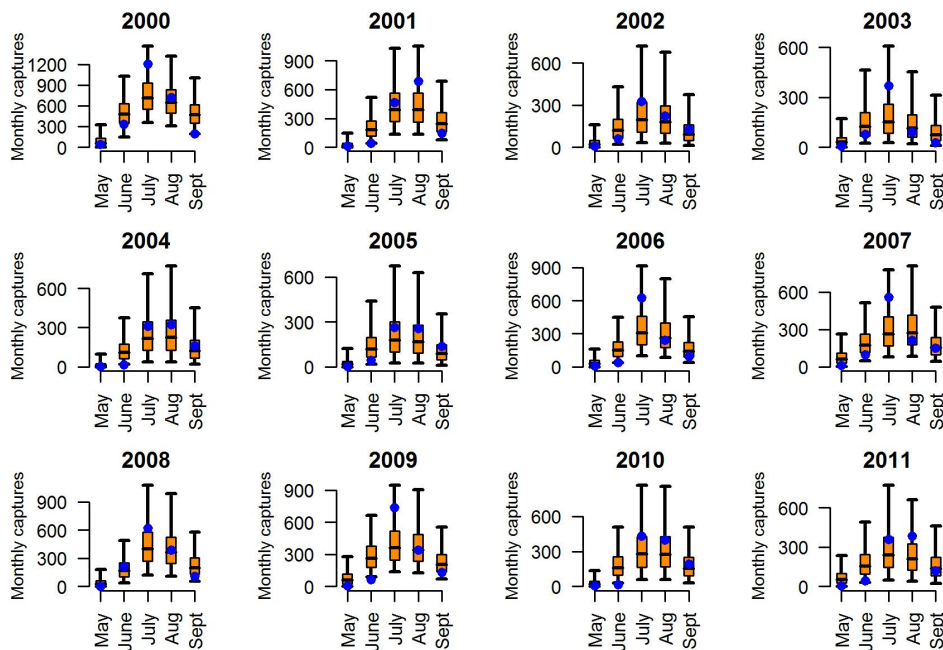


Figure 2.9: **Model fit for monthly captures.** Boxplots (2.5%, 25%, 75% and 97.5% quantile and median) of fitted posterior distribution for *Cx. pipiens* monthly captures. Blue dots represent the observed values.

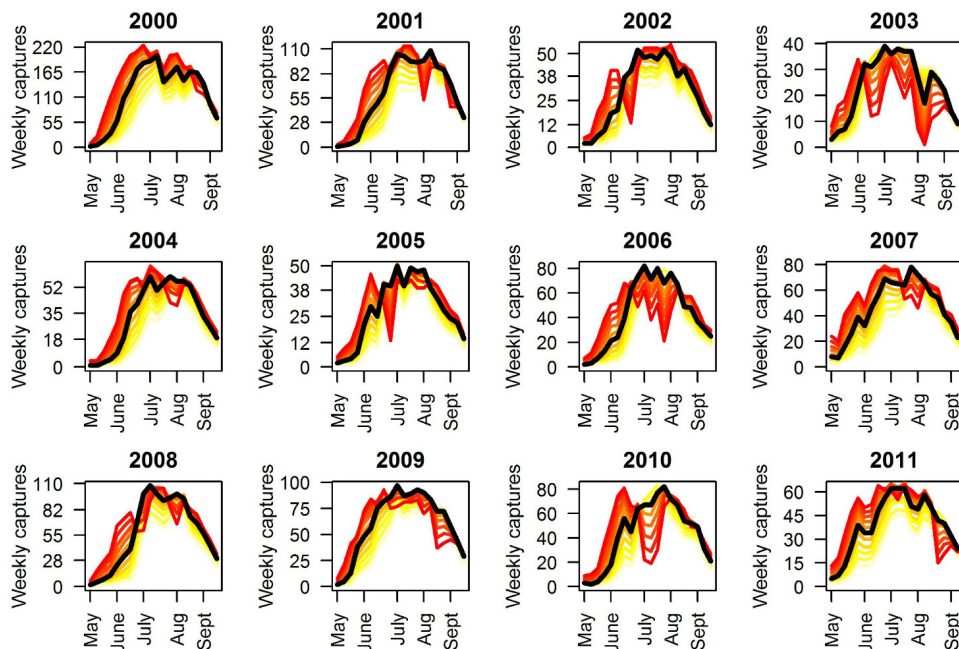


Figure 2.10: **Effect of temperature on *Cx. pipiens*.** Predicted captures (median values) for 10 different scenarios obtained varying daily temperature T from $T - 2.5^\circ\text{C}$ (light yellow) to $T + 2.5^\circ\text{C}$ (dark red) with a step of 0.5°C . Black lines represent the median of the fit using daily temperature T , as shown in Figure 2.1.

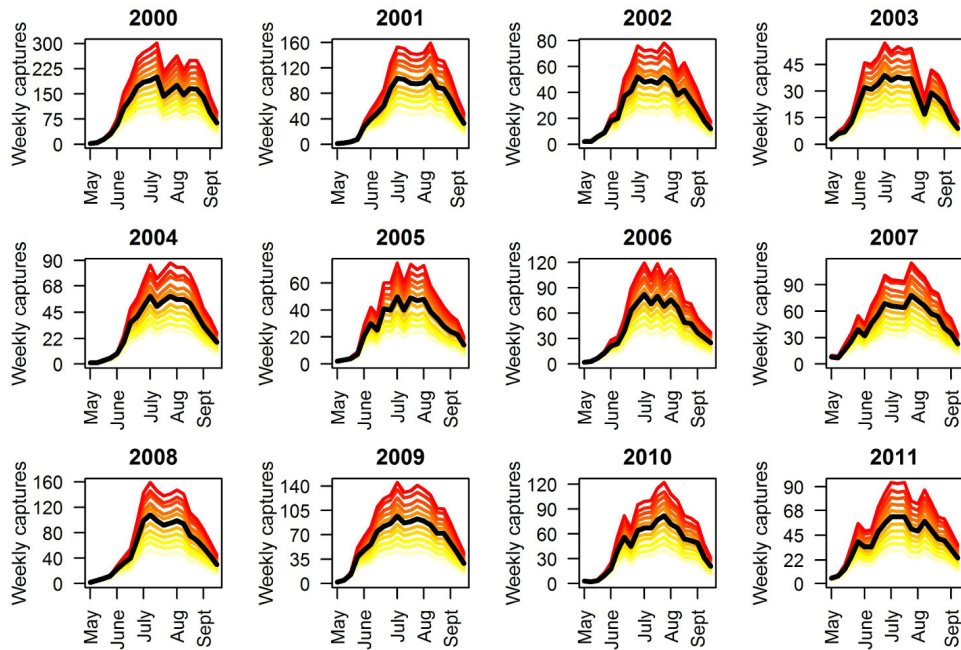


Figure 2.11: **Effect of the carrying capacity on *Cx. pipiens*.** Predicted captures (median values) for 10 different scenarios obtained changing the density-dependent factor K from $K \cdot 0.5$ (light yellow) to $K \cdot 1.5$ (dark red) with a step of $K \cdot 0.1$. Black lines represent the median of the fit, using K , as shown in Figure 2.1.

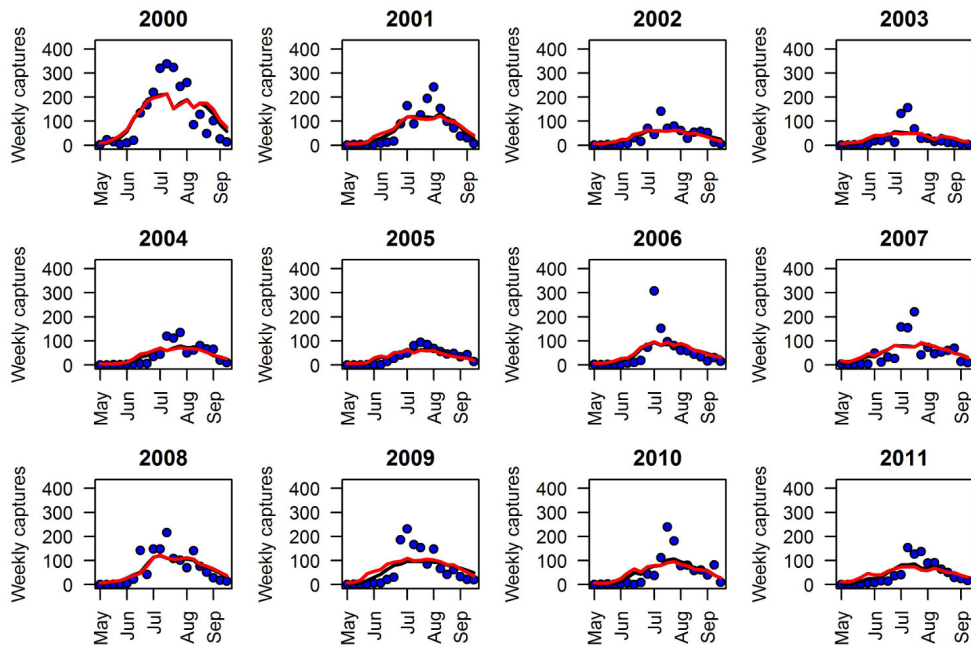


Figure 2.12: **Comparison of fit.** Average number of weekly captured *Cx. pipiens* during the twenty-week survey period observed in Piedmont region from 2000 to 2011 (blue points) and median predictions by model simulation based on the estimated posterior distribution of free parameters by assuming α and β to be seasonal independent (red line) and by considering different α and β for each considered year (black line).

3 The effect of interspecific competition on the temporal dynamics of *Aedes albopictus* and *Culex pipiens*

Giovanni Marini^{a,b}, Giorgio Guzzetta^c, Frederic Baldacchino^a, Daniele Arnoldi^a, Fabrizio Montarsi^d, Gioia Capelli^d, Annapaola Rizzoli^a, Stefano Merler^c, Roberto Rosá^a

a: Department of Biodiversity and Molecular Ecology, Research and Innovation Centre, Fondazione Edmund Mach, San Michele all'Adige (TN), Italy

b: Department of Mathematics, University of Trento, Trento, Italy

c: Bruno Kessler Foundation, Trento, Italy

d: Laboratory of Parasitology, Istituto Zooprofilattico Sperimentale delle Venezie, Padova, Italy

Parasites & Vectors 2017; 10: 102

3.1 Introduction

A fundamental concept in ecology is that competition for limited resources can take place between individuals of the same species, i.e. intraspecific competition, or between individuals of different species, i.e. interspecific competition. In interspecific competition, individuals of different species compete for the same resource (e.g. food or living space) therefore limiting resource availability for the other species. Such competition could lead to the exclusion of the weaker species but also to coexistence equilibrium via different mechanisms, such as differential resource use and spatial or temporal variations in habitat conditions (Tilman, 1982; Leishman *et al.*, 2014).

Among mosquito species, interspecific competition plays a key role in structuring the community at the larval stage in water-filled containers (Juliano, 2009). In Europe, *Aedes albopictus* and *Culex pipiens* are two of the most widely spread mosquito species (Farajollahi *et al.*, 2011; Schaffner *et al.*, 2013; Medlock *et al.*, 2012). While *Cx. pipiens* is indigenous, *Ae. albopictus* is native to Asia and was introduced in several European countries at the end of the last century (Schaffner *et al.*, 2013); since then, *Ae. albopictus* rapidly spread in urban and suburban environments, occupying a habitat already exploited by *Cx. pipiens*. These two species are vectors of many arboviruses. *Ae. albopictus* can transmit dengue, chikungunya, Zika and West Nile viruses (Chouin-Carneiro *et al.*, 2016-03-03; Fortuna *et al.*, 2015; Paupy *et al.*, 2009; Vega-Rua *et al.*, 2013, 2014; Wong *et al.*, 2013), while *Cx. pipiens* is the most important vector of West Nile virus in Europe (Zeller & Schuffenecker, 2004). Local vector abundance, which drives the pathogen-transmission dynamics (Colborn *et al.*, 2013; Kilpatrick & Pape, 2013), might be influenced by interspecific competition. Furthermore, larval competition might have indirect effects on epidemiological risks by altering mosquito-virus interactions in adult females (Alto & Lounibos, 2013); in particular, different *Aedes* mosquitoes (including *Ae. albopictus*, *Ae. aegypti* and *Ae. triseriatus*) bred in conditions of nutritional

stress imposed by the interspecific competition were more susceptible to infection and more able to transmit various pathogens such as dengue, Sindbis and LaCrosse viruses (Alto *et al.*, 2005, 2008; Bevins, 2007). In addition, adult survival, and consequently the length of infectious period for infected females (i.e. their vectorial capacity), might be influenced by interspecific interactions occurred at the larval stage (Costanzo *et al.*, 2011; Reiskind & Lounibos, 2009). Therefore, competition between different mosquito species, especially at the aquatic stages, may have important consequences on the epidemiology of mosquito-borne infections and their potential control strategies (Juliano, 2009).

Previous laboratory studies show that *Ae. albopictus* is a strong competitor against other species; *Ae. albopictus* larvae have been shown to negatively affect the growth and survival of larvae from other mosquito species bred in the same site, including *Ae. aegypti* (Murrell & Juliano, 2008; O'Neal & Juliano, 2013), *Ae. japonicus* (Armistead *et al.*, 2008), *Ae. triseriatus* (Livdahl & Willey, 1991; Novak *et al.*, 1993), *Ae. koreicus* (F. Balacchino, unpublished observations) and *Culex pipiens* (Carrieri *et al.*, 2003; Costanzo *et al.*, 2005). *Ae. albopictus* larvae, on the other hand, were substantially unaffected by the presence of *Cx. pipiens* larvae. This asymmetric interspecific competition has been attributed to a higher efficiency of *Ae. albopictus* in converting food to biomass (Carrieri *et al.*, 2003). The strength of competition effects has been shown to depend on food resource types (Costanzo *et al.*, 2011) and temperature, with a maximal effect on *Cx. pipiens* larval mortality observed at temperatures above 25°C (Carrieri *et al.*, 2003).

In nature, *Ae. albopictus* and *Cx. pipiens* can exploit common water-filled containers as larval habitats. Generally, *Ae. albopictus* prefers ovipositing in small natural and artificial containers, while *Cx. pipiens* prefers larger water bodies (Carrieri *et al.*, 2003; Becker *et al.*, 2010). However, these two species can share medium size containers. In northern Italy, during entomological surveys in the summer of 1996 and 1997, *Ae. albopictus* and *Cx. pipiens* were detected together in 67% of larval habitats, especially drums, buckets, catch basins and tires (Carrieri *et al.*, 2003). Thus, coexistence between these two species could be shaped by both interspecific competition and niche differentiation involving temporal and spatial factors (Leisnham *et al.*, 2014; Juliano, 2009).

The temporal patterns of local populations of *Ae. albopictus* and *Cx. pipiens* in Northern Italy can be highly variable depending on climate and landscape ((Roiz *et al.*, 2011) and Chapter 1), but generally *Cx. pipiens* is active earlier than *Ae. albopictus* (Carrieri *et al.*, 2003; Verna, 2015). *Cx. pipiens* larvae appear in springtime and peak in July, while *Ae. albopictus* larvae appear several weeks after *Cx. pipiens* and peak in September (Carrieri *et al.*, 2003). Different temporal profiles may be driven by different life history strategies and patterns of survival, oviposition and egg hatching under variable environments (Carrieri *et al.*, 2003; Costanzo *et al.*, 2005). In the case of *Cx. pipiens*, only adult females undergo diapause, and shortening photoperiods induce diapause in a growing number of newly emerged adult females (Denlinger & Armbruster, 2014; Spielman & Wong, 1973). Early in the mosquito breeding season, overwintering females of *Cx. pipiens* begin to lay eggs on water surface. In contrast, *Ae. albopictus* overwinters as diapausing eggs (Becker *et al.*, 2010), which hatch several weeks after *Cx. pipiens* eggs; then newly emerged *Ae. albopictus* females lay eggs above the water line, and hatching is induced by submergence after precipitations. This asynchrony in hatching between the two species allows *Cx. pipiens* larvae to develop in the absence of *Ae. albopictus* and provides to *Cx. pipiens* a refuge from competition (Costanzo *et al.*, 2005) early in the season. Furthermore, high temperatures observed in summertime decrease *Cx. pipiens* adult survival (Ciota *et al.*, 2014; Ruybal *et al.*, 2016), while *Ae. albopictus* is better

adapted to warmer conditions (Delatte *et al.*, 2009). Therefore, environmental conditions can create a “temporal niche” effect, allowing a shift in breeding seasons of the two species. Nonetheless, the “temporal niche” effect is not always sufficient to explain the observed temporal profiles of competing mosquito species (Leisnham *et al.*, 2014).

Disentangling the ecological mechanisms that drive mosquito population dynamics might be difficult with a simple statistical analysis of the observed capture pattern. However, mechanistic models incorporate a range of biological processes that drive mosquito population dynamics. Therefore, they are more suitable to investigate the main determinants of dynamical patterns, such as the effect of temporal niches and interspecific competition. Several mechanistic models have been used to describe the population dynamics of single mosquito species, including *Ae. albopictus* (Erickson *et al.*, 2010; Poletti *et al.*, 2011; Tran *et al.*, 2013) and *Cx. pipiens* (Gong *et al.*, 2011; Loncaric & Hackenberger, 2013). In this study, we describe and interpret, in a robust mathematical framework, observed differences in temporal patterns of *Ae. albopictus* and *Cx. pipiens*, aiming to disentangle the contribution of the temporal niche effect and interspecific competition on their population dynamics.

To this aim, we develop a mathematical model that describes temporal variations of population dynamics of both species and allows for interspecific interactions at the larval stages, as previously evaluated in laboratory conditions. To the best of our knowledge, this is one of the first efforts to assess the impact of *Ae. albopictus* and *Cx. pipiens* ecological interactions in natural conditions.

3.2 Methods

3.2.1 Study area and mosquito data

The study was carried out in the provinces of Belluno (46°08'2"N, 12°12'56"E) and Trento (46°04'00"N, 11°07'00"E), Northern Italy. This mountainous area covers a large part of the Dolomites and the Southern Alps. The climate is temperate-oceanic with four main areas: sub-Mediterranean (close to Lake Garda with mild winters), subcontinental (the main valleys with more severe winters), continental (the alpine valleys) and alpine (the areas above the tree line) (Neteler *et al.*, 2011).

We performed entomological surveillance of several mosquito species in the provinces of Trento and Belluno during 2014 and 2015. Mosquitoes were collected using Biogents Sentinel traps (BG trap; Biogents AG, Regensburg, Germany) baited with commercial lures from the same producer and CO₂ from dry ice. The BG trap has been demonstrated to collect a great variety of species and is efficient for both *Ae. albopictus* and *Cx. pipiens* when baited with CO₂, especially in an urban environment (Luhken *et al.*, 2014). Trapping locations were chosen within three municipalities of Belluno province (Belluno, Feltre, Santa Giustina) and three of Trento province (Borgo Valsugana, Riva del Garda, Trento) (see Figure 3.1).

A total of 73 BG traps were located within urban and peri-urban areas at altitudes ranging from 75m to about 640m above sea level. As recommended by the manufacturer, traps were placed in shaded positions sheltered from wind and rainfall. In 2014, 39 traps were positioned while in 2015 the number of traps was reduced to 34; 28 trapping sites were shared among the two years. BG traps ran for 24h, approximately every two weeks, from the end of April to the beginning of November. Mosquito sex and species were identified using taxonomic keys (Severini *et al.*, 2009). The number of capture ses-

sions differed from trap to trap because of logistic reasons, ranging from a minimum of 8 to a maximum of 15.

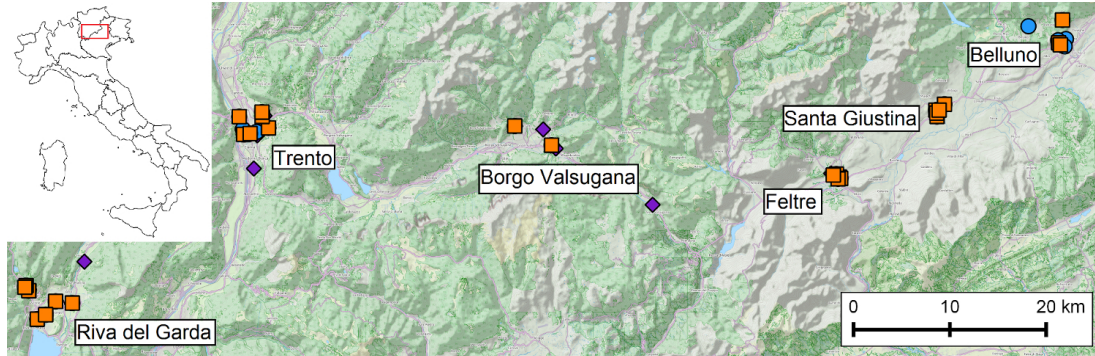


Figure 3.1: **Map of the study area.** Selected trap locations (purple diamonds: 2014; blue circles: 2015; orange squares: both years).

3.2.2 Delay analysis

We analysed temporal shifts between pairs of time series of captured female adults of *Cx. pipiens* and *Ae. albopictus*, observed at the same site and year. To this aim, we estimate the time lag T between the two time series at which the cross-correlation function ρ reaches its maximum (see (Jacovitti & Scarano, 1993) for details):

$$T = \arg \max_{\tau} \rho_{XY}(\tau) = \arg \max_{\tau} \sum_{t=1}^m X(t)Y(t + \tau).$$

More specifically, $\rho_{XY}(\tau)$ is the cross-correlation function, X and Y are the time series for *Cx. pipiens* and *Ae. albopictus* respectively, m is the length of the time series expressed in weeks. T measures the time lag (in weeks) between the two time series and it is labelled throughout the chapter as the “interspecific delay” between *Ae. albopictus* and *Cx. pipiens* temporal dynamics.

3.2.3 Environmental data

Original land surface temperature (LST) data were obtained from the MODIS version 5 LST products MOD11A1 and MYD11A1 (Wan, 2014). We used the average daily temperature and a spatial resolution of 250 m (Metz *et al.*, 2014).

There was a striking difference in recorded temperatures between the two considered years (see Figures 3.2a and 3.2b); specifically, for the 28 sites sampled in both years, the difference in the average daily temperature during summer months (July to September) between 2014 and 2015 (Figure 3.2c) is close to 5°C, with average observed temperatures of 20.6°C and 25.5°C for the two years respectively. For comparison, the average temperature for this period computed over years 2004-2013 is about 21.9°C (Meteotrentino, 2016), so that the two years of study represent the extremes of a wide range of possible temperature scenarios. Daylight lengths for the centroid of the study region during the considered period were obtained from the US Naval Observatory (United States Naval Meteorology and Oceanography Command, 2013).

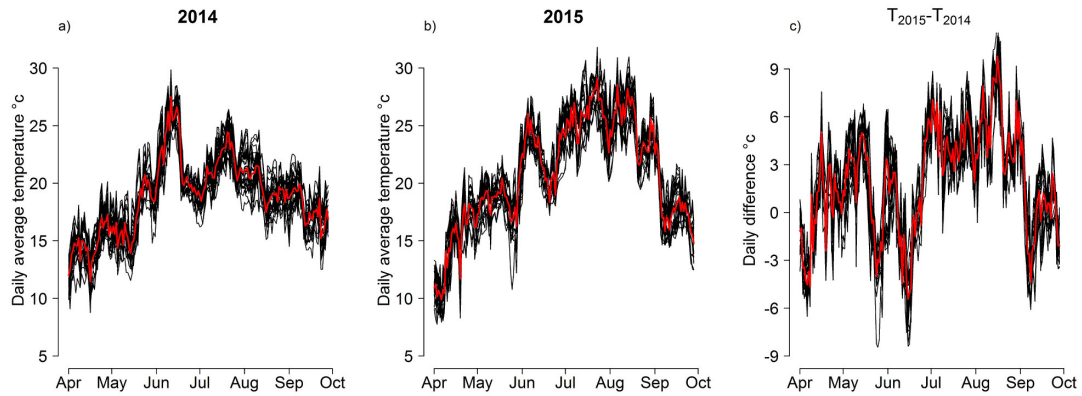


Figure 3.2: **Daily temperature at study sites.** (a) Daily average temperatures from the 39 trap locations in 2014 (black lines) and average across all sites (red line); (b) daily average temperatures from the 34 trap locations in 2015 (black lines) and average across all sites (red line); (c) daily average temperature difference between 2015 and 2014 from the 28 sites represented in both years.

3.2.4 Population model

We developed a mathematical model of the abundance of the two vector species based on the *Ae. albopictus* model proposed in (Poletti *et al.*, 2011; Guzzetta *et al.*, 2016a,b) and on the *Cx. pipiens* model proposed in Chapter 2. The original models account for the population dynamics of each species by considering temperature-dependent development and mortality rates and intraspecific larval density dependent factors; the model for *Cx. pipiens* also includes a photoperiod-dependent diapause rate for pupae. Here, we include the effect of asymmetric interspecific competition, by adding a mortality term for *Cx. pipiens* larvae proportional to the larval abundance of *Ae. albopictus* in the same site. Given that the effect of interspecific competition weakens for temperatures below 20°C (Carrieri *et al.*, 2003), we set the competition coefficient to zero for average daily temperatures less than 15°C, and to a constant value, estimated via model calibration, otherwise.

The model was calibrated using a Markov chain Monte Carlo (MCMC) approach applied to the Poisson likelihood of observing the empirical capture data, given the model-predicted abundance. The model has five free model parameters: two daily capture rates of adult mosquitoes (one for *Ae. albopictus* and one for *Cx. pipiens*); an intraspecific larval density dependent factor for each species, representing the availability of suitable breeding sites and food resources at a given site; and the interspecific larval competition coefficient, which increases the mortality of *Cx. pipiens* larvae proportionally to the abundance of *Ae. albopictus* larvae. The posterior distribution of parameters was obtained by a random-walk Metropolis-Hastings sampling (Gilks *et al.*, 1996), using uniform prior distributions and normal jumps.

To evaluate the hypothesis of interspecific competition, we calibrated a simplified model representing the assumption of independent populations, where the larval competition coefficient was fixed to zero. We then compared the goodness of fit of the two models (with and without competition) using the Deviance Information Criterion (DIC) (Spiegelhalter *et al.*, 2002, 2014). The model including competition was preferred to the model with independent populations when its DIC value was lower by a minimum threshold, which

was conservatively set to four (compared to a minimum recommended threshold of 2 (Spiegelhalter *et al.*, 2002)).

All relevant details on model equations, calibration procedure, model selection and sensitivity analysis of model results with respect to model selection criteria are reported in Section 3.A.

3.3 Results

The total number of trapped female *Ae. albopictus* and *Cx. pipiens* in all sites and years was 4566 and 8362 respectively. As can be noted in Figure 2.2, *Cx. pipiens* abundance was similar between the two years (54% of total captured in 2014) while the majority of *Ae. albopictus* were captured in 2015 (69% of total). This is likely because 2015 was warmer and therefore more suitable for *Ae. albopictus*.

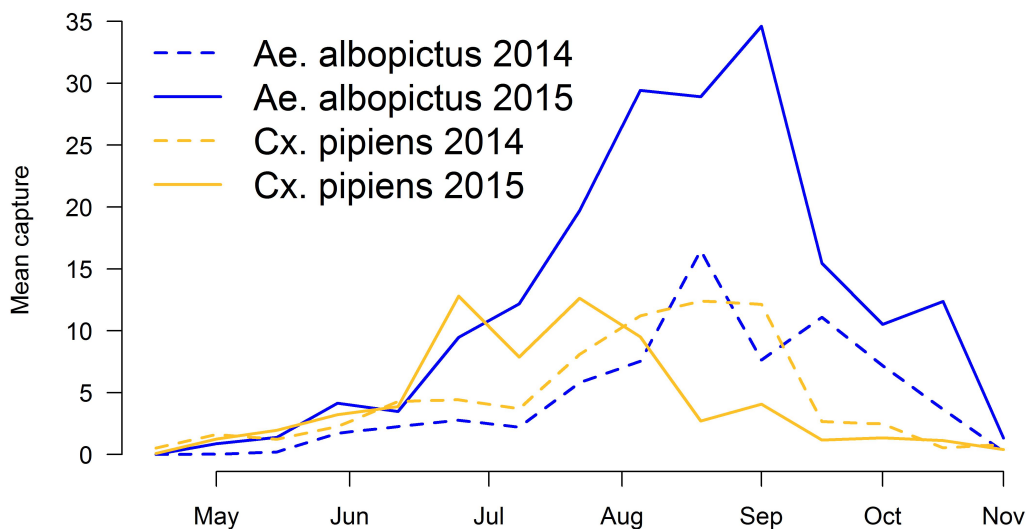


Figure 3.3: **Mosquito temporal dynamics.** Number of adult female mosquito captures for the two species (*Ae. albopictus* in blue and *Cx. pipiens* in yellow), averaged over all sites, for 2014 and 2015 (dashed and continuous lines respectively).

Cx. pipiens shows different patterns between the two considered years. In fact, in 2015 *Cx. pipiens* abundance starts declining earlier in the season, in conjunction with the increase of *Ae. albopictus* abundance, while in 2014 the two species show a more synchronous pattern. On the other hand, temporal dynamics of *Ae. albopictus* does not show substantial inter-annual differences.

Figure 3.4 presents the distribution of interspecific delays computed over all available time series. We can note that temporal profiles of *Ae. albopictus* are delayed, with respect to *Cx. pipiens* from the same site and year, by more than 4 weeks (29 days) on average; a higher delay was recorded in 2015 (37 days) with respect to 2014 (22 days)

(t-test p-value = 0.05). Figure 3.5 illustrates two examples of capture patterns associated with an average delay of four weeks (Fig. 3.5a) and no delay (Fig. 3.5b).

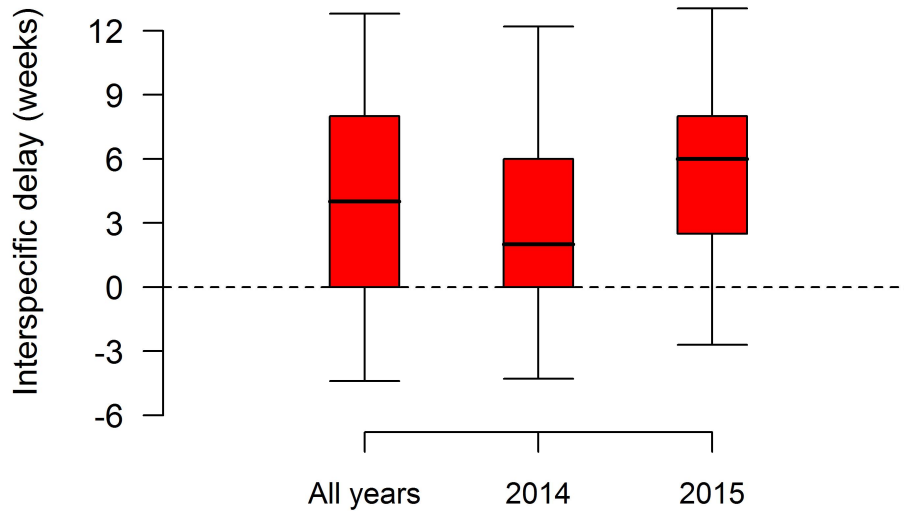


Figure 3.4: **Interspecific delay.** The interspecific delay (in weeks, median, quartiles and 95% quantiles) computed for *Ae. albopictus* and *Cx. pipiens* capture patterns. Distributions are shown for all time series combined and aggregated by year.

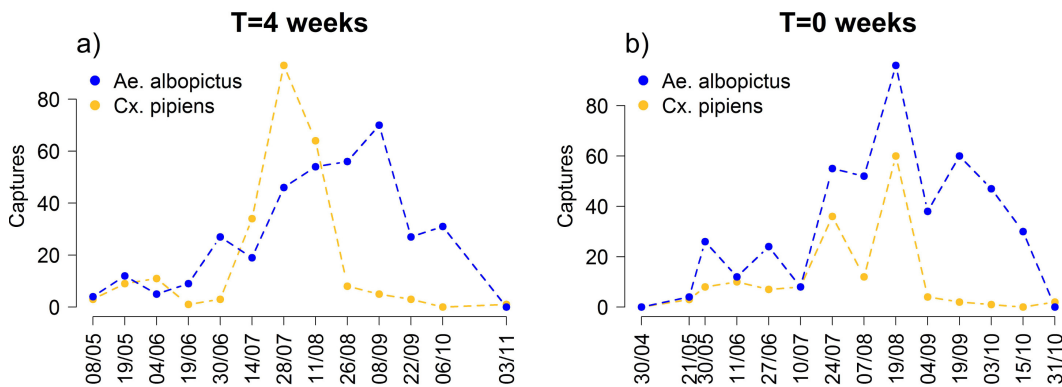


Figure 3.5: **Two examples of recorded temporal patterns with different interspecific delay.** T = 4 weeks (a), no delay, i.e. T=0 (b). *Ae. albopictus* (blue) and *Cx. pipiens* (yellow) recorded captures from two datasets.

For 29 time series (around 40%) the model with competition assumption was better ($\Delta DIC > 4$) at explaining the observed capture dynamics; of these, the large majority (22) were time series from 2015 (see Table 3.1). On the other hand, 44 time series (around 60%) were better described ($\Delta DIC < 4$) by the model without the competition assumption; of these, 32 were time series observed in 2014 (Table 3.1). An overall comparison of

selected model fits for all time series can be seen in Figure 3.12.

| | All time series | Competition (%) | Independent populations (%) |
|-----------|-----------------|-----------------|-----------------------------|
| All years | 73 | 29 (40%) | 44 (60%) |
| 2014 | 39 | 7 (18%) | 32 (82%) |
| 2015 | 34 | 22 (65%) | 12 (35%) |

Table 3.1: **Number of time series by year and selected model.** Time series, classified according to model selection based on the Deviance Information Criterion, are shown for grouped and separated years. Percentages are computed by row.

In Figure 3.6, we show the distribution of interspecific delays aggregated by the selected model (competition vs. independent populations) and by year. In sites with competition, *Ae. albopictus* capture patterns had a systematic and large positive delay with respect to *Cx. pipiens* (average 51 days considering the two years combined). Conversely, in sites where the independent population model prevailed, the average interspecific delay was lower (14 days considering the two years combined). There were no significant differences between average delays from the same group and different years.

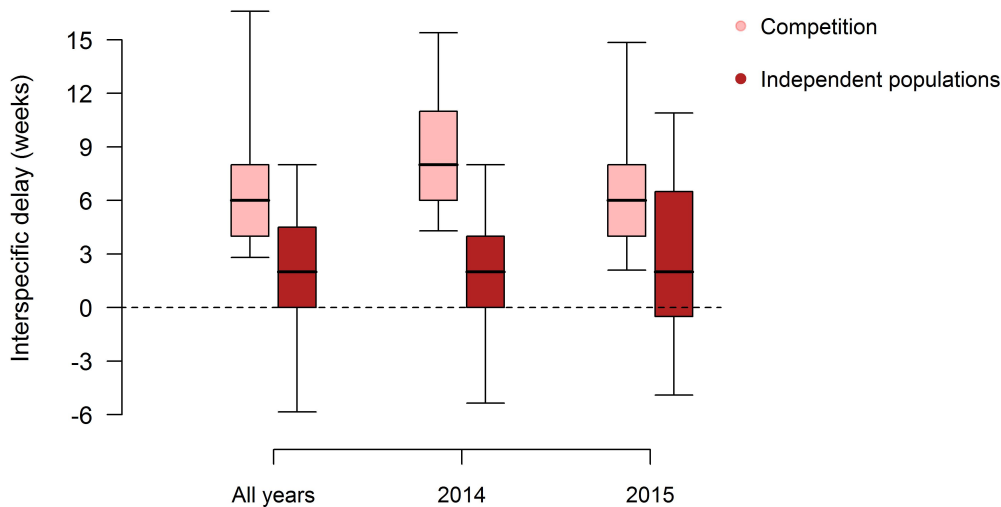


Figure 3.6: **Interspecific delay by selected model.** The interspecific delay (in weeks, median, quartiles and 95% quantiles) computed for *Ae. albopictus* and *Cx. pipiens* capture patterns by the selected model. Distributions are shown for all time series combined and aggregated by year.

We analysed the average numbers of mosquitoes captured per session and site, aggregated by selected model and year (Figure 3.7). In 2014, when competition was rare, abundances of *Cx. pipiens* and *Ae. albopictus* were not significantly different within competition time series compared to those without; however, in 2015 competition was much more common, and both *Ae. albopictus* and *Cx. pipiens* were significantly more

abundant within competition sites (t-test $t=-3.2873$, $df=23.758$, $p\text{-value}=0.003$). This result suggests that high mosquito densities might have increased the chance of competition in 2015, possibly because of the increased likelihood of shared oviposition sites. Interestingly, despite the higher mortality of *Cx. pipiens* larvae in competition sites, we did not find an overall reduction in *Cx. pipiens* captures in 2015 respect to 2014 within competition sites. This seemingly counterintuitive result can be better interpreted by considering temporal dynamics (Figure 3.3): in the early part of the 2015 season, *Cx. pipiens* were much more abundant than in the same period of 2014, because of improved environmental conditions; however, with the rapid expansion of *Ae. albopictus*, the 2015 abundance of *Cx. pipiens* fell briskly, offsetting the advantage of the first part of the season.

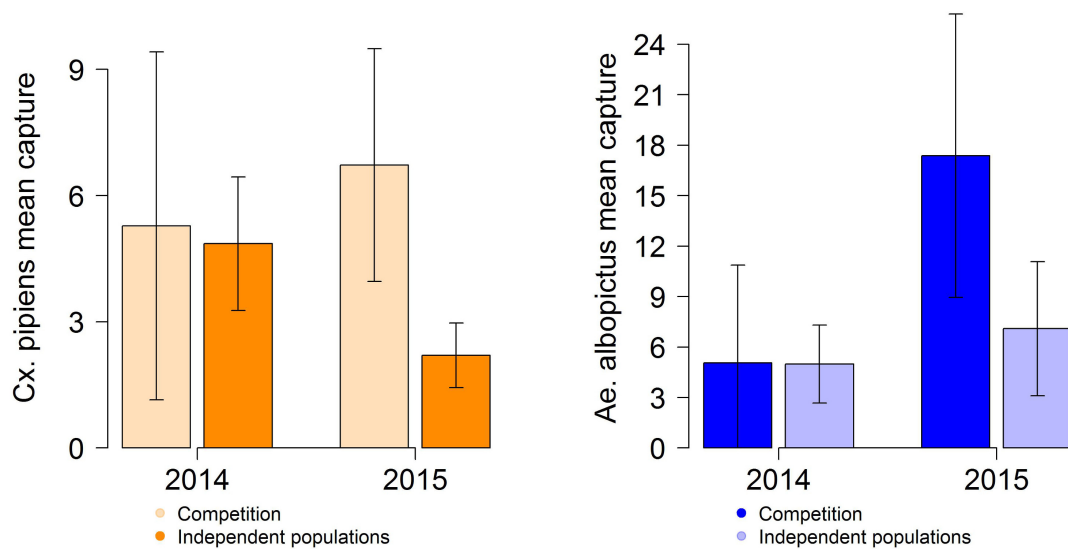


Figure 3.7: **Average recorded captures by selected model.** Average number of captured *Cx. pipiens* and *Ae. albopictus* per site by selected model and year. Black lines represent the 95% confidence intervals.

Considering only sites with competition, the model predicted a reduction for the average *Cx. pipiens* abundance by 49.2% (95% quantiles: 14-74%), compared to predictions obtained with independent populations. The onset of competition effects (defined as the first date at which relative differences between the *Cx. pipiens* populations predicted by models with and without competition exceed 10%) ranged from the end of April to the middle of July, with median centred on the first ten days of June.

3.4 Discussion

In this study, we analysed time series of *Ae. albopictus* and *Cx. pipiens* captures in northern Italy. The observed dynamics of the two species show, in several cases, a marked misalignment in temporal patterns, with a delay of *Ae. albopictus* abundance patterns with respect to *Cx. pipiens*. We showed that these temporal shifts could be explained by two alternative mechanisms: temporal niche effects and asymmetric interspecific larval competition. Under the assumption that the two populations do not interfere with

each other in a given area, a temporal niche effect may occur, depending on environmental variables (e.g. temperature, photoperiod), when the two species reach their peak of abundance at different times of the year. On the other hand, in general, competition causes more pronounced delays between the dynamics of the two species. That is due to an increase of *Cx. pipiens* larval mortality in the presence of *Ae. albopictus* within the same breeding site, inducing an anticipated decline of *Cx. pipiens* adult population.

An asymmetric competition between *Ae. albopictus* and *Cx. pipiens* has been observed and replicated in several laboratory experiments (Carrieri *et al.*, 2003; Costanzo *et al.*, 2005), but its importance in the natural environment has not been assessed before. According to our modelling results, asymmetric interspecific competition explained well the seasonal patterns of *Cx. pipiens* in many sampling sites. Specifically, in 2015 the model with competition assumption better described empirical observations in 65% of the considered sites, compared to only 18% in 2014. Our results suggest that this difference was associated with higher temperatures in 2015 than in 2014, which caused both a direct increase in the competition effect (Carrieri *et al.*, 2003) and an increase of *Ae. albopictus* densities due to a considerable reduction in the development time of immature stages (Delatte *et al.*, 2009). High *Ae. albopictus* densities may increase the chance of oviposition in shared containers (Costanzo *et al.*, 2011). Furthermore, drier conditions observed in summer 2015 (about 122mm total precipitations on average, compared to 355mm in 2014 (Meteo trentino, 2016)) likely reduced the number of small rain-filled containers available for *Ae. albopictus*, pushing females to oviposit in medium containers with the presence of *Cx. pipiens* larvae. Thus, the larval habitats of *Ae. albopictus* and *Cx. pipiens* might have overlapped more under such conditions, leading to a greater frequency of interspecific competition (Carrieri *et al.*, 2003). Abiotic factors in 2015 were also more favourable for *Cx. pipiens*, but the adverse effects of competition strongly limited their increase with respect to 2014. In particular, we estimated a relative reduction of *Cx. pipiens* abundance due to competition of about 50% on average (and up to 70% in some sites), compared to equivalent environmental conditions where competition was discounted.

Under natural conditions, competition occurs within breeding sites where the two species happen to oviposit together, mainly in urban and peri-urban areas. Adults of *Ae. albopictus* and *Cx. pipiens* captured in a given trap emerged from various breeding sites present in the neighbourhood of the trap location. Among these breeding sites, some are colonized by a single larval species, while others are colonized by both species, where they then compete for resources. Therefore, our sampling procedure can only weigh the average effect of competition in the neighbourhood of the trapping site. Our criterion for model selection was designed conservatively to identify sites where competition has a strong overall effect on the temporal patterns of mosquito abundance (see section 3.A.3). It is likely that competition occurs, to a lower degree, even in trapping sites that were not classified as “competition” sites. To explore the robustness of results with respect to the model selection criterion, we did a sensitivity analysis by using different score functions for model selection and considering different threshold values. Results confirmed our main conclusions and suggested that competition may shape *Cx. pipiens* dynamics from 30% to 50% of all datasets (see section 3.A.4 for details).

For the sake of simplicity, in this study we assumed competition would affect only *Cx. pipiens* larval survival. It has been shown that interspecific competition at this stage might also increase *Cx. pipiens* larval developmental time (Costanzo *et al.*, 2005) and reduce the body size of newly emerged adults (Costanzo *et al.*, 2011; Carrieri *et al.*,

2003), with possible negative implications for female fecundity and longevity (Costanzo *et al.*, 2011). Moreover, the body size has been associated with female susceptibility to virus infection (Alto & Lounibos, 2013; Bevins, 2007), and female longevity is a main component of the vectorial capacity. Non-lethal effects are more likely to have an impact at low densities of *Ae. albopictus* larvae (Costanzo *et al.*, 2005; Carrieri *et al.*, 2003), i.e. in situations where the independent population hypothesis could not be rejected by the present analysis, or at poor food resource conditions (Costanzo *et al.*, 2011). Thus, the inclusion of non-lethal effects in the competition model might unveil an even more widespread importance of competition effects on vector populations and arbovirus transmission. However, abundance data provided by mosquito trapping only give information on the cumulative effects of competition on the adult population; therefore, they are insufficient to distinguish the relative contribution of different competition effects. We chose to only model increased larval mortality, being the strongest competition outcome (Costanzo *et al.*, 2005; Carrieri *et al.*, 2003) and the one most directly affecting the adult population. Nonetheless, quantitative experiments collecting further data on non-lethal competition effects might improve the development of models and foster our understanding of ecological mechanisms. In addition, given the importance of climatic factors in shaping mosquito population dynamics, important additional insights will be needed, from further experiments, to quantify the effect of temperature on the strength of lethal and non-lethal effects of interspecific competition (Carrieri *et al.*, 2003).

3.5 Conclusions

We found that interspecific competition between *Cx. pipiens* and *Ae. albopictus* is common in temperate climates and it is enhanced by higher mosquito densities produced by higher temperatures. Drier weather conditions may also induce a higher overlap of breeding sites for different mosquito species, increasing the overall chances for competition. We have shown that competition amplifies the temporal separation between seasonal patterns of the two species, with *Cx. pipiens* arising early and declining more quickly with the rise of *Ae. albopictus*. Finally, we have shown that competition induces significant reductions in the total abundance of *Cx. pipiens*.

Understanding the interaction between climatic variables, competition and resulting vector abundances can be important to improve our estimates of epidemiological risks for arboviruses for which *Cx. pipiens* and *Ae. albopictus* are competent vectors, and for the assessment of vector control strategies (Baldacchino *et al.*, 2015; Bellini *et al.*, 2014). Furthermore, recent findings have shown that interspecific competition at the larval stage may affect strongly the viral competence of adult mosquitoes (Alto & Lounibos, 2013) as well as their vectorial capacity by modifying their longevity (Costanzo *et al.*, 2011; Reiskind & Lounibos, 2009). If similar effects exist in the competition between *Ae. albopictus* and *Cx. pipiens*, they would significantly impact the viral susceptibility and transmission potential of local mosquito populations and should therefore be considered in the estimation of outbreak risks (Guzzetta *et al.*, 2016a,b).

Acknowledgments

We thank Francesca Bussola, Charlotte Lap ere, Sara Carlin, Graziana Da Rold, Marco Dal Pont, Nicola Ferro Milone, Luca Tripepi, for mosquito collection and Markus Neteler

and Markus Metz for providing Land Surface Temperature data. Authors wish to thank Joanne Lello for her help in the proofreading of the manuscript.

3.A Supporting Information

3.A.1 Model calibration

The model accounts for the seven *Cx. pipiens* and four *Ae. Albopictus* life stages, namely eggs (E_c and E_a), the four *Cx. pipiens* larval instars ($L_{1c}, L_{2c}, L_{3c}, L_{4c}$) and one *Ae. albopictus* larval stage (L_a), pupae (P_c and P_a), non-diapausing *Cx. female* adults (A_c) and *Ae. female* adults (A_a). The ODE version of the model is based on the following system of equations:

$$\begin{aligned}
 E'_c &= \frac{n_{E_c}}{d_{A_c}} A_c - (\mu_{E_c} + \tau_{E_c}) E_c \\
 E'_a &= \frac{n_{E_a}}{d_{A_a}} A_a - (\mu_{E_a} + \tau_{E_a}) E_a \\
 L'_{1c} &= \tau_{E_c} E_c - \left(\tau_{L_{1c}} + \mu_{L_{1c}} \left(1 + \frac{L_c + \alpha L_a}{K_c} \right) \right) L_{1c} \\
 L'_{2c} &= \tau_{L_{1c}} L_{1c} - \left(\tau_{L_{2c}} + \mu_{L_{2c}} \left(1 + \frac{L_c + \alpha L_a}{K_c} \right) \right) L_{2c} \\
 L'_{3c} &= \tau_{L_{2c}} L_{2c} - \left(\tau_{L_{3c}} + \mu_{L_{3c}} \left(1 + \frac{L_c + \alpha L_a}{K_c} \right) \right) L_{3c} \\
 L'_{4c} &= \tau_{L_{3c}} L_{3c} - \left(\tau_{L_{4c}} + \mu_{L_{4c}} \left(1 + \frac{L_c + \alpha L_a}{K_c} \right) \right) L_{4c} \\
 L'_a &= \tau_{E_a} E_a - \left(\tau_{L_a} + \mu_{L_a} \left(1 + \frac{L_a}{K_a} \right) \right) L_a \\
 P'_c &= \tau_{L_{4c}} L_{4c} - (\tau_{P_c} + \mu_{P_c}) P_c \\
 P'_a &= \tau_{L_a} L_a - (\tau_{P_a} + \mu_{P_a}) P_a \\
 A'_c &= \frac{1}{2} \tau_{P_c} (1 - p) P_c - \mu_{A_c} A_c - \chi_C \beta_c A_c \\
 A'_a &= \frac{1}{2} \tau_{P_a} P_a - \mu_{A_a} A_a - \chi_C \beta_a A_a \\
 C'_c &= \chi_C \beta_c A_c \\
 C'_a &= \chi_C \beta_a A_a
 \end{aligned} \tag{3.1}$$

where

- $\tau_{E_c}, \tau_{E_a}, \tau_{L_{1c}}, \tau_{L_{2c}}, \tau_{L_{3c}}, \tau_{L_{4c}}, \tau_{L_a}, \tau_{P_c}, \tau_{P_a}$ are the temperature dependent developmental rates driving the transitions of the two vector species across the different life stages considered;
- $\mu_{E_c}, \mu_{E_a}, \mu_{L_{1c}}, \mu_{L_{2c}}, \mu_{L_{3c}}, \mu_{L_{4c}}, \mu_{L_a}, \mu_{P_c}, \mu_{P_a}, \mu_{A_a}, \mu_{A_c}$ are the temperature dependent death rates associated with the different stages;
- n_{E_c} and n_{E_a} are the number of eggs laid in one oviposition for a female of *Cx. pipiens* and *Ae. albopictus* respectively;
- d_{A_c} and d_{A_a} are the length of the gonotrophic cycles of the two species;
- K_a and K_c are density-dependent scaling factors driving the carrying capacity for the larval stages;
- p is the probability (depending on daylight duration) that a fully developed *Cx. pipiens* pupa becomes a diapausing adult;
- α represents the increase in mortality of *Cx. pipiens* larval stages due to competition with *Ae. albopictus*. Its value is 0 if the daily temperature is below 15°C;
- β_a and β_c are the adult capture rates;
- χ_C is a function of time defined equal to 1 when the trap is open and 0 otherwise;
- L_c represents the total *Cx. pipiens* larval population, i.e. $L_c = L_{1c} + L_{2c} + L_{3c} + L_{4c}$;

- C_a and C_c represent the cumulative number of captured female adult mosquitoes for *Ae. albopictus* and *Cx. pipiens* respectively.

Since only female adult mosquitoes are explicitly considered in the model, the term $1/2$ in the equation for the adults accounts for the sex ratio (Delatte *et al.*, 2009; Vinogradova, 2011). Moreover, given that diapausing *Cx. pipiens* females do not take blood meals before overwintering (Denlinger & Armbruster, 2014), they are unlikely to be captured by using the considered traps. Consequently, only non-diapausing female adults are considered in the model.

We implemented model 3.1 as a discrete-time stochastic version, with time-step $\Delta t = 1$ day, in order to account for the stochastic nature of the processes. Precisely, the model is a Markov chain whose states represent the integer number of individuals in all developmental stages. Transition probabilities are built according to Poisson distributions whose means are obtained from the rate in system 3.1. The seasonal dynamics of the mosquito population of each site is simulated from April 1 (corresponding to approximately one month before the first reported capture session) to October 31. Since, to the best of our knowledge, no data are available regarding the overwintering of *Cx. pipiens* and *Ae. albopictus*, we initialize the system with 100 non-diapausing *Cx. pipiens* adults and 10000 *Ae. albopictus* eggs. Preliminary model simulations showed no significant change of the model's behavior for different initial conditions.

Mortality and developmental rates across different vector life stages have been modeled as a function of temperature as presented in (Poletti *et al.*, 2011) and Chapter 2. The probability p for a developed *Cx. pipiens* pupa to become a diapausing adult is a function of daylight duration as presented in Chapter 2. The average number of eggs laid n_{E_a} and n_{E_c} per oviposition were fixed to 60 (Poletti *et al.*, 2011) and 190 (Chapter 2) respectively. The duration of the gonotrophic cycle d_{A_a} is a function of temperature as in (Poletti *et al.*, 2011), while d_{A_c} is fixed to 5.54 days (Faraj *et al.*, 2006).

We assumed that, for each capture session, the number of captured female adult mosquitoes follows a Poisson distribution with mean obtained from the model; therefore, for each dataset, the likelihood of the observed data given a parameter set θ has been defined as

$$L = \prod_{i=1}^h e^{-\tilde{A}_i(\theta)} \frac{\tilde{A}_i(\theta)^{A_i}}{A_i!} \cdot e^{-\tilde{C}_i(\theta)} \frac{\tilde{C}_i(\theta)^{C_i}}{C_i!}$$

where i runs over the number of capture sessions h , A_i (C_i) is the observed number of captured *Ae. albopictus* (*Cx. pipiens*) adults at capture session i and $\tilde{A}_i(\theta)$ ($\tilde{C}_i(\theta)$) is the predicted number of captures of *Ae. albopictus* (*Cx. pipiens*) at capture session i simulated by the model with parameters $\theta = (\alpha, \beta, K_a, K_c)$.

3.A.2 Model output

Figure 3.8 shows an example of the temporal dynamics of larvae and adults for both species predicted by the two models in a given site and year. During spring months (April and May), the presence of *Ae. albopictus* larvae is limited by the relatively low temperatures and both models predict the same expansion of *Cx. pipiens* larvae and adults. Afterwards (beginning of June), increasing temperatures cause the rise of the *Ae. albopictus* population; consequently, the model with competition predicts a sharp fall of the larval (Fig. 3.8a) and adult (Fig. 3.8b) *Cx. pipiens* abundances. On the other hand, with the independent populations model, the decline of *Cx. pipiens* adults begins in late summer (August), when higher temperatures increase their mortality and

progressively shortening photoperiods induce diapause in a growing number of newly emerged adult females. *Ae. albopictus* adults are better suited to higher temperatures and do not diapause, therefore their decline does not start until mid-September (Fig. 3.8b).

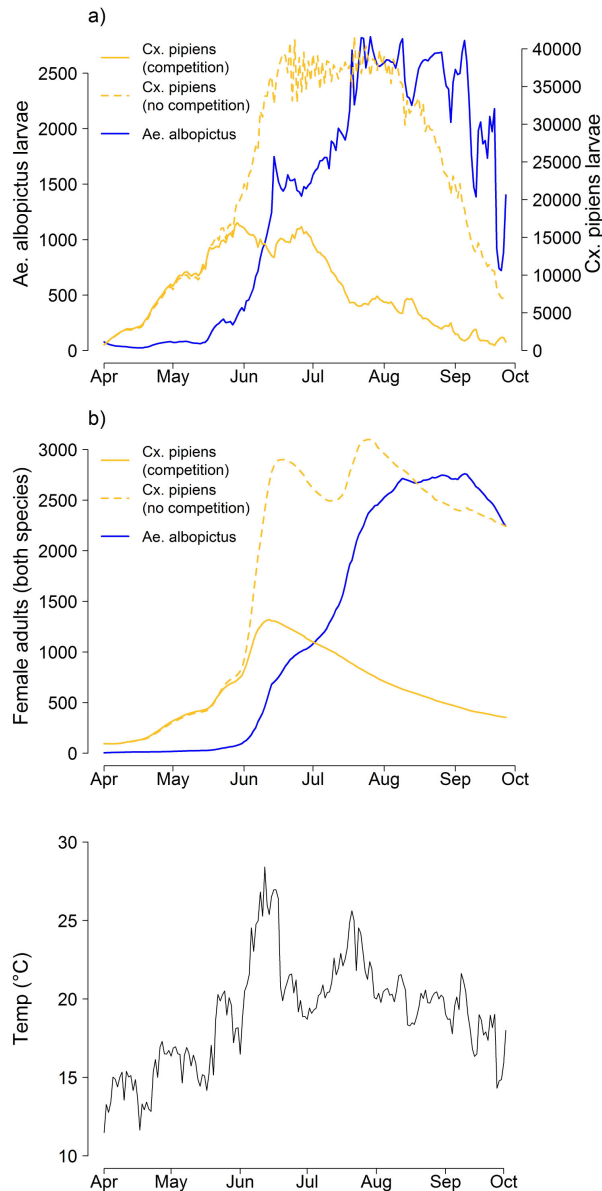


Figure 3.8: **Example of predicted populations.** Example of average larval (a) and adults (b) populations predicted by the two considered models in a selected site. Lower panel shows the recorded temperature.

3.A.3 Model fit

The model fits the observed data quite well. In fact, about 75% of the recorded weekly captures lies in the 95% Credible Interval (CI) of model predictions with both assump-

| All years | All datasets | $\Delta DIC > 2$ | | $\Delta AIC > 2$ | | $\Delta AIC > 4$ | | $\Delta AIC > 7$ | |
|-----------|--------------|------------------|-----------------------------|------------------|-----------------------------|------------------|-----------------------------|------------------|-----------------------------|
| | | Competition (%) | Independent populations (%) |
| 2014 | 73 | 34 (47%) | 39 (53%) | 29 (40%) | 44 (60%) | 23 (32%) | 50 (68%) | 18 (25%) | 55 (75%) |
| 2015 | 34 | 9 (23%) | 30 (77%) | 7 (18%) | 32 (82%) | 5 (13%) | 34 (87%) | 4 (10%) | 35 (90%) |
| 2015 | 34 | 25 (74%) | 9 (26%) | 22 (65%) | 12 (35%) | 18 (53%) | 16 (47%) | 14 (41%) | 20 (59%) |

Table 3.2: Number of datasets by year, selected model and DIC and AIC threshold.

tions. In sites where the competition model was selected, the 95% CI of captured females predicted by the independent population model included the observed *Cx. pipiens* captures in 65% of data points overall, compared to 72% in the competition model. As expected, both models fitted equally well *Ae. albopictus* data, with about 80% of observations lying within the 95% CI of model predictions.

3.A.4 DIC and AIC analysis

We compared the goodness of fit of the model with interspecific competition against that of the model with independent populations (i.e. with α set equal to 0), using the Deviance Information Criterion (DIC):

$$DIC = E(D) + \frac{1}{2} \text{var}(D)$$

where $D = -2 \ln L$, $E(D)$ is the average value of D and $\text{var}(D)$ is its variance.

Models with smaller DIC should be preferred. In fact, if the likelihood L is high (closer to 1) then $\ln L$ is closer to 0. Moreover, $\text{var}(D)$ increases with model complexity: in this way, the DIC penalizes models with a higher number of free parameters. We denote with DIC_α the value obtained with the interspecific competition model and with DIC_0 the value associated with the independent populations model. Generally, model selection using the DIC criterion only requires a model to have a lower DIC than the alternative (corresponding to $\Delta DIC = DIC_0 - DIC_\alpha > 0$) (Spiegelhalter *et al.*, 2002). Considering the high stochastic noise in the capture data and the number of free parameters in our models, we conservatively restricted this criterion in such a way to minimize the risk of false positives on the existence of competition (Spiegelhalter *et al.*, 2002), by fixing a higher threshold on the minimum ΔDIC , i.e. $\Delta DIC > 4$. However, since the value of the threshold is arbitrary, we tested the robustness of our results by using a looser threshold, set to $\Delta DIC > 2$ as well as a different score function for model selection, namely, the Akaike Information Criterion, AIC (Burnham & Anderson, 2002). AIC is defined as

$$AIC = 2K - E(D)$$

Where K is the number of the model parameters. Analogously to the DIC criterion, we selected models based on the value of on ΔAIC with respect to three standard threshold values (namely, 2, 4 and 7) (Burnham & Anderson, 2002; Burnham *et al.*, 2011).

By loosening the DIC threshold, we included 5 additional datasets in the competition group (see Table 3.2). The AIC yielded results very similar to the DIC, although slightly more conservative for corresponding values of the threshold. As reported in Table 3.2 and Figures 3.9 and 3.10, qualitative results presented in the main text do not change significantly when applying a different threshold on DIC or when using the AIC with either threshold.

3.A.5 Estimates of the competition-dependent additional mortality

The ratio $z = \frac{\alpha}{K_c}$ defines the mortality rate of *Cx. pipiens* larvae due to each additional *Ae. albopictus* larva in the breeding site. Figure 3.11 shows that estimates of z for sites

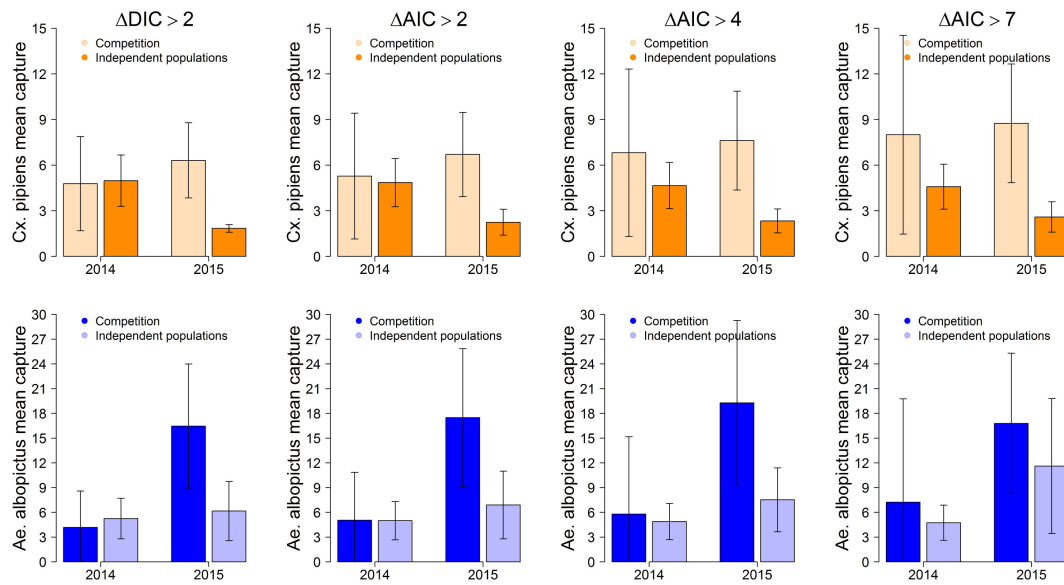


Figure 3.9: Average number of captured *Cx. pipiens* (panels in the upper row) and *Ae. albopictus* (panels in the lower row) per site by criterion of model selection ($\Delta DIC > 2$, $\Delta AIC > 2$, $\Delta AIC > 4$ and $\Delta AIC > 7$, from left to right) by selected model and year.

more strongly associated with competition ($\Delta DIC > 4$) are on average significantly higher (t-test p-value < 0.05) than those associated to independent populations ($\Delta DIC < 0$): in other words, the competition model tended to be rejected when the estimated value of the competition-dependent mortality was closer to zero. The distribution of z values in sites with uncertain attribution (characterized by intermediate values of ΔDIC) was in between the two cases: this result mirrors the fact that competition has a nuanced, rather than an on/off effect on mosquito abundance.

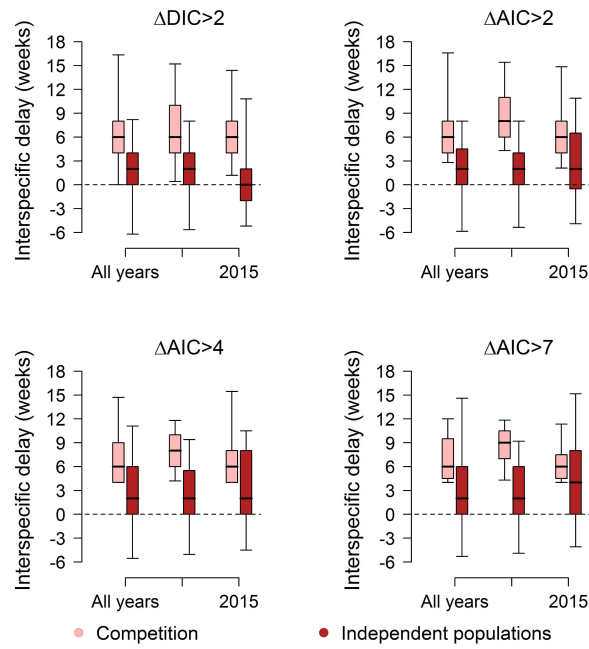


Figure 3.10: The interspecific delay (in weeks, median, quartiles and 95% credible intervals) computed for *Ae. albopictus* and *Cx. pipiens* capture patterns by criterion of model selection. Distributions are shown for all datasets combined and aggregated by year.

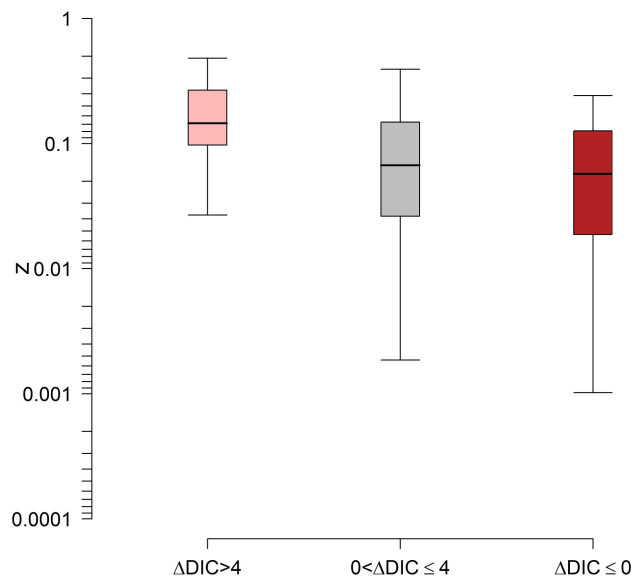


Figure 3.11: Boxplot (2.5%, 25%, 75% and 97.5% quantile and median) of estimated posterior distribution of z by ΔDIC .

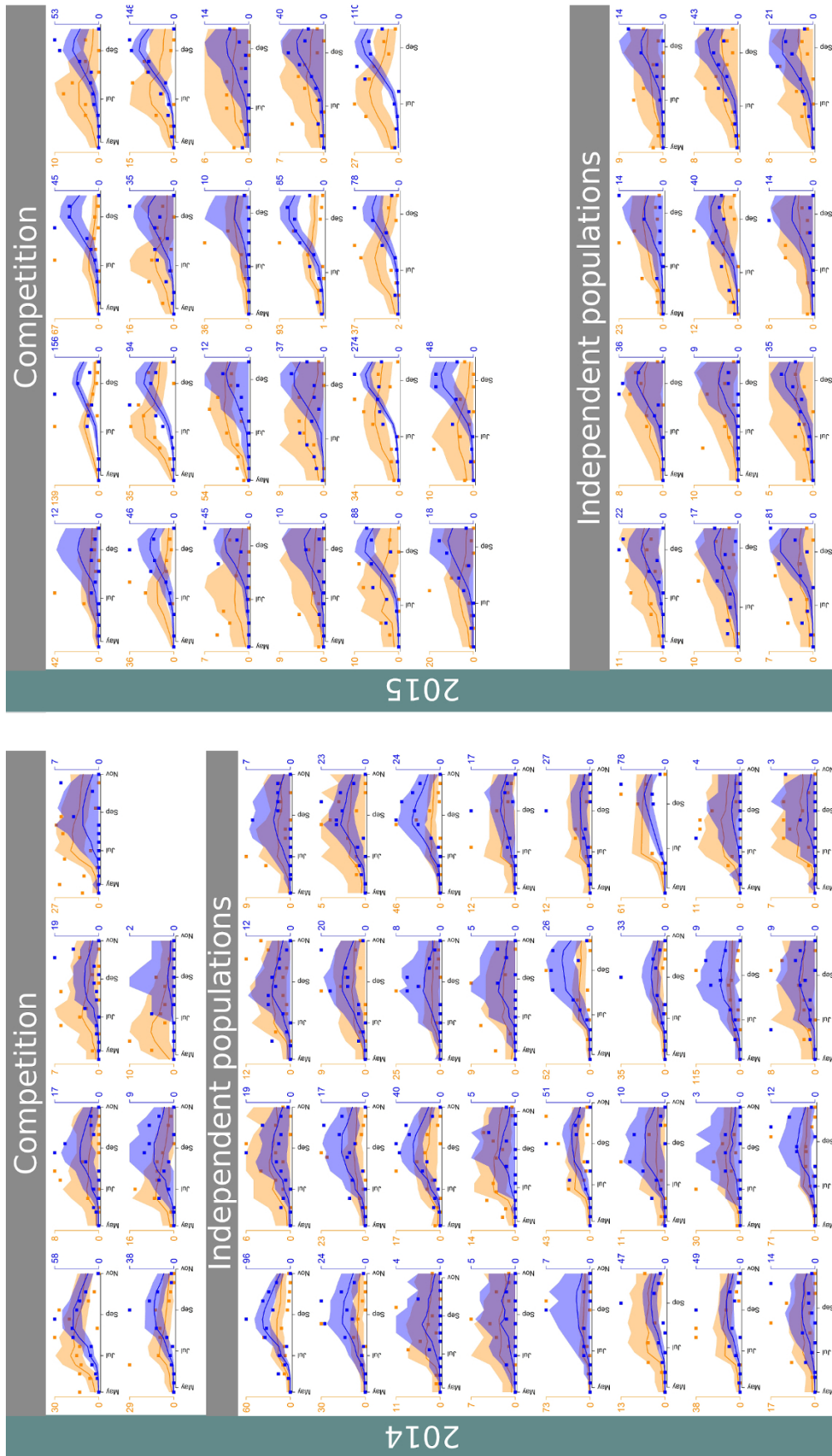


Figure 3.12: Model fit for *Cx. pipiens* (orange) and *Ae. albopictus* (blue) in the 73 datasets from 2014; sites where the competition model was selected are shown in the first two rows. Right side: datasets from 2015; sites where the competition model was selected are shown in the first six rows. Squares: capture data; lines and shaded areas: posterior model estimates with 95% credible intervals.

4 Exploring vector-borne infection ecology in multi-host communities: a case study of West Nile virus

Giovanni Marini^{a,b}, Andrea Pugliese^b, Roberto Rosá^a, Hans Heesterbeek^c

a: Department of Biodiversity and Molecular Ecology, Research and Innovation Centre, Fondazione Edmund Mach, San Michele all'Adige (TN), Italy

b: Department of Mathematics, University of Trento, Trento, Italy

c: Faculty of Veterinary Medicine, University of Utrecht, Yalelaan 7, 3584 CL Utrecht, The Netherlands

Journal of Theoretical Biology 2017; 415: 58-69

4.1 Introduction

Ecological interactions within and between species, such as competition and consumer-resource relations, can be influenced by infection dynamics of pathogens and parasites, and vice versa. A recent attempt to more systematically address their mutual interactions (Roberts & Heesterbeek, 2013) has focused on invasion of infection into ecological communities. For this purpose, they computed the basic reproduction number \mathcal{R}_0 , defined as the average number of new cases of an infection caused by one typical infected individual, in a population consisting of susceptibles only (Diekmann *et al.*, 2010).

Following Roberts & Heesterbeek (2013), we investigate the case of a vector-borne infection spreading in a population where different species of hosts compete with each other, for instance for food or habitat, and where the vector bites the hosts according to its feeding preferences. Several papers investigating an infection spreading into competing hosts have been published (Bowers & Turner, 1997; Han & Pugliese, 2009; Bokil & Manore, 2013), but to the best of our knowledge none analyzing the case of a vector-borne infection. In this type of infection, the pathogen is usually transmitted to and from the host when the latter is bitten by the vector to obtain a blood meal required for reproduction.

We focus on mosquito-borne infections and analyze a basic system where one vector species takes blood meals from two competent host species that compete ecologically. We show how to compute \mathcal{R}_0 allowing for different reservoir host competence (i.e. probability of transmitting the pathogen to the vector). As a prototypical example, we consider West Nile virus (WNV) in an ecosystem composed of two avian host species. However, the formula for \mathcal{R}_0 is easily generalizable to ecosystems of arbitrary numbers of host and non-host species that interact by competition and/or food web relations (Roberts & Heesterbeek, 2013).

WNV is a flavivirus first isolated in Uganda in 1937 (Smithburn *et al.*, 1940) and now present on every continent (Reisen, 2013). It is maintained in a bird-mosquito transmission cycle primarily involving mosquitoes belonging to *Culex* species, of which the

pipiens sub-complex is thought to be one of the most important in Europe (Zeller & Schuffenecker, 2004) and North America (Reisen, 2013). Humans and other mammals (e.g. horses) are considered dead-end hosts, i.e. they can not transmit the virus.

Culex mosquitoes and WNV have a broad host range, and mosquito feeding preferences can change during the season. In fact mosquitoes seem to preferentially bite certain hosts more than others, even if they are less available (Kilpatrick *et al.*, 2006a; Thiemann *et al.*, 2011; Simpson *et al.*, 2012; Taylor *et al.*, 2012; Rizzoli *et al.*, 2015); moreover its preferences seem to change during the breeding season (Kilpatrick *et al.*, 2006b; Thiemann *et al.*, 2011; Burkett-Cadena *et al.*, 2012).

Many models have been proposed to study West Nile virus dynamics among different bird species (Cruz-Pacheco *et al.*, 2005, 2012; Maidana & Yang, 2011; Simpson *et al.*, 2012) but they do not explicitly investigate ecological interactions between the hosts or the effects of changes in host preference over the season. Our aim is to investigate how ecological interactions, such as competition, and shifting mosquito feeding preferences can affect the invasion of a pathogen and therefore change the outcome relatively to a baseline scenario which does not include such features.

4.2 The model

We analyze the simplest case with only two competing species, both competent hosts for an infection transmitted by a vector with population size V . In addition, we assume that hosts can not recover, but may die due to the infection. To this aim, we develop a compartmental model similar to the one proposed by Lord *et al.* (1996) with hosts and vectors classified according to whether they are susceptible S or infected I . Although vector-borne infections are usually transmitted only by the vector, we consider also the possibility of host-to-host transmission, as this has been shown to be possible for West Nile virus among crows by Komar *et al.* (2003).

To model the competition among birds we assume, as in (Gamarra *et al.*, 2005), that they both follow a Lotka-Volterra dynamics. In addition, the mosquito population dynamics is assumed to be density dependent; in particular, we assume that density can affect larval development and survival, as observed by Agnew *et al.* (2010).

The equations of the model are

$$\begin{cases} N_1' &= r_1 \left(1 - \frac{N_1 + c_{12}N_2}{K_1}\right) N_1 - \alpha_1 I_1 \\ N_2' &= r_2 \left(1 - \frac{N_2 + c_{21}N_1}{K_2}\right) N_2 - \alpha_2 I_2 \\ V' &= (n_E \sigma b_{max} (1 - \rho_V V) - \mu_V) V \\ I_1' &= \left[p_{V1} b_1 \frac{I_V}{N_1} + \beta_{11} p_{11} \frac{I_1}{N_1} + \beta_{12} p_{21} \frac{I_2}{N_2} \right] S_1 - \left(\alpha_1 + \mu_1 + r_1 \frac{a_{11}N_1 + a_{12}c_{12}N_2}{K_1} \right) I_1 \\ I_2' &= \left[p_{V2} b_2 \frac{I_V}{N_2} + \beta_{22} p_{22} \frac{I_2}{N_2} + \beta_{21} p_{12} \frac{I_1}{N_1} \right] S_2 - \left(\alpha_2 + \mu_2 + r_2 \frac{a_{22}N_2 + a_{21}c_{21}N_1}{K_2} \right) I_2 \\ I_V' &= \left[p_{1V} b_1 \frac{I_1}{N_1} + p_{2V} b_2 \frac{I_2}{N_2} \right] S_V + (q_V n_E \sigma b_{max} (1 - \rho_V V) - \mu_V) I_V \end{cases} \quad (4.1)$$

where

- $N_i = S_i + I_i$ is the number of individuals of species i with $i \in \{1, 2\}$;
- $r_i = \eta_i - \mu_i > 0$ is the growth rate of species $i \in \{1, 2\}$, where η_i and μ_i are the birth and death rate respectively. They are assumed not to be influenced by the vector. Each species has a certain carrying capacity K_i ;

- c_{ij} represents the effect of competition of species j on species i with $i, j \in \{1, 2\}, i \neq j$;
- $\alpha_{ij} \in [0, 1]$ is the proportion of competition from species j that affects the death rate of species i with $i, j \in \{1, 2\}$;
- n_E is the number of eggs laid by a gravid mosquito and σ is the probability that an egg becomes an adult;
- b_{max} is the vector biting rate, which can be thought of as the inverse of the length of the gonotrophic cycle, i.e. the interval spanned between the blood meal and the oviposition. Bites are divided between the two host populations with b_1, b_2 , denoting the biting rates on species 1 and 2 respectively, and therefore $b_{max} = b_1 + b_2$;
- $\rho_V < 1$ is the density dependent factor on vector fecundity. We can then define K_V as the vector carrying capacity, as follows:

$$K_V := \frac{1}{\rho_V} \left(1 - \frac{\mu_V}{n_E \sigma b_{max}} \right).$$

- μ_V is the vector death rate;
- α_i is the additional death rate for species i due to the infection;
- p_{ij} is the probability that an infected individual of type $i \in \{1, 2, V\}$ infects a susceptible individual of type $j \in \{1, 2, V\}$, given contact or bite;
- β_{ij} is the direct transmission rate between host species i and j ;
- q_V is the probability of vertical transmission, i.e. the probability that an infected mosquito passes the virus to its offspring.

If there is no infection, the Jacobian of system (4.1) at the Infection-free Equilibrium is given by

$$J = \begin{pmatrix} C & D \\ 0 & H \end{pmatrix}$$

where

$$C = \begin{pmatrix} \frac{r_1}{K_1} (K_1 - c_{12}N_2 - 2N_1) & -\frac{c_{12}r_1N_1}{K_1} & 0 \\ -\frac{c_{21}r_2N_2}{K_2} & \frac{r_2}{K_2} (K_2 - c_{21}N_1 - 2N_2) & 0 \\ 0 & 0 & n_E \sigma b_{max} (1 - 2\rho_V V) - \mu_V \end{pmatrix}$$

represents the ecological community dynamics of the two host species and the vector. The lower 3×3 matrix H in the Jacobian represents the epidemiological dynamics of the two host species and the vector species:

$$H = \begin{pmatrix} p_{11}\beta_{11} - (\alpha_1 + \tilde{\mu}_1) & \frac{\beta_{12}p_{21}N_1}{N_2} & p_{V1}b_1 \\ \frac{p_{12}\beta_{21}N_2}{N_1} & \beta_{22}p_{22} - (\alpha_2 + \tilde{\mu}_2) & p_{V2}b_2 \\ \frac{p_{1V}b_1V}{N_1} & \frac{p_{2V}b_2V}{N_2} & q_V n_E \sigma b_{max} (1 - \rho_V V) - \mu_V \end{pmatrix}$$

where $\tilde{\mu}_i = \mu_i + r_i \frac{\alpha_{ii}N_i + \alpha_{ij}c_{ij}N_j}{K_i}$ with $i \in \{1, 2\}$.

The matrix D in the upper right corner is

$$D = \begin{pmatrix} -\alpha_1 & 0 & 0 \\ 0 & -\alpha_2 & 0 \\ 0 & 0 & 0 \end{pmatrix}.$$

The infection-free non trivial equilibrium is

$$N_1^* = \frac{K_1 - c_{12}K_2}{1 - c_{12}c_{21}}, \quad N_2^* = \frac{K_2 - c_{21}K_1}{1 - c_{12}c_{21}}, \quad V^* = K_V \quad (4.2)$$

which exists (i.e. $N_1^* \geq 0, N_2^* \geq 0, V^* \geq 0$) and is stable provided

$$K_i > c_{ij}K_j, \quad \mu_V < n_E \sigma b_{max}.$$

We observe that $N_i^*/K_i > N_j^*/K_j$ (i.e. population size of species i is depressed by competition less than species j) when $c_{ji} \frac{K_i}{K_j} > c_{ij} \frac{K_j}{K_i}$. In particular when $K_i = K_j$ (which can also be assumed through an appropriate scaling) we can equate size of competition coefficients with depression of population size.

As in (Roberts & Heesterbeek, 2013) we write $H = T + \Sigma$ where T is the epidemiological transmission matrix

$$T = \begin{pmatrix} p_{11}\beta_{11} & \frac{\beta_{12}p_{21}N_1^*}{N_2^*} & p_{V1}b_1 \\ \frac{p_{12}\beta_{21}N_2^*}{N_1^*} & \beta_{22}p_{22} & p_{V2}b_2 \\ \frac{p_{1V}b_1V^*}{N_1^*} & \frac{p_{2V}b_2V^*}{N_2^*} & q_V n_E \sigma b_{max} (1 - \rho_V V^*) \end{pmatrix}$$

and Σ is the epidemiological transition matrix

$$\Sigma = \begin{pmatrix} -(\alpha_1 + \tilde{\mu}_1) & 0 & 0 \\ 0 & -(\alpha_2 + \tilde{\mu}_2) & 0 \\ 0 & 0 & -\mu_V \end{pmatrix}$$

and therefore the so called next-generation matrix with large domain (Diekmann *et al.*, 2010) is

$$\mathcal{K} = -T\Sigma^{-1} = \begin{pmatrix} \frac{p_{11}\beta_{11}}{(\alpha_1 + \tilde{\mu}_1)} & \frac{\beta_{12}p_{21}N_1^*}{N_2^*(\alpha_2 + \tilde{\mu}_2)} & \frac{p_{V1}b_1}{\mu_V} \\ \frac{p_{12}\beta_{21}N_2^*}{N_1^*(\alpha_1 + \tilde{\mu}_1)} & \frac{\beta_{22}p_{22}}{(\alpha_2 + \tilde{\mu}_2)} & \frac{p_{V2}b_2}{\mu_V} \\ \frac{p_{1V}b_1V^*}{N_1^*(\alpha_1 + \tilde{\mu}_1)} & \frac{p_{2V}b_2V^*}{N_2^*(\alpha_2 + \tilde{\mu}_2)} & q_V \end{pmatrix}$$

and \mathcal{R}_0 is the dominant eigenvalue of \mathcal{K} .

4.2.1 Infections without horizontal transmission

This is probably the most common case, since, as explained above, most vector-borne infections are transmitted only by the vector, so $p_{ij} = 0, i, j \in \{1, 2\}$. In this case the next-generation matrix becomes

$$\mathcal{K} = \begin{pmatrix} 0 & 0 & \frac{p_{V1}b_1}{\mu_V} \\ 0 & 0 & \frac{p_{V2}b_2}{\mu_V} \\ \frac{p_{1V}b_1V^*}{N_1^*(\alpha_1 + \tilde{\mu}_1)} & \frac{p_{2V}b_2V^*}{N_2^*(\alpha_2 + \tilde{\mu}_2)} & q_V \end{pmatrix}$$

and the formula for \mathcal{R}_0 is

$$\mathcal{R}_0 = \frac{1}{2} \left(\sqrt{\frac{4p_{V1}p_{1V}b_1^2 V^*}{\mu_V(\alpha_1 + \tilde{\mu}_1) N_1^*} + \frac{4p_{V2}p_{2V}b_2^2 V^*}{\mu_V(\alpha_2 + \tilde{\mu}_2) N_2^*} + q_V^2} + q_V \right) \quad (4.3)$$

with N_1^*, N_2^*, V^* as in (4.2).

We note that the biting rates b_1, b_2 play a crucial role for \mathcal{R}_0 , which depends also on the vector to host ratio which is in turn driven by the competition coefficients and the carrying capacities.

In order to make (4.3) more perspicuous, we can simplify it by assuming that an infected vector passes the pathogen to any susceptible host with same probability $p_{V1} = p_{V2} = p_{VH}$ and that it can not transmit the virus to its offspring (so $q_V = 0$). We can further assume that mosquitoes bite hosts according to their density, so $b_i = b_{max} \frac{N_i}{N_1 + N_2}$ with $i \in \{1, 2\}$. In this case (4.3) reduces to

$$\mathcal{R}_0 = \frac{b_{max}}{N_1^* + N_2^*} \sqrt{\frac{p_{VH}V^*}{\mu_V}} \sqrt{\frac{p_{1V}N_1^*}{\alpha_1 + \tilde{\mu}_1} + \frac{p_{2V}N_2^*}{\alpha_2 + \tilde{\mu}_2}}. \quad (4.4)$$

From (4.4) we see that competition does not affect \mathcal{R}_0 linearly. In fact, for fixed c_{21} , increasing c_{12} will decrease N_1^* while at the same time N_2^* and $\tilde{\mu}_1$ will increase. Thus one term inside the square root will increase with c_{12} while the other will decrease; as a consequence, the overall effect on \mathcal{R}_0 is not straightforward.

4.2.2 Horizontal transmission

In this case we assume, as observed for WNV (Komar *et al.*, 2003), that horizontal transmission can happen only between individuals belonging to the same species, so $p_{ij} = 0, i \neq j$. In this case

$$\mathcal{K} = \begin{pmatrix} \frac{p_{11}\beta_{11}}{(\alpha_1 + \tilde{\mu}_1)} & 0 & \frac{p_{V1}b_1}{\mu_V} \\ 0 & \frac{p_{22}\beta_{22}}{(\alpha_2 + \tilde{\mu}_2)} & \frac{p_{V2}b_2}{\mu_V} \\ \frac{p_{1V}b_1V^*}{N_1^*(\alpha_1 + \tilde{\mu}_1)} & \frac{p_{2V}b_2V^*}{N_2^*(\alpha_2 + \tilde{\mu}_2)} & q_V \end{pmatrix}.$$

\mathcal{R}_0 is then the largest root of a 3-rd order equation. We will consider some numerical examples in the next section.

Finally, in order to investigate the combined effect of horizontal and vector transmission, we consider, for the sake of simplicity, that there is only one host species, say species 1. Then, with only horizontal transmission

$$\mathcal{R}_0^h = \frac{p_{11}\beta_{11}}{(\alpha_1 + \tilde{\mu}_1)},$$

while, with only vector transmission (and $q_V = 0$),

$$\mathcal{R}_0^V = \sqrt{\frac{p_{V1}p_{1V}b_1^2V^*}{\mu_V N_1^*(\alpha_1 + \tilde{\mu}_1)}}.$$

When both transmission routes operate, one obtains

$$\mathcal{R}_0 = \sqrt{\left(\frac{p_{11}\beta_{11}}{4(\alpha_1 + \tilde{\mu}_1)}\right)^2 + \frac{p_{V1}p_{1V}b_1^2V^*}{\mu_V N_1^*(\alpha_1 + \tilde{\mu}_1)} + \frac{p_{11}\beta_{11}}{\alpha_1 + \tilde{\mu}_1}} = \frac{\mathcal{R}_0^h}{2} + \sqrt{\frac{(\mathcal{R}_0^h)^2}{4} + (\mathcal{R}_0^V)^2}. \quad (4.5)$$

From (4.5) we see that $\mathcal{R}_0 \leq (>)1 \iff \mathcal{R}_0^h + (\mathcal{R}_0^V)^2 \leq (>)1$.

4.3 Numerical example

Here, we present a numerical example to explore the influence of vector and host ecology, in our setting, on invasion of the infectious agent. In particular, we study the invasion of WNV with two bird species. We selected their respective parameters among the most competent species, that are American crow (*Corvus brachyrhynchos*, species 1) and House finch (*Haemorrhous mexicanus*, species 2), as found in (Komar *et al.*, 2003). We assume horizontal transmission only in species 1 (American crow), since Komar *et al.* (2003) found its occurrence in this species only, and assume $p_{22} = 0$.

Finally, we also assume that the vector has a fixed daily biting rate $b_{max} = b_1 + b_2$. The baseline parameters, with their description, are reported in Table 4.1.

| Parameter | Description | Value | Source |
|----------------------------------|--|---------|-------------------------------------|
| p_{V1}, p_{V2} | Transmission probability mosquito to bird | 0.88 | (Turell <i>et al.</i> , 2001) |
| p_{1V} | Transmission probability species 1 to mosquito | 0.5 | (Komar <i>et al.</i> , 2003) |
| p_{2V} | Transmission probability species 2 to mosquito | 0.28 | (Komar <i>et al.</i> , 2003) |
| $p_{11}\beta_{11}$ | Contact transmission rate in crows | 0.33 | (Hartemink <i>et al.</i> , 2007) |
| μ_V | Death rate in mosquitoes (/day) | 0.08 | (Hartemink <i>et al.</i> , 2007) |
| q_V | Transovarial transmission rate | 0.004 | (Hartemink <i>et al.</i> , 2007) |
| α_1 | Species 1 WNV-related mortality rate (/day) | 0.2 | (Komar <i>et al.</i> , 2003) |
| α_2 | Species 2 WNV-related mortality rate (/day) | 0.11 | (Komar <i>et al.</i> , 2003) |
| n_E | Number of mosquito eggs in one batch | 200 | (Hartemink <i>et al.</i> , 2007) |
| σ | Survival probability egg to female mosquito | 0.1 | (Hartemink <i>et al.</i> , 2007) |
| μ_1, μ_2 | Bird death rate | 0.001 | (Bowman <i>et al.</i> , 2005) |
| r_1, r_2 | Bird growth rate | 0.5 | (Bowman <i>et al.</i> , 2005) |
| $\frac{K_V}{(K_1 + K_2)}$ | Mosquito to bird ratio | 5 | (Cruz-Pacheco <i>et al.</i> , 2005) |
| K_1, K_2 | Carrying capacities for birds | 1000 | Assumption |
| $a_{11}, a_{12}, a_{21}, a_{22}$ | Proportion of competition affecting the death rate | Varying | |

Table 4.1: parameters.

4.3.1 Effect of vector and host ecology on \mathcal{R}_0

We assume that the vector bites its hosts according to their density with a fixed daily rate $b_{max} = 0.2$, and $a_{11} = a_{22} = a_{12} = a_{21} = 0.5$. In Figure 4.1 the effect of competition on \mathcal{R}_0 is shown. In Figure 4.1a (left panel) we can see that for a fixed value of c_{ij} , increasing c_{ji} will increase \mathcal{R}_0 and the highest values are reached when c_{12} is particularly large, so when species 1 (which has a higher probability of transmitting the virus to the vector) is much less abundant than the other. The lowest values are expected when the competition is not very high. We remark that \mathcal{R}_0 is always greater than 1 and, as expected from formula (4.5), it is also greater than the one computed without vector transmission. In fact in this latter case $\mathcal{R}_0^h \sim 0.73$ (see Section 4.A), thus mosquitoes are crucial for the pathogen invasion and transmission.

Figure 4.1b (right panel) shows how \mathcal{R}_0 is influenced by competition and its contribution to the death rate, represented by a_{12}, a_{21} . \mathcal{R}_0 is greater when host death rates are less affected by competition (as this increases expected life of infected individuals) and, in all three cases, it increases linearly with $c_{12} = c_{21}$. Since the three cases ($a_{12} = a_{21} = 0.1, 0.5, 0.9$) do not differ substantially, from now on we consider only the

case with $a_{12} = a_{21} = a_{22} = a_{11} = 0.5$. As observed in many field studies, *Cx. pipiens* may

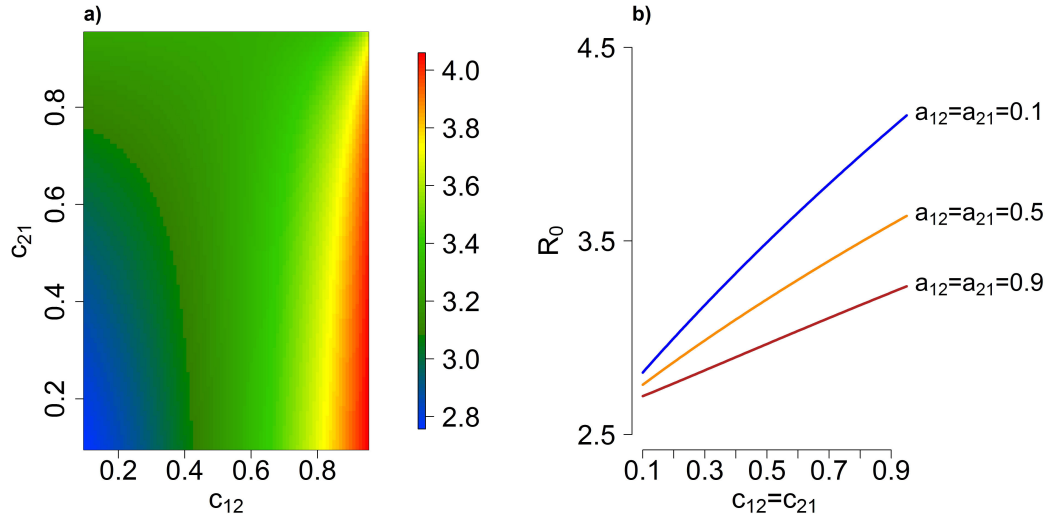


Figure 4.1: Panel a) \mathcal{R}_0 according to the competition coefficients with $a_{12} = a_{21} = 0.5$. Panel b) \mathcal{R}_0 according to the competition coefficients (only for the case $c_{21} = c_{12}$) and three different values for $a_{12} = a_{21}$. In both panels $b_{max} = 0.2$.

show different feeding preferences for different avian species (Kilpatrick *et al.*, 2006a; Simpson *et al.*, 2012; Thiemann *et al.*, 2011). We say that a species, say i , is preferred if $\frac{b_i}{b_{max}} > \frac{N_i}{N_i+N_j}$, i.e. its fraction of bites is higher than its frequency. Hence we can model the mosquito biting preference introducing, as in (Simpson *et al.*, 2012), the feeding preference index $\delta_V, \delta_V \geq 1$. According to this the biting rates become

$$b_i = b_{max} \frac{\delta_V N_i}{\delta_V N_i + N_j}, \quad b_j = b_{max} \frac{N_j}{\delta_V N_i + N_j}.$$

We study the cases $b_{max} = 0.1, 0.2, 0.3$; as the biting rate can be interpreted as the reciprocal of the duration of the gonotrophic cycle, we are assuming that it varies between 3 and 10 days, that seems to be a realistic estimate (Faraj *et al.*, 2006; Jones *et al.*, 2012). Figure 4.2 shows how the value of \mathcal{R}_0 depends on the values of the different ecological ingredients (competition coefficients c_{12}, c_{21} and vector feeding preference δ_V). Continuous lines represent the case when species 1 is preferred, while dashed lines when the vector prefers species 2. On the x -axis δ_V , the feeding preference index, ranges from 1 to 10. Different panels refer to different values of (c_{12}, c_{21}) that assume respectively the values of (0.1, 0.5, 0.9).

In every case we observe that $\mathcal{R}_0 > 1$, so the infection-free equilibrium will always be unstable.

The interplay of both competition and feeding preference is rather complex; however we see that they both affect significantly \mathcal{R}_0 . Higher values of \mathcal{R}_0 can be observed when the vector prefers to feed on the less abundant host. For example, if species 1 is preferred and $c_{12} = 0.9, c_{21} = 0.1$ (i.e. species 1 is less abundant than species 2), we can observe that \mathcal{R}_0 reaches its maximum values. Conversely, if the most abundant species is preferred, \mathcal{R}_0 does not seem to increase significantly if δ_V increases. Actually, it may slightly decrease: for instance if $c_{12} = 0.5, c_{21} = 0.1, b_{max} = 0.1$ and species 2, the less infectious one, is

preferred, then \mathcal{R}_0 is 1.49, 1.46, 1.49, 1.5 for $\delta_V = 1, 2, 3, 4$ respectively (see blue dashed line in upper central panel). Eventually, we can also note that if no species is ecologically advantaged (i.e. $c_{12} = c_{21}$, panels on the diagonal), then the patterns are quite similar but the values are higher when competition is strong ($c_{12} = c_{21} = 0.9$) and if species 1 is preferred.

Figure 4.2 shows the case with both horizontal and vector transmission. The results for the model considering only vector transmission are very similar and presented in Section 4.A.

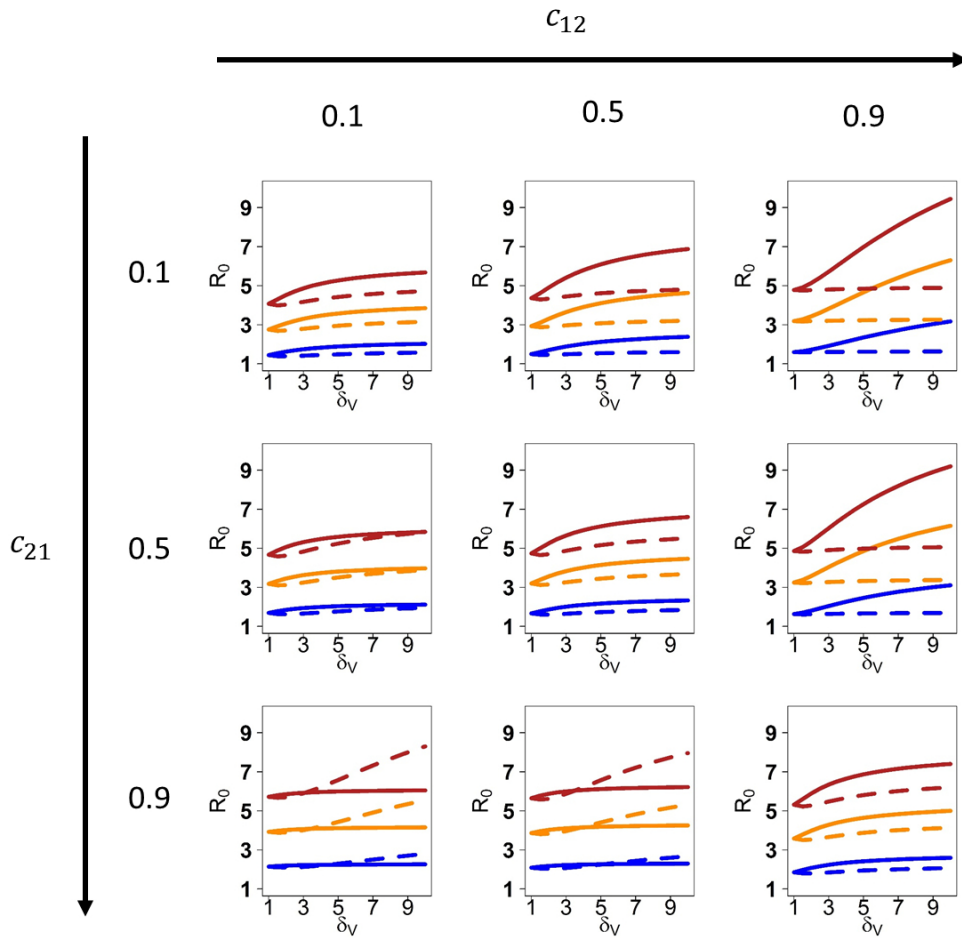


Figure 4.2: \mathcal{R}_0 with $b_{max} = 0.1$ (blue), 0.2 (orange) and 0.3 (red) as function of the competition coefficients $c_{12}, c_{21} \in \{0.1, 0.5, 0.9\} \times \{0.1, 0.5, 0.9\}$ and the feeding preference index δ_V ranging from 1 to 10. Continuous (dashed) lines regard the case when species 1 (2) is preferred.

4.3.2 Effect of competition and shifting mosquito feeding preference on infection seasonal dynamics

To model a typical season, we add another host type M , representing a mammal species, individuals of which are bitten at rate b_M . They do not have any interaction with other hosts and we assume they are a closed population. Moreover, we assume that they are dead-end hosts, so they do not infect the vector, and that they can recover and become immune for life.

Hence, we add to system (4.1) the three following equations

$$\begin{cases} N'_M &= 0 \\ I'_M &= p_{VM} b_M I_V \frac{S_M}{N_M} - \alpha_M I_M \\ R'_M &= R_M + \alpha_M I_M \end{cases}$$

The description of the new parameters and their values are reported in Table 4.2. As far as we know, there are no empirical estimates for the probability of transmission to any mammal species. Hence in our simulations we consider two values for p_{VM} . In the first case we assume $p_{VM} = p_{V1} = p_{V2} = 0.88$ as in (Bowman *et al.*, 2005), in the other case we assume p_{VM} value and order of magnitude less than p_{V1}, p_{V2} , i.e. $p_{VM} = 0.088$.

An important ecological aspect that affects mosquito seasonal dynamics is the diapause (Denlinger & Armbruster, 2014). It is a common mechanism adopted by mosquitoes to survive winter; in the case of *Cx. pipiens*, only adult females undergo diapause, i.e. they do not lay new eggs until the following spring. Daylight duration plays a key role in its activation (Spielman & Wong, 1973; Denlinger & Armbruster, 2014). To take into account this feature, we introduce a new variable γ , which is the function of the daylight duration following the experiment in (Spielman & Wong, 1973) presented in Chapter 2. It ranges from 0 to 1 and it is shown in Figure 4.3 (dotted line in panel d). The equation for V in (4.1) is replaced by

$$V' = [n_E \sigma \gamma b_{max} (1 - \rho_V V) - \mu_V] V.$$

The simulations start on June 1 in a given year with an infected bird belonging to species 1 and lasts 6 months. γ is modeled according to the daylight duration recorded at 46°N latitude, as presented in Figure 2.7.

Instead of simulating the deterministic system (4.1), we consider a Markov chain whose transition probabilities corresponds to the rates of the differential equations in (4.1) (see Section 4.A for more details). We decided to follow a stochastic approach to be able to account for demographic stochasticity, relevant for instance at the invasion stage.

| Parameter | Description | Value | Source |
|------------|--|---------|-------------------------------|
| N_M | Number of mammals | 1000 | Assumption |
| α_M | Recovery rate from WNV for dead end hosts (/day) | 0.07 | (Bowman <i>et al.</i> , 2005) |
| p_{VM} | Transmission probability mosquito to mammal | Varying | |

Table 4.2: Mammal parameters.

Baseline case

Here we present the outcome of the model when inter-species competition is absent, i.e. $c_{12} = c_{21} = 0$, the vector does not have a preferred avian species (i.e. $\delta_V = 1$) and its biting

rate is $b_{max} = 0.2$. So for each host type $i \in \{1, 2, M\}$ the biting rate is

$$b_i = b_{max} \frac{N_i}{N_1 + N_2 + N_M}.$$

Figure 4.3 shows the prevalence, i.e. the number of infected divided by the total number of individuals, for each host type i and the vector during the season. Avian species 1 experiences a higher infection than the other two host populations. Highest prevalence in the vector is recorded very late in the season; this may be due to our assumption that towards the end of the season almost no mosquitoes reproduce, as γ is very close to zero, and therefore the influx of susceptible vectors is very low in that period. Maximal prevalence in the host species is expected much earlier. For mammal, this occurs two months after the beginning of the season (10th of August), when $p_{VM} = p_{V1} = p_{V2}$ (black line in panel c), or around three months after the beginning (middle of September), when $p_{VM} = p_{V1} \cdot 10^{-1}$ (red line in panel c), similar to what happens in the avian populations.

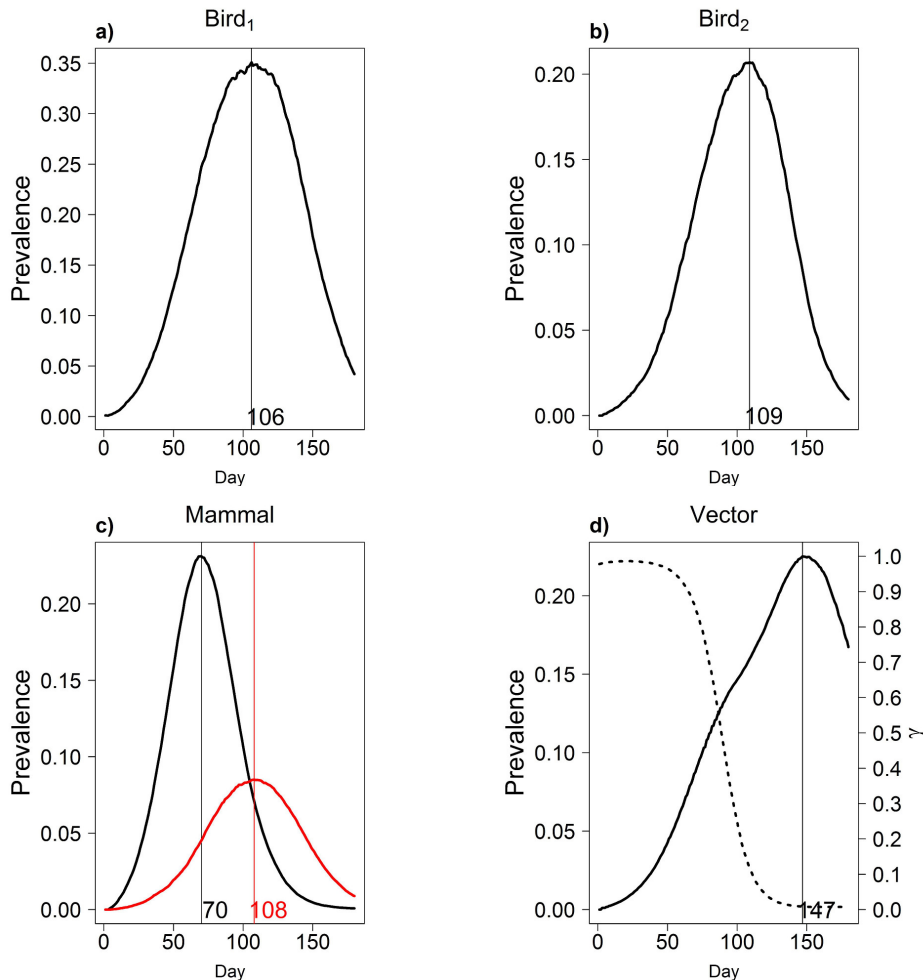


Figure 4.3: Prevalence for the three host types (panels a-c) and the vector (panel d). Black (red) line in panel c represent the outcome with $p_{VM} = 0.88$ (0.088). The vertical lines show the day at which the maximal prevalence is reached. Parameter γ is shown in panel d (dotted line).

Including feeding preference shift only

For the sake of simplicity we assume, in this Subsection, that there is no competition, i.e. $c_{12} = c_{21} = 0$, and that there is no preference between the two avian species, i.e. $\delta_V = 1$, but there is preference between birds and mammals. In particular this preference, which shifts through the season, is modeled according to the functions presented in (Kilpatrick *et al.*, 2006b). More specifically, we assume that at time t the vector bites a host of type $i \in \{bird, M\}$ with probability $f_i(t)$ with $f_{bird}(t) + f_M(t) = 1$. Therefore the biting rates are

$$b_i(t) = f_i(t)b_{max} \quad i \in \{bird, M\}$$

with $f_i(t)$ as shown in Figure 4.4 (panels a-c) and

$$b_i = b_{bird} \frac{N_i}{N_i + N_j} \quad i, j \in \{1, 2\}.$$

The inclusion of shifts in feeding preference significantly affects virus spread. As shown in Figure 4.4, the highest prevalences for all populations occur earlier compared to the scenario in which the biting rates are time independent (Figure 4.3). More precisely, they are expected about two months (beginning of August) after the introduction of the first infected bird. The two avian species exhibit a similar pattern, but we can note that, compared to the baseline case, the prevalences have a much higher maximum (about 60%), and they decrease to zero more quickly.

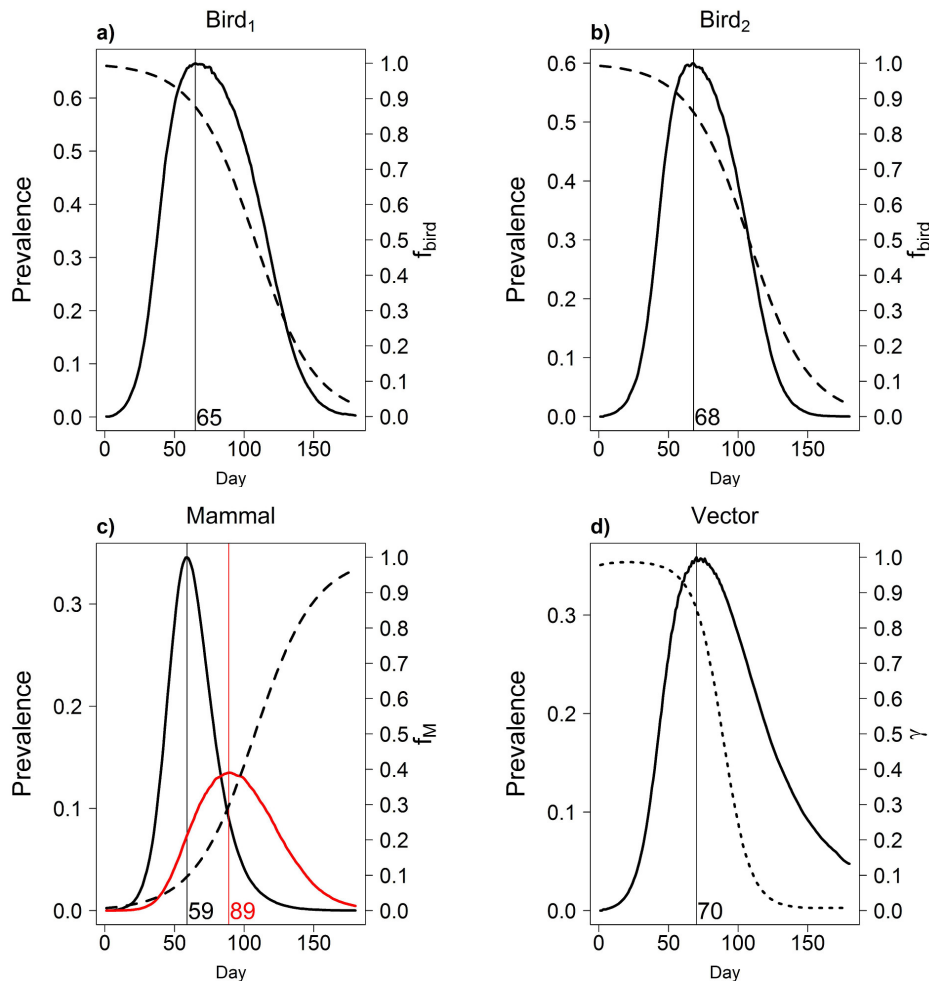


Figure 4.4: Prevalence for the three host types (panels a-c) and the vector (panel d). Black (red) line in panel c represent the outcome with $p_{VM} = 0.88$ (0.088). The shifting mosquito feeding preferences are represented in panel a, b ($f_{bird}(t)$) and c ($f_M(t)$) with dashed lines. The vertical lines show the times when the maximal prevalence is reached. The function γ (diapause rate) is shown in panel d (dotted line).

The complete model without feeding preference shift

In this case we allow c_{12} and c_{21} to be different from 0, while $b_{max} = 0.2$ as previously and $p_{VM} = 0.88$ as in (Bowman *et al.*, 2005). We explore a range of c_{12}, c_{21} combinations, with $(c_{12}, c_{21}) \in (0.05, 1) \times (0.05, 1)$. Moreover, we study three cases of vector preference for birds: no preference, preference for species 1 or for species 2, in which cases $\delta_V = 5$.

The inclusion of competition produces rather different outcomes, depending on vector preference, as shown in Figure 4.5, where the central column presents the no-preference case while the first and third column show the cases of preference for species 1 and 2 respectively. When there is no preference between the two bird species, all four populations present smaller maximal prevalences if the species with higher infectiousness (1) is less abundant, i.e. if it is severely affected by the competition with the other ($c_{12} \gg c_{21}$). The same observation can be made for the vector in the case it prefers the more infectious bird species (1), and when this latter has a strong ecological disadvantage ($c_{12} > 0.6$). For avian species, the maximal prevalence is higher for the preferred bird population. Moreover, for the preferred avian species (say i), its highest maximal prevalence values are reached when $c_{ij} \gg c_{ji}$, i.e. when it has a strong ecological disadvantage. This corresponds to what found for the value of \mathcal{R}_0 in Section 4.3.1.

If species 1 (with higher probability of infecting the vector) is preferred, then the maximal prevalence for both host and vector population is recorded much earlier in the season compared to when the vector prefers species 2 or there is no preference between them (see Figure 4.6, blue boxplots). Moreover, as shown in Figure 4.9, if this host type is also extremely affected by competition with the other species, then the vector maximal prevalence is expected less than two months after the beginning of the epidemics, so much earlier with respect to cases with low competition coefficients values.

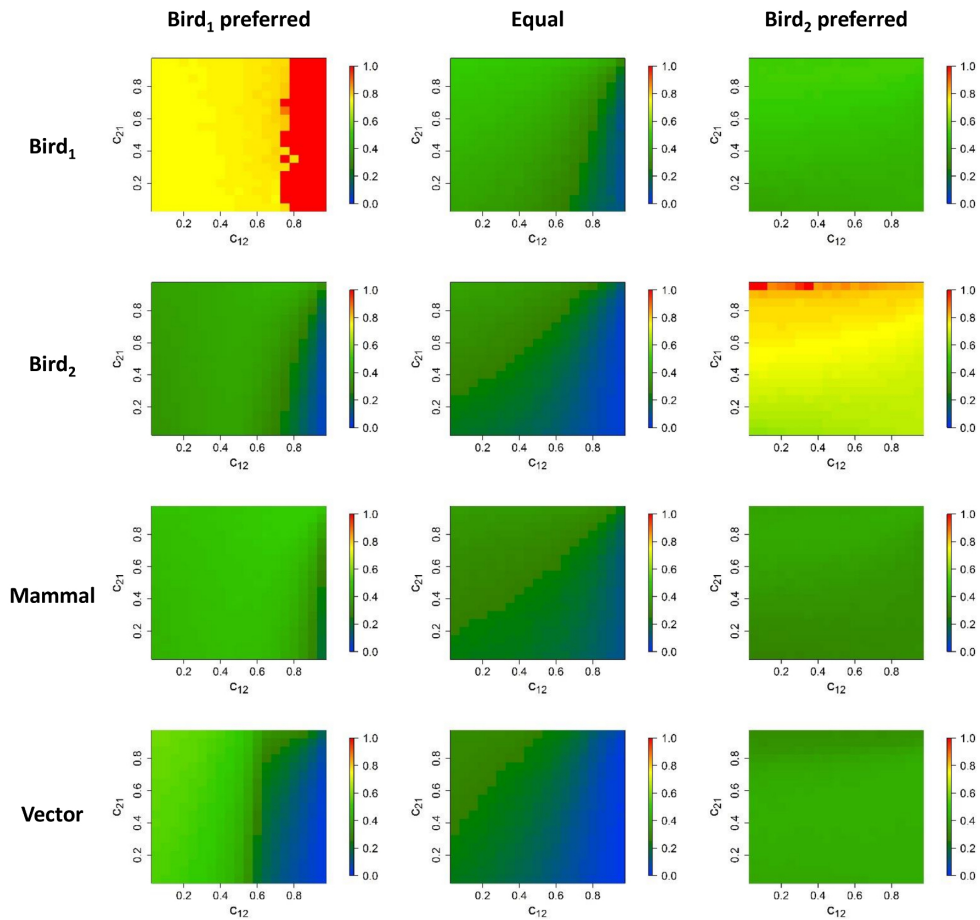


Figure 4.5: Prevalence for the three host types and the vector for the model without feeding preference shift, where species 1 (left) or species 2 (right) is preferred ($\delta_V = 5$), or there is no preference ($\delta_V = 1$, center). Values range from 0 (dark blue) to 1 (bright red). Avian species 1 is assumed to be more infectious than species 2 ($p_{1V} > p_{2V}$).

The complete model with feeding preference shift

In this Subsection, we study how the virus circulation is affected by competition with the time-dependent biting rates as presented in Figure 4.4.

As shown in Figure 4.7, if the vector changes its feeding preference during the season, then the expected maximal prevalence in vector, hosts and mammals increases in comparison with the case with constant preference. This is consistent with what observed when we investigated the case with time-dependent biting rates but without competition.

If there is no preference between the two bird populations (central column), it can be seen that the lowest maximal prevalences are expected when the competition is not particularly high, similarly to what we observed for \mathcal{R}_0 in Figure 4.1. On the other hand, if there is a preference for species i , its maximal prevalence is much higher than that of the other avian population. Furthermore, if the preferred host species is strongly affected by competition (large c_{ij}), both avian maximal prevalences are larger, consistent with the computation of \mathcal{R}_0 in Section 4.3.1 and with the simulations presented when we studied the same scenario with time-independent biting rates.

In this case, infection prevalence in mammals and vector is not significantly affected by bird competition and its value is around 50% for every (c_{12}, c_{21}) combination.

As found previously in the case without preference between birds and no competition, assuming a shifting mosquito feeding preference causes a large anticipation of the time when maximal prevalence is reached. In fact, as shown in Figure 4.6, avian and vector infection prevalence peaks are expected to occur from two to three months earlier respectively. Moreover, the maximal prevalence is recorded earlier in the season when mosquitoes prefer to feed on the more infectious avian species (see Figure 4.6, orange boxplots), while there does not seem to be a significant difference between the cases $\delta_V = 1$ and $\delta_V = 5$ when species 2 is preferred.

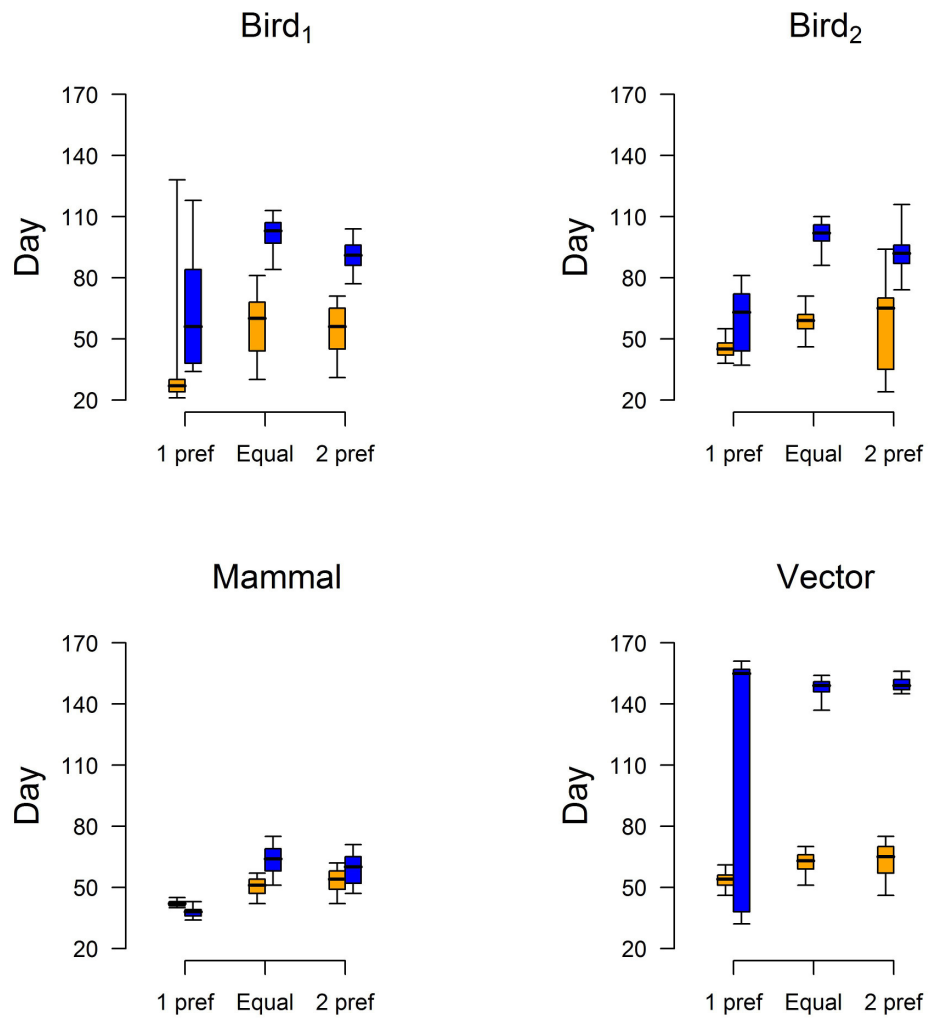


Figure 4.6: Boxplot (2.5%, 25%, 75% and 97.5% quantile and median) of the maximal prevalence recording time (number of days after the introduction of the first infected host) in the cases with competition coefficients $(c_{12}, c_{21}) \in (0.05, 1) \times (0.05, 1)$, and where species 1 or species 2 is preferred ($\delta_V = 5$), and when there is no preference ($\delta_V = 1$) with (without) the assumption of shifting vector feeding preference in orange (in blue). Whiskers: 2.5% and 97.5% quantiles; box: 25% and 75% quantiles; thick line: median.

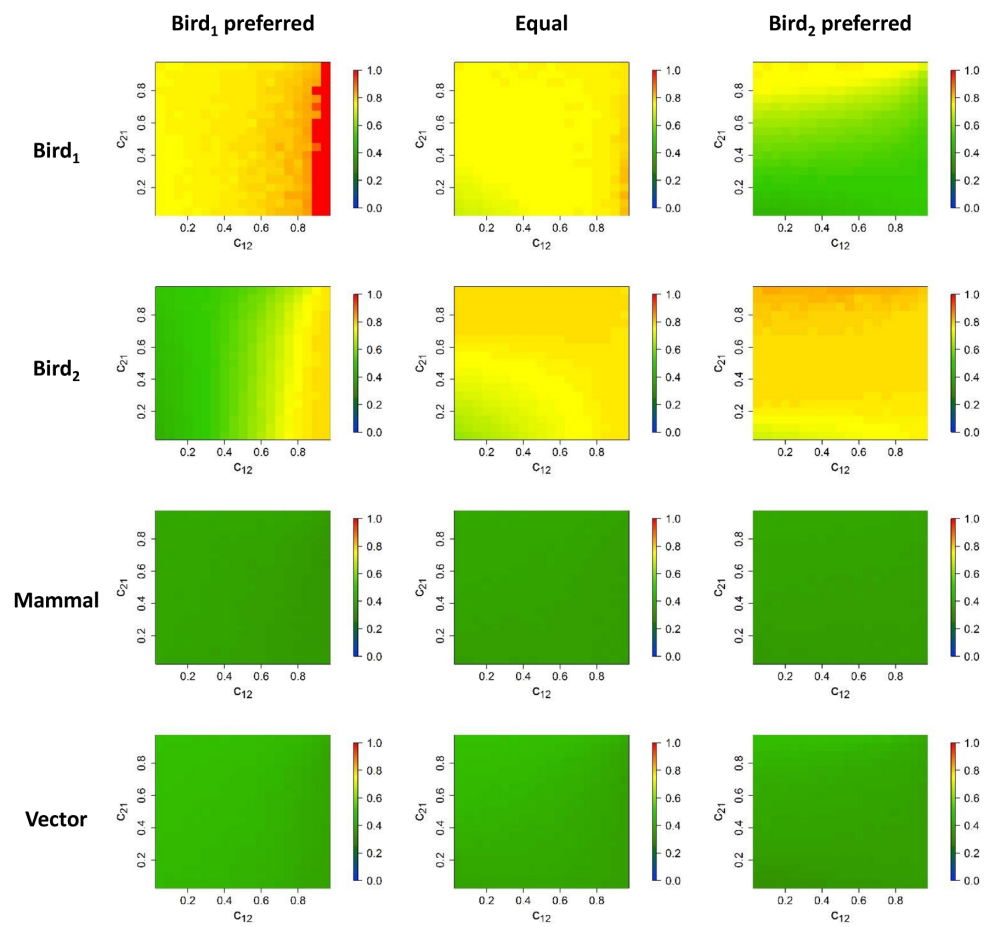


Figure 4.7: Prevalence for the three host types and the vector in the cases with competition and time-dependent biting rates, where species 1 (left) or species 2 (right) is preferred ($\delta_V = 5$), or there is no preference ($\delta_V = 1$, center). Values range from 0 (dark blue) to 1 (bright red).

4.4 Conclusions

In this paper, we presented a mathematical framework to investigate a vector-borne infection spreading in a multi-host community where individuals can interact with each other epidemiologically as well as ecologically (in particular by competition), following the study presented in (Roberts & Heesterbeek, 2013) and the model proposed in (Lord *et al.*, 1996).

We observed that competition may increase \mathcal{R}_0 by decreasing host population sizes (and thus increasing vector/host ratios), but that at the same time it might decrease host life expectancy and in this way decrease \mathcal{R}_0 . A general pattern of the effect of competition on \mathcal{R}_0 is therefore difficult to establish, as the influence on infection dynamics very much depends on the ecological particularities of the system one studies. \mathcal{R}_0 is also strongly influenced by the vectors' biting rate, but also by vector feeding preferences, which may cause a large increase of \mathcal{R}_0 if the less abundant host is the preferred one. On the other hand, \mathcal{R}_0 might be smaller if the vector tends to feed on the less competent host.

In order to be able to obtain more precise conclusions, we focused on a particular case, the spread of West Nile Virus within an avian population composed by two different species that share the same habitat and compete for resources. We explored a wide range of values for the ecological ingredients, such as ecological interactions and vector feeding preference, using epidemiological parameter values that have been estimated for WNV. We found that \mathcal{R}_0 can be strongly influenced by competition and feeding preferences (see Figures 4.1 and 4.2).

We also used the model, parameterized for WNV, to simulate seasonal epidemics, and thus studying the effect of competition and vector preference on transient dynamics. This model included also dead-end hosts, typically mammals for WNV, and allowed for a shifting preference of vectors, from birds in the first part of the season to mammals in the second part, as shown to occur in natural systems by Kilpatrick *et al.* (2006b), Thiemann *et al.* (2011) and Burkett-Cadena *et al.* (2012). One effect of the presence of dead-end hosts is a dilution effect (Keesing *et al.*, 2006), as they decrease the circulation of the virus by wasting, from the pathogen transmission point of view, a proportion of the vector bites. This effect is no longer observed when assuming time-dependent vector feeding preference; in fact, in this case mosquitoes bite only competent hosts at the beginning of the season, enhancing the increase of infection prevalence; indeed, the virus would circulate among mosquitoes with a higher incidence than in the case when mosquitoes are assumed to feed also on mammals, which are assumed to be dead-end hosts. From the simulations, it also appears that, with shifting vector preferences, infection prevalence in dead-end hosts and vectors is not influenced by bird competition (compare Figures 4.5 and 4.7), which in this case affects infection spread only among avian populations.

Shifting feeding preference during a season has another important consequence: the times of highest prevalence in a season are recorded around the same period for both vectors and birds, i.e. about two months after the start of the epidemics. This result agrees with actual observations. For instance, Bell *et al.* (2005), Lukacik *et al.* (2006) and Reisen *et al.* (2010) recorded the highest WNV prevalence in mosquitoes in August in different parts of North America, while Nemeth *et al.* (2007) and Kwan *et al.* (2010) noted that the highest records of WNV avian cases are during summer (June-July). On the other hand, if it is assumed that vector feeding preferences are fixed throughout the season, one can see that the prevalence peaks later in the season and in vectors later than in birds. We argue that the assumption of changing feeding preferences is impor-

tant when studying the seasonal pattern of infections in vector-borne pathogen models. The model considered here does not attempt to be realistic for any specific infection, even though some assumptions and parameter values have been tailored for WNV. In reality, *Culex* mosquitoes bite a large number of bird and mammal species, some of which will be dead-end hosts, others will be of different competence for the transmission of WNV (Komar *et al.*, 2003). The model we studied considered only two avian species, both highly competent. Possibly, the rather high prevalence of WNV in the simulations, as well as the high values of \mathcal{R}_0 , are an artifact arising from this simplified situation. Another questionable assumption is that birds are not allowed to recover, though antibody-positive birds are not difficult to find in endemic areas (Jozan *et al.*, 2003; Mckee *et al.*, 2015). Including a compartment of recovered birds would not change the values of \mathcal{R}_0 but would certainly decrease infection prevalence.

Despite these limitations, we believe that this study of a simplified situation gave important insights on the importance of ecological interactions and vector feeding preferences in shaping infection dynamics in a multi-host-vector system.

4.A Supporting Information

Details on model simulations

We simulated the model presented in the main text with a stochastic approach by considering a Markov chain whose transition probabilities are equal to the rates present in the differential equations. More specifically, we chose a time step $\Delta t = 1$ day and updated each class of the system from time t to time $t + 1$ according to binomial processes. For instance, the number of new infected individuals of species 2 at day $t + 1$ will be given by

$$B\left(\frac{p_{V2}b_2I_V(t)}{N_2(t)}, S_2(t)\right).$$

For each studied case (so for instance for each competition coefficients combination) we performed 100 stochastic simulations and considered their average.

\mathcal{R}_0 without vector transmission

If we assume the pathogen can be passed horizontally among individuals of only one species, say 1, then, using the same notation of the main text, $\mathcal{R}_0^h = \frac{\beta_{11}p_{11}}{a_1 + \tilde{\mu}_1}$ where

$\tilde{\mu}_1 = \mu_1 + r_1 \frac{a_{11}N_1^* + a_{12}c_{12}N_2^*}{K_1}$, $N_1^* = \frac{K_1 - c_{12}K_2}{1 - c_{12}c_{21}}$, $N_2^* = \frac{K_2 - c_{21}K_1}{1 - c_{12}c_{21}}$. If, as in the main text, $a_{12} = a_{21} = a$ and $K_1 = K_2 = K$, then

$$\begin{aligned} \tilde{\mu}_1 &= \mu_1 + r_1 \frac{a_{11}N_1^* + a_{12}c_{12}N_2^*}{K_1} = \mu_1 + r_1 \frac{aN_1 + ac_{12}N_2}{K} \\ &= \mu_1 + \frac{r_1}{K} \left(a \frac{K - c_{12}K}{1 - c_{12}c_{21}} + ac_{12} \frac{K - c_{21}K}{1 - c_{12}c_{21}} \right) \\ &= \mu_1 + r_1 \frac{a}{1 - c_{12}c_{21}} (1 - c_{12} + c_{12}(1 - c_{21})) = \mu_1 + r_1 a \end{aligned}$$

Thus using the values proposed in the main text $\beta_{11}p_{11} = 0.33$, $\alpha_1 = 0.2$, $r_1 = a = 0.5$, $\mu_1 = 0.001$, we get $\mathcal{R}_0^h \sim 0.73$.

\mathcal{R}_0 and seasonal dynamics without horizontal transmission

Here we assume there is no horizontal transmission between species 1 individuals ($p_{11} = 0$), $b_{max} = 0.2$, $\delta_V = 1$ and $p_{VM} = p_{V1}$. As reported in Figure 4.8, in this case \mathcal{R}_0 is substantially equal to the one computed with $p_{11} \neq 0$.

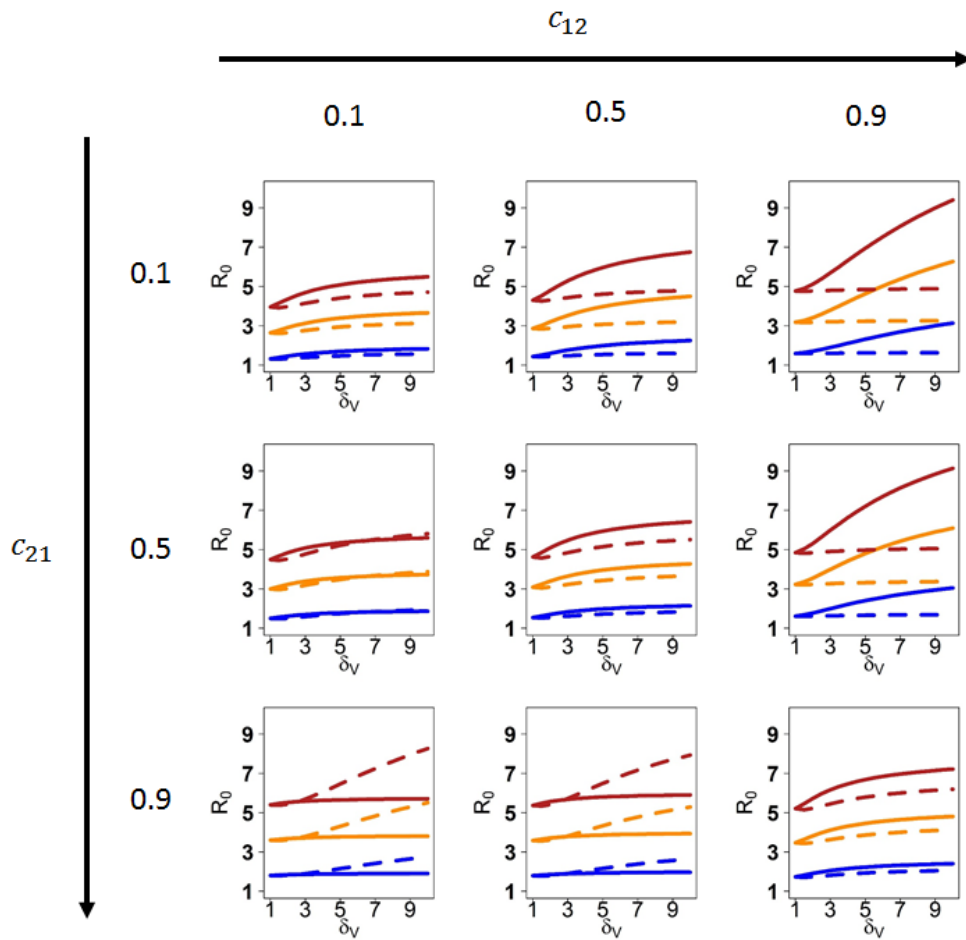


Figure 4.8: \mathcal{R}_0 in the case $p_{11} = 0$ with $b_{max} = 0.1$ (blue), 0.2 (orange) and 0.3 (red) as function of the competition coefficients $c_{12}, c_{21} \in \{0.1, 0.5, 0.9\} \times \{0.1, 0.5, 0.9\}$ and the feeding preference index δ_V ranging from 1 to 10. Continuous (dashed) lines regard the case when species 1 (2) is preferred.

Infection peak times for the complete model without feeding preference shift

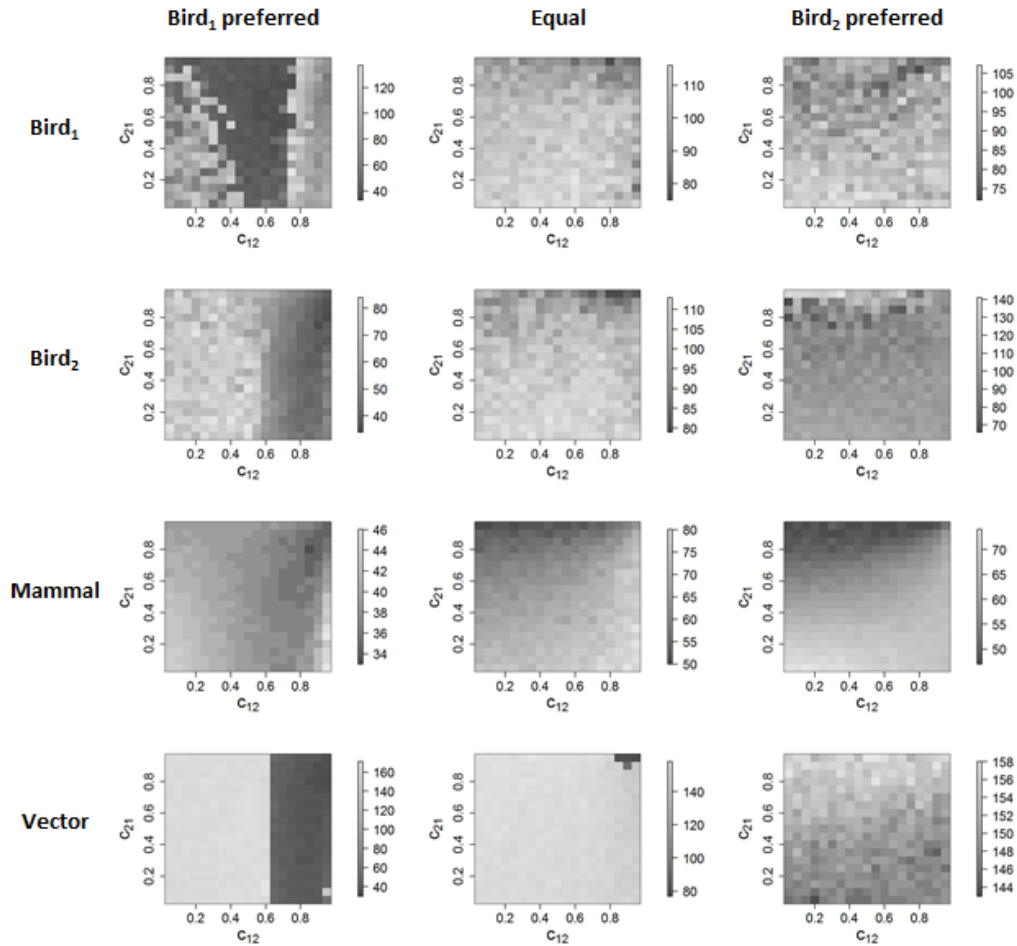


Figure 4.9: Maximal prevalence recording time (number of days after the introduction of the first infected host) for cases species 1 (left) and species 2 (right) preferred and no preference (center) with competition.

Conclusions

In this thesis, that is a collection of scientific articles, we have seen that mathematical models represent a very helpful tool to investigate vector-borne infections, in particular from the vector dynamics perspective. The statistical and mechanistic models developed throughout my work provided new important insights on the dynamics of *Cx. pipiens* mosquitoes and its dependence on different external factors. We observed that mosquito abundance depends strongly on several abiotic factors, especially temperature and rain-falls. In this context, the model developed in Chapter 2 allowed us to explore several what-if scenarios, providing interesting insights on how possible climatic changes could affect the future density of this vector. Furthermore, we presented one of the first efforts of modeling the effect of intraspecific competition between *Cx. pipiens* and *Ae. albopictus*. We highlighted that what so far observed only in laboratory experiments might occur also in natural conditions and that *Cx. pipiens* abundance might be strongly affected by this invasive species.

The models presented in my thesis can be used not only to investigate *Cx. pipiens* population dynamics but can be adapted to answer other important epidemiological questions. In fact, the model presented in Chapter 2 can be used to study the spread of WNV during a typical breeding season, or any other potential virus that sees *Cx. pipiens* as competent vector, by adding for instance one or more classes of hosts (eg. birds, mammals) and by dividing the vector population into susceptible and infected compartments. Understanding the interaction between climatic variables and vector abundance can be crucial to improve our estimates of epidemiological risks for arboviruses for which *Cx. pipiens* is a competent vector, and also for the assessment of vector control strategies.

As we noted in Chapter 4, such possible epidemiological model could be greatly improved by carefully evaluating *Cx. pipiens* feeding preference in the considered study area, allowing for a more precise determination of the infection risk.

The extension developed in Chapter 3 can be also adapted for an epidemiological framework. Still focusing on a *Cx. pipiens*-borne infection, one could investigate how competition with *Ae. albopictus* might affect the transmission of the transmitted pathogen. Interspecific competition negatively affects *Cx. pipiens* abundance and thus it might limit the circulation of the infection. Besides, recent findings have shown that interspecific competition at the larval stage may affect strongly the viral competence of adult mosquitoes of several *Aedes* and *Culex* species. If similar effects exist in the competition between *Ae. albopictus* and *Cx. pipiens*, they would significantly impact the viral susceptibility and transmissibility of local mosquito populations and should therefore be considered in the estimation of outbreak risks.

Although based on very simple assumptions, the results provided in Chapter 4 highlight that ecological interactions between different hosts might strongly affect pathogen transmission. This model, easily adaptable to other vector-borne infections, represents one of the first attempts to study the interaction of ecological processes and the epidemiology of vector-borne infections. This research topic should be definitely studied more deeply in the future, also in the case of other vector-borne pathogens. For instance, Lyme disease, transmitted by ticks to mammal hosts including humans, or African trypanosomiasis, transmitted by the tsetse fly to humans and other animal species.

To conclude, we can affirm that interspecific interactions are crucial also in science: in fact, my thesis is the result of cross-contamination processes between different research fields (mathematics, statistics, biology, entomology, epidemiology, etc.). Using mathematics we can help in answering different biological and epidemiological questions very important for entomologists and public health authorities, providing very helpful insights on *Cx. pipiens* and WNV dynamics. Moreover, we offered various ideas for possible future studies, which I hope other scientists (modelers, data analysts, etc.) will find intriguing and stimulating.

Acknowledgments

First of all I would like to thank Roberto and Andrea, for their precious help and guidance during these three years. This thesis would not have been possible without you and your stimulating supervision. Thank you so much for all the time you spent for me and for having given me the opportunity to travel and meet a lot of new interesting people.

I am very grateful to all the Fondazione Bruno Kessler team. Stefano, Piero and Giorgio taught me a lot on mathematical modeling, coding, writing scientific papers and more generally what "doing research" means. Thank you guys!

The six months I spent in Utrecht were a very satisfying experience, which widened my mathematical knowledge as well as my research interests. Thank you Hans for your great patience, friendliness and your countless helpful suggestions.

I want to thank the LExEM project (funded by the Autonomous Province of Trento - Bando Grandi Progetti 2012) and the FIRS>T research school of the Research and Innovation Centre at Fondazione Edmund Mach, which funded my scholarship and made my research possible. Thanks to all the people involved in the project, it's been a pleasure to work with you!

Thanks to all my friends spread throughout the world, who always encouraged and supported me. Although impossible to name everyone, I want you to know I've been very lucky to meet you and share many different moments of my life with you.

My family always believed in me and allowed me to choose and build my future. Thank you so much for all your patience and support over all these years, without you I would never have got this far.

Last but not least a big thank goes to Marco, who has always been a huge fixed point in my life, even in the most stressful and hard times.

Bibliography

- Agnew, P., Haussy, C., & Michalakis, Y. 2010. Effects of density and larval competition on selected life history traits of *Culex pipiens quinquefasciatus* (Diptera: Culicidae). *Journal of Medical Entomology*, **37**(5), 732–755.
- Akaike, H. 1974. A new look at the statistical model identification. *IEEE Transactions on Automatic Control*, **19**(6), 716–723.
- Alto, B.W., & Lounibos, L.P. 2013. Vector competence for arboviruses in relation to the larval environment of mosquitoes. *Pages 81–101 of: Ecology of parasite-vector interactions*. Ecology and control of vector-borne diseases, no. 3. Wageningen Academic Publishers.
- Alto, B.W., Lounibos, L.P., Higgs, S., & Juliano, S.A. 2005. Larval competition differentially affects arbovirus infection in *Aedes* mosquitoes. *Ecology*, **86**(12), 3279–3288.
- Alto, B.W., Lounibos, L.P., Mores, C.N., & Reiskind, M.H. 2008. Larval competition alters susceptibility of adult *Aedes* mosquitoes to dengue infection. *Proceedings of the Royal Society B: Biological Sciences*, **275**(1633), 463–471.
- ArboNET, Arboviral Diseases Branch, Centers for Disease Control and Prevention. 2014. *West Nile virus disease cases reported to CDC by week of illness onset, 1999-2014*. www.cdc.gov/westnile/resources/pdfs/data/4-wnv-week-onset_1999-2014_06042015.pdf. Accessed: 2015-06-23.
- Arifin, S.M.N., Zhou, Y., Davis, G.J., Gentile, J.E., Madey, G.R., & Collins, F.H. 2014. An agent-based model of the population dynamics of *Anopheles gambiae*. *Malaria Journal*, **13**, 424.
- Armistead, J.S., Arias, J.R., Nishimura, N., & Lounibos, L.P. 2008. Interspecific larval competition between *Aedes albopictus* and *Aedes japonicus* (Diptera : Culicidae) in northern Virginia. *Journal of Medical Entomology*, **45**(4), 629–637.
- Arpa Piemonte. 2014. *Dati Ambientali*. <http://www.arpa.piemonte.it/dati-ambientali>. Accessed: 2014-06-23.
- Baldacchino, F., Caputo, B., Chandre, F., Drago, A., della Torre, A., Montarsi, F., & Rizzoli, A. 2015. Control methods against invasive *Aedes* mosquitoes in Europe: a review. *Pest Management Science*, **71**(11), 1471–1485.

- Barton, K. 2013. *Package 'MuMIn'*.
- Barzon, L., Pacenti, M., Franchin, E., Lavezzo, E., Masi, G., Squarzon, L., Pagni, S., Toppo, S., Russo, F., Cattai, M., Cusinato, R., & Palu, G. 2013. Whole genome sequencing and phylogenetic analysis of West Nile virus lineage 1 and lineage 2 from human cases of infection, Italy, August 2013. *Euro Surveillance: Bulletin Europeen Sur Les Maladies Transmissibles = European Communicable Disease Bulletin*, **18**(38).
- Beck-Johnson, L.M., Nelson, W.A., Paaijmans, K.P., Read, A.F., Thomas, M.B., & Bjornstad, O.N. 2013. The Effect of Temperature on Anopheles Mosquito Population Dynamics and the Potential for Malaria Transmission. *Plos One*, **8**(11), e79276.
- Becker, N. 1997. Microbial control of mosquitoes: management of the upper rhine mosquito population as a model programme. *Parasitology Today*, **13**(12), 485–487.
- Becker, N., Petric, D., Zgomba, M., Boase, C., Dahl, C., Madon, M., & Kaiser, A. 2010. *Mosquitoes and their control*. Springer.
- Bell, J.A., Mickelson, N.J., & Vaughan, J.A. 2005. West Nile virus in host-seeking mosquitoes within a residential neighborhood in Grand Forks, North Dakota. *Vector-borne and Zoonotic Diseases*, **5**(4).
- Bellini, R., Zeller, H., & Van Bortel, W. 2014. A review of the vector management methods to prevent and control outbreaks of West Nile virus infection and the challenge for Europe. *Parasites & Vectors*, **7**, 323.
- Bernard, K.A., Maffei, J.G., Jones, S.A., Kauffman, E B., Ebel, G., Dupuis, A.P., Ngo, K.A., Nicholas, D.C., Young, D.M., Shi, P.Y., Kulasekera, V.L., Eidson, M., White, D.J., Stone, W.B., Kramer, L.D., & NY State West Nile Virus Surveillance Team. 2001. West Nile virus infection in birds and mosquitoes, New York State, 2000. *Emerging Infectious Diseases*, **7**(4), 679–685.
- Bevins, S.N. 2007. Invasive mosquitoes, larval competition, and indirect effects on the vector competence of native mosquito species (Diptera: Culicidae). *Biological Invasions*, **10**(7), 1109–1117.
- Bisanzio, D., Giacobini, M., Bertolotti, L., Mosca, A., Balbo, L., Kitron, U., & Vazquez-Prokopec, G. M. 2011. Spatio-temporal patterns of distribution of West Nile virus vectors in eastern Piedmont Region, Italy. *Parasites & Vectors*, **4**(1), 230.
- Bokil, V.A., & Manore, C.A. 2013. Linking population dynamics and disease models for multi-host pathogen systems: implications for pathogen and species invasion. *Journal of Biological Systems*, **21**(4).
- Bolker, B.M. 2008. *Ecological models and data in R*. Princeton University Press.
- Bowers, R.G., & Turner, J. 1997. Community Structure and the Interplay between Interspecific Infection and Competition. *Journal of Theoretical Biology*, **187**, 95–109.
- Bowman, C., Gumel, A.B., van den Driessche, P., Wu, J., & Zhu, H. 2005. A mathematical model for assessing control strategies against West Nile virus. *Bulletin of Mathematical Biology*, **67**, 1107–1133.

- Box, G.E.P., & Cox, D.R. 1964. An Analysis of Transformations. *Journal of the Royal Statistical Society. Series B (Methodological)*, **26**(2), 211–252.
- Brown, H., Diuk-Wasser, M., Andreadis, T., & Fish, D. 2008. Remotely-Sensed Vegetation Indices Identify Mosquito Clusters of West Nile Virus Vectors in an Urban Landscape in the Northeastern United States. *Vector-Borne and Zoonotic Diseases*, **8**(2), 197–206.
- Burkett-Cadena, N.D., Hassan, H.K., Eubanks, M.D., Cupp, E.W., & Unnasch, T.R. 2012. Winter severity predicts the timing of host shifts in the mosquito *Culex erraticus*. *Biology Letters*, **8**(4), 567–569.
- Burnham, Kenneth P., Anderson, David R., & Huyvaert, Kathryn P. 2011. AIC model selection and multimodel inference in behavioral ecology: some background, observations, and comparisons. *Behavioral Ecology and Sociobiology*, **65**(1), 23–35.
- Burnham, K.P., & Anderson, D.R. 2002. *Model selection and multimodel inference: a practical information-theoretic approach*. Springer.
- Cailly, P., Tran, A., Balenghien, T., L'Ambert, G., Toty, C., & Ezanno, P. 2012. A climate-driven abundance model to assess mosquito control strategies. *Ecological Modelling*, **227**, 7–17.
- Calistri, P., Giovannini, A., Savini, G., Monaco, F., Bonfanti, L., Ceolin, C., Terregino, C., Tamba, M., Cordioli, P., & Lelli, R. 2010. West Nile Virus Transmission in 2008 in North-Eastern Italy. *Zoonoses and Public Health*, **57**(3), 211–219.
- Campbell, G., Marfin, A., Lanciotti, R., & Gubler, D. 2002. West Nile virus. *The Lancet Infectious Diseases*, **2**(9), 519–529.
- Carrieri, M., Bacchi, M., Bellini, R., & Maini, S. 2003. On the Competition Occurring Between *Aedes albopictus* and *Culex pipiens* (Diptera: Culicidae) in Italy. *Environmental Entomology*, **32**(6), 1313–1321.
- Chouin-Carneiro, T., Vega-Rua, A.S., Vazeille, M., Yebakima, A., Girod, R., Goindin, D., Dupont-Rouzeyrol, M., Lourenco-de Oliveira, R., & Failloux, A. 2016-03-03. Differential Susceptibilities of *Aedes aegypti* and *Aedes albopictus* from the Americas to Zika Virus. *PLOS Negl Trop Dis*, **10**(3), e0004543.
- Chowell, G., Diaz-Duenas, P., Miller, J.C., Alcazar-Velazco, A., Hyman, J.M., Fenimore, P.W., & Castillo-Chavez, C. 2007. Estimation of the reproduction number of dengue fever from spatial epidemic data. *Mathematical Biosciences*, **208**(2), 571–589.
- Chuang, T., Henebry, G.M., Kimball, J.S., VanRoekel-Patton, D.L., Hildreth, M.B., & Wimberly, M.C. 2012. Satellite microwave remote sensing for environmental modeling of mosquito population dynamics. *Remote Sensing of Environment*, **125**, 147–156.
- Ciota, A.T., Matakchiero, A.C., Kilpatrick, A.M., & Kramer, L.D. 2014. The Effect of Temperature on Life History Traits of *Culex* Mosquitoes. *Journal of Medical Entomology*, **51**(1), 55–62.
- Cleckner, H.L., Allen, T.R., & Bellows, A.S. 2011. Remote Sensing and Modeling of Mosquito Abundance and Habitats in Coastal Virginia, USA. *Remote Sensing*, **3**(12), 2663–2681.

- Clements, A.N. 1992. *The Biology of Mosquitoes: Development, nutrition, and reproduction*. Chapman & Hall.
- Colborn, J.M., Smith, K.A., Townsend, J., Damian, D., Nasci, R.S., & Mutebi, J. 2013. West Nile virus outbreak in Phoenix, Arizona—2010: entomological observations and epidemiological correlations. *Journal of the American Mosquito Control Association*, **29**(2), 123–132.
- Costanzo, K.S., Mormann, K., & Juliano, S.A. 2005. Asymmetrical Competition and Patterns of Abundance of *Aedes albopictus* and *Culex pipiens* (Diptera: Culicidae). *Journal of medical entomology*, **42**(4), 559–570.
- Costanzo, K.S., Muturi, E.J., Lampman, R.L., & Alto, B.W. 2011. The Effects of Resource Type and Ratio on Competition With *Aedes albopictus* and *Culex pipiens* (Diptera: Culicidae). *Journal of Medical Entomology*, **48**(1), 29–38.
- Cruz-Pacheco, G., Esteva, L., Montano-Hirose, J.A., & Vargas, C. 2005. Modelling the dynamics of West Nile virus. *Bulletin of Mathematical Biology*, **67**, 1157–1172.
- Cruz-Pacheco, G., Esteva, L., & Vargas, C. 2012. Multi-species interactions in West Nile virus infection. *Journal of Biological Dynamics*, **6**(2), 281–298.
- Degaetano, A.T. 2005. Meteorological effects on adult mosquito (*Culex*) populations in metropolitan New Jersey. *International journal of biometeorology*, **49**(5), 345–353.
- Deichmeister, J.M., & Telang, A. 2011. Abundance of West Nile virus mosquito vectors in relation to climate and landscape variables. *Journal of vector ecology: journal of the Society for Vector Ecology*, **36**(1), 75–85.
- Delatte, H., Gimonneau, G., Triboire, A., & Fontenille, D. 2009. Influence of temperature on immature development, survival, longevity, fecundity, and gonotrophic cycles of *Aedes albopictus*, vector of chikungunya and dengue in the Indian Ocean. *Journal of Medical Entomology*, **46**(1), 33–41.
- Delbart, N., Kergoat, L., Le Toan, T., Lhermitte, J., & Picard, G. 2005. Determination of phenological years in boreal regions using normalized difference water index. *Remote Sensing of Environment*, **97**(1), 26–38.
- Denlinger, D.L., & Armbruster, P.A. 2014. Mosquito diapause. *Annual Review of Entomology*, **59**, 73–93.
- Diekmann, O., Heesterbeek, J.A.P., & Roberts, M. 2010. The construction of next-generation matrices for compartmental epidemic models. *Interface*, **7**(47), 873–885.
- Diuk-Wasser, M. A., Brown, H. E., Andreadis, T. G., & Fish, D. 2006. Modeling the spatial distribution of mosquito vectors for West Nile virus in Connecticut, USA. *Vector borne and zoonotic diseases (Larchmont, N.Y.)*, **6**(3), 283–295.
- ECA&D project. 2013. *Home European Climate Assessment & Dataset*. <http://www.ecad.eu>.
- Eirayah, E., & Abugroun, Na. 1983. Effect of Temperature on Hatching Eggs and Embryonic Survival in the Mosquito *Culex-Quinquefasciatus*. *Entomologia Experimentalis Et Applicata*, **33**(3), 349–351.

- Erickson, R.A., Presley, S.M., Allen, L.J.S., Long, K R., & Cox, S.B. 2010. A stage-structured, *Aedes albopictus* population model. *Ecological Modelling*, **221**(9), 1273–1282.
- Estallo, E.L., Luduena-Almeida, F.F., Visintin, A.M., Scavuzzo, C.M., Lamfri, M.A., Introini, M.V., Zaidenberg, M., & Almiron, W.R. 2012. Effectiveness of normalized difference water index in modelling *Aedes aegypti* house index. *International Journal of Remote Sensing*, **33**(13), 4254–4265.
- European Centre for Disease Prevention and Control. 2013. *Annual epidemiological report reporting on 2010 surveillance data and 2011 epidemic intelligence data*. European Centre for Disease Prevention and Control.
- European Centre for Disease Prevention and Control. 2014. *Annual epidemiological report 2014 - emerging and vector-borne diseases*. European Centre for Disease Prevention and Control.
- European Centre for Disease Prevention and Control. 2016. *West Nile fever maps*. http://ecdc.europa.eu/en/healthtopics/west_nile_fever/West-Nile-fever-maps/pages/index.aspx. Accessed: 2017-01-11.
- European Environment Agency. 2014. *Corine Land Cover 2000-2006 changes*. <http://www.eea.europa.eu/data-and-maps/data/corine-land-cover-2000-2006>.
- Fan, G., Liu, J., van den Driessche, P., Wu, J., & Zhu, H. 2010. The impact of maturation delay of mosquitoes on the transmission of West Nile virus. *Mathematical Biosciences*, **228**, 119–126.
- Faraj, C., Elkohli, M., & Lyagoubi, M. 2006. Cycle gonotrophique de *Culex pipiens* (Diptera: Culicidae), vecteur potentiel du virus West Nile, au Maroc : estimation de la durée en laboratoire. *Bulletin de la Societe de pathologie exotique*, **99**(2), 119–121.
- Farajollahi, A., Fonseca, D.M., Kramer, L.D., & Kilpatrick, A.M. 2011. "Bird biting" mosquitoes and human disease: A review of the role of *Culex pipiens* complex mosquitoes in epidemiology. *Infection Genetics and Evolution*, **11**(7), 1577–1585.
- Fortuna, C., Remoli, M. E., Severini, F., Di Luca, M., Toma, L., Fois, F., Bucci, P., Boccolini, D., Romi, R., & Ciufolini, M.G. 2015. Evaluation of vector competence for West Nile virus in Italian *Stegomyia albopicta* (= *Aedes albopictus*) mosquitoes. *Medical and Veterinary Entomology*, **29**(4), 430–433.
- Gaibani, P., Cavrini, F., Gould, E.A., Rossini, G., Pierro, A., Landini, M.P., & Sambri, V. 2013. Comparative Genomic and Phylogenetic Analysis of the First Usutu Virus Isolate from a Human Patient Presenting with Neurological Symptoms. *Plos One*, **8**(5).
- Gamarra, J., Montoya, J., Alonso, D., & Sola, R.V. 2005. Competition and introduction regime shape exotic bird communities in Hawaii. *Biological Invasions*, **7**, 297–307.
- Gardner, A.M., Anderson, T.K., Hamer, G.L., Johnson, D.E., Varela, K.E., Walker, E.D., & Ruiz, M.O. 2013. Terrestrial vegetation and aquatic chemistry influence larval mosquito abundance in catch basins, Chicago, USA. *Parasites & Vectors*, **6**(1), 9.

- Geery, P.R., & Holub, R.E. 1989. Seasonal abundance and control of *Culex* spp. in catch basins in Illinois. *Journal of the American Mosquito Control Association*, **5**(4), 537–540.
- Gilks, W.R., Richardson, S., & Spiegelhalter, D. 1996. *Markov Chain Monte Carlo in practice*. Chapman & Hall.
- Gong, H., DeGaetano, A.T., & Harrington, L.C. 2011. Climate-based models for West Nile *Culex* mosquito vectors in the Northeastern US. *International Journal of Biometeorology*, **55**(3), 435–446.
- Guzzetta, G., Poletti, P., Montarsi, F., Baldacchino, F., Capelli, G., Rizzoli, A., Rosá, R., & Merler, S. 2016a. Assessing the potential risk of Zika virus epidemics in temperate areas with established *Aedes albopictus* populations. *Eurosurveillance*, **21**(15).
- Guzzetta, G., Montarsi, F., Baldacchino, F., Metz, M., Capelli, G., Rizzoli, A., Pugliese, A., Rosá, R., Poletti, P., & Merler, S. 2016b. Potential Risk of Dengue and Chikungunya Outbreaks in Northern Italy Based on a Population Model of *Aedes albopictus* (Diptera: Culicidae). *PLoS neglected tropical diseases*, **10**(6), e0004762.
- Han, L., & Pugliese, A. 2009. Epidemics in two competing species. *Nonlinear Analysis: Real World Applications*, **10**, 723–744.
- Hartemink, N.A., Davis, S.A., Reiter, P., Hubalek, Z., & Heesterbeek, J.A.P. 2007. The importance of bird-to-bird transmission for the establishment of West Nile Virus. *Vector-Borne and Zoonotic Diseases*, **7**, 575–584.
- Haylock, M.R., Hofstra, N., Klein Tank, A.M.G., Klok, E.J., Jones, P.D., & New, M. 2008. A European daily high-resolution gridded data set of surface temperature and precipitation for 1950–2006. *Journal of Geophysical Research: Atmospheres*, **113**.
- Iyer, A.V., & Kousoulas, K.G. 2013. A Review of Vaccine Approaches for West Nile Virus. *International Journal of Environmental Research and Public Health*, **10**(9), 4200–4223.
- Jacovitti, G., & Scarano, G. 1993. Discrete time techniques for time delay estimation. *IEEE Transactions on Signal Processing*, **41**(2), 525–533.
- Jones, C.E., Lounibos, L.P., Marra, P.P., & Kilpatrick, A.M. 2012. Rainfall influences survival of *Culex pipiens* (Diptera: Culicidae) in a residential neighborhood in the mid-Atlantic United States. *Journal of Medical Entomology*, **49**(3), 467–473.
- Jouda, F., Perret, J., & Gern, L. 2004. *Ixodes ricinus* density, and distribution and prevalence of *Borrelia burgdorferi sensu lato* infection along an altitudinal gradient. *Journal of Medical Entomology*, **41**(2), 162–169.
- Jozan, M., Evans, R., R.McLean, Hall, R., Tangredi, B., Reed, L., & Scott, J. 2003. Detection of West Nile Virus Infection in birds in the United States by blocking ELISA and immunohistochemistry. *Vector-borne and Zoonotic Diseases*, **3**(3), 99–110.
- Juliano, S.A. 2009. Species interactions among larval mosquitoes: context dependence across habitat gradients. *Annual Review of Entomology*, **54**, 37–56.

- Keesing, F., Holt, R.D., & Ostfeld, R.S. 2006. Effects of species diversity on disease risk. *Ecology Letters*, **9**(4), 485–498.
- Kemeny, J.G., & Snell, J.L. 1976. *Finite Markov Chains*. Springer-Verlag.
- Kilpatrick, A.M., & Pape, W.J. 2013. Predicting Human West Nile Virus Infections With Mosquito Surveillance Data. *American Journal of Epidemiology*, **178**(5), 829–835.
- Kilpatrick, A.M., Kramer, L.D., Campbell, S.R., Alleyne, E.O., Dobson, A.P., & Daszak, P. 2005. West Nile Virus Risk Assessment and the Bridge Vector Paradigm. *Emerging Infectious Diseases*, **11**(3), 425–429.
- Kilpatrick, A.M., Daszak, P., Jones, M.J., Marra, P.P., & Kramer, L.D. 2006a. Host heterogeneity dominates West Nile virus transmission. *Proceedings of the Royal Society B*, **273**, 2327–2333.
- Kilpatrick, A.M., Kramer, L.D., Jones, M.J., Marra, P.P., & Daszak, P. 2006b. West Nile Virus epidemics in North America are driven by shifts in mosquito feeding behaviour. *Plos Biology*, **4**.
- Kilpatrick, A.M., Meola, M.A., Moudy, R.M., & Kramer, L.D. 2008. Temperature, Viral Genetics, and the Transmission of West Nile Virus by *Culex pipiens* Mosquitoes. *PLoS Pathog*, **4**(6), e1000092.
- Komar, N., Langevin, S., Hinten, S., Nemeth, N., Edwards, E., Hettler, D., Davis, B., Bowen, R., & Bunning, M. 2003. Experimental Infection of North American Birds with the New York 1999 Strain of West Nile Virus. *Emerging Infectious Diseases*, **9**, 311–322.
- Kwan, J.L., Klugh, S., Madon, M. B., & Reisen, W.K. 2010. West Nile virus emergence and persistence in Los Angeles, California, 2003-2008. *American Journal of Tropical Medicine and Hygiene*, **83**(2), 400–412.
- Leisnham, P.T., LaDeau, S.L., & Juliano, S.A. 2014. Spatial and Temporal Habitat Segregation of Mosquitoes in Urban Florida. *PLOS ONE*, **9**(3), e91655.
- Livdahl, T.P., & Willey, M.S. 1991. Prospects for an invasion: competition between *Aedes albopictus* and native *Aedes triseriatus*. *Science (New York, N.Y.)*, **253**(5016), 189–191.
- Loetti, V., Schweigmann, N., & Burrioni, N. 2011. Development rates, larval survivorship and wing length of *Culex pipiens* (Diptera: Culicidae) at constant temperatures. *Journal of Natural History*, **45**(35), 2203–2213.
- Loncaric, Z., & Hackenberger, B.K. 2013. Stage and age structured *Aedes vexans* and *Culex pipiens* (Diptera: Culicidae) climate-dependent matrix population model. *Theoretical Population Biology*, **83**, 82–94.
- Lord, C.C., Woolhouse, M.E.J., Heesterbeek, J.A.P., & Mellor, P.S. 1996. Vector-borne diseases and the basic reproduction number: a case study of African horse sickness. *Medical and Veterinary Entomology*, **10**, 19–28.
- Luhken, R., Pfitzner, W.P., Borstler, J., Garms, R., Huber, K., Schork, N., Steinke, S., Kiel, E., Becker, N., Tannich, E., & Kruger, A. 2014. Field evaluation of four widely used mosquito traps in Central Europe. *Parasites & Vectors*, **7**(1), 268.

- Lukacik, G., Anand, M., Shusas, E.J., Howard, J.J., Oliver, J., Chen, H., Backenson, P.B., Kauffman, E.B., Berndard, K.A., Kramer, L.D., & White, D.J. 2006. West Nile virus surveillance in mosquitoes in New York state, 2000-2004. *Journal of the American Mosquito Control Association*, **22**(2), 264–271.
- Lundstrom, J.O., Lindstrom, K.M., Olsen, B., Dufva, R., & Krakower, D.S. 2001. Prevalence of Sindbis virus neutralizing antibodies among Swedish passerines indicates that thrushes are the main amplifying hosts. *Journal of Medical Entomology*, **38**(2), 289–297.
- Maidana, N.A., & Yang, H.M. 2011. Dynamic of West Nile virus transmission considering several coexisting avian populations. *Mathematical and Computer Modelling*, **53**, 1247–1260.
- McFeeters, S.K. 2013. Using the Normalized Difference Water Index (NDWI) within a Geographic Information System to Detect Swimming Pools for Mosquito Abatement: A Practical Approach. *Remote Sensing*, **5**(7), 3544–3561.
- Mckee, E.M., Walker, E.D., Anderson, T.K., Kitron, U.D., Brawn, J.D., Krebs, B.L., Newman, C., Ruiz, M.O., Levine, R.S., Carrington, M.E., McLean, R.G., Goldberg, T.L., & Hamer, G.L. 2015. West Nile virus antibody decay rate in free-ranging birds. *Journal of Wildlife Diseases*, **51**(3), 601–608.
- Medlock, J.M., Hansford, K.M., Schaffner, F., Versteirt, V., Hendrickx, G., Zeller, H., & Van Bortel, W. 2012. A review of the invasive mosquitoes in Europe: ecology, public health risks, and control options. *Vector Borne and Zoonotic Diseases (Larchmont, N.Y.)*, **12**(6), 435–447.
- Meteotrentino. 2016. *Meteotrentino*. <http://www.meteotrentino.it/>. Accessed: 2016-11-16.
- Metz, M., Rocchini, D., & Neteler, M. 2014. Surface Temperatures at the Continental Scale: Tracking Changes with Remote Sensing at Unprecedented Detail. *Remote Sensing*, **6**(5), 3822–3840.
- Monaco, F., Lelli, R., Teodori, L., Pinoni, C., Di Gennaro, A., Polci, A., Calistri, P., & Savini, G. 2010. Re-Emergence of West Nile Virus in Italy. *Zoonoses and Public Health*, **57**(7), 476–486.
- Morin, C.W., & Comrie, A.C. 2010. Modeled response of the West Nile virus vector *Culex quinquefasciatus* to changing climate using the dynamic mosquito simulation model. *International Journal of Biometeorology*, **54**(5), 517–529.
- Mulatti, P., Ferguson, H.M., Bonfanti, L., Montarsi, F., Capelli, G., & Marangon, S. 2014. Determinants of the population growth of the West Nile virus mosquito vector *Culex pipiens* in a repeatedly affected area in Italy. *Parasites & Vectors*, **7**, 26.
- Murrell, E.G., & Juliano, S.A. 2008. Detritus Type Alters the Outcome of Interspecific Competition Between *Aedes aegypti* and *Aedes albopictus* (Diptera: Culicidae). *Journal of Medical Entomology*, **45**(3), 375–383.

- Nemeth, N.M., Beckett, S., Edwards, E., Klenk, K., & Komar, N. 2007. Avian mortality surveillance for West Nile virus in Colorado. *American Journal of Tropical Medicine and Hygiene*, **76**(3), 431–437.
- Neteler, M. 2010. Estimating Daily Land Surface Temperatures in Mountainous Environments by Reconstructed MODIS LST Data. *Remote Sensing*, **2**(1), 333–351.
- Neteler, M., Roiz, D., Rocchini, D., Castellani, C., & Rizzoli, A. 2011. Terra and Aqua satellites track tiger mosquito invasion: modelling the potential distribution of *Aedes albopictus* in north-eastern Italy. *International Journal of Health Geographics*, **10**, 49.
- Neteler, M., Bowman, M.H., Landa, M., & Metz, M. 2012. GRASS GIS: A multi-purpose open source GIS. *Environmental Modelling & Software*, **31**, 124–130.
- Niebylski, M.L., & Craig, G.B. 1994. Dispersal and Survival of *Aedes-Albopictus* at a Scrap Tire Yard in Missouri. *Journal of the American Mosquito Control Association*, **10**(3).
- Novak, M.G., Higley, L.G., Christianssen, C.A., & Rowley, W.A. 1993. Evaluating Larval Competition Between *Aedes albopictus* and *A. triseriatus* (Diptera: Culicidae) through Replacement Series Experiments. *Environmental Entomology*, **22**(2), 311–318.
- O’Neal, P.A., & Juliano, S.A. 2013. Seasonal variation in competition and coexistence of *Aedes* mosquitoes: stabilizing effects of egg mortality or equalizing effects of resources? *Journal of Animal Ecology*, **82**(1), 256–265.
- Osório, H.C., Zé-Zé, L., Amaro, F., Nunes, A., & Alves, M.J. 2014. Sympatric occurrence of *Culex pipiens* (Diptera, Culicidae) biotypes *pipiens*, *molestus* and their hybrids in Portugal, Western Europe: feeding patterns and habitat determinants. *Medical and Veterinary Entomology*, **28**(1), 103–109.
- Pan, Y., & Jackson, R.T. 2008. Ethnic difference in the relationship between acute inflammation and serum ferritin in US adult males. *Epidemiology and Infection*, **136**(3), 421–431.
- Paupy, C., Delatte, H., Bagny, L., Corbel, V., & Fontenille, D. 2009. *Aedes albopictus*, an arbovirus vector: From the darkness to the light. *Microbes and Infection*, **11**(14), 1177–1185.
- Pawelek, K.A., Niehaus, P., Salmeron, C., Hager, E.J., & Hunt, G. J. 2014. Modeling Dynamics of *Culex pipiens* Complex Populations and Assessing Abatement Strategies for West Nile Virus. *Plos One*, **9**(9), e108452.
- Pecorari, M., Longo, G., Gennari, W., Grottola, A., Sabbatini, A., Tagliazucchi, S., Savini, G., Monaco, F., Simone, M., Lelli, R., & Rumpianesi, F. 2009. First human case of Usutu virus neuroinvasive infection, Italy, August-September 2009. *Euro surveillance : bulletin Europeen sur les maladies transmissibles = European communicable disease bulletin*, **14**(50).
- Poletti, P., Messeri, G., Ajelli, M., Vallorani, R., Rizzo, C., & Merler, S. 2011. Transmission Potential of Chikungunya Virus and Control Measures: The Case of Italy. *PLoS ONE*, **6**(5), e18860.

- R Development Core Team. 2008. *R: A Language and Environment for Statistical Computing*. R Foundation for Statistical Computing, Vienna, Austria. ISBN 3-900051-07-0.
- Reisen, W.K. 2013. Ecology of West Nile Virus in North America. *Viruses*, **5**, 2079–2105.
- Reisen, W.K., Lothrop, H.D., Wheeler, S.S., Kennington, M., Gutierrez, A., Fang, Y., Garcia, S., & Lothrop, B. 2008. Persistent West Nile virus transmission and the apparent displacement St. Louis encephalitis virus in southeastern California, 2003-2006. *Journal of Medical Entomology*, **45**(3), 494–508.
- Reisen, W.K., Wheeler, S.S., Garcia, S., & Fang, Y. 2010. Migratory birds and the dispersal of Arboviruses in California. *American Journal of Tropical Medicine and Hygiene*, **83**(4), 808–815.
- Reiskind, M. H., & Lounibos, L. P. 2009. Effects of intraspecific larval competition on adult longevity in the mosquitoes *Aedes aegypti* and *Aedes albopictus*. *Medical and Veterinary Entomology*, **23**(1), 62–68.
- Rizzoli, A., Hauffe, H.C., Tagliapietra, V., Neteler, M., & Rosá, R. 2009. Forest Structure and Roe Deer Abundance Predict Tick-Borne Encephalitis Risk in Italy. *PLoS ONE*, **4**(2), e4336.
- Rizzoli, A., Bolzoni, L., Chadwick, E.A., Capelli, G., Montarsi, F., Grisenti, M., de la Puente, J. M., Munoz, J., Figuerola, J., Soriguer, R., Anfora, G., Di Luca, M., & Rosá, R. 2015. Understanding West Nile virus ecology in Europe: *Culex pipiens* host feeding preference in a hotspot of virus emergence. *Parasites & Vectors*, **8**, 213.
- Roberts, M.G., & Heesterbeek, J.A.P. 2013. Characterizing the next-generation matrix and basic reproduction number in ecological epidemiology. *Journal of Mathematical Biology*, **66**, 1045–1064.
- Roerink, G.J., Menenti, M., & Verhoef, W. 2000. Reconstructing cloudfree NDVI composites using Fourier analysis of time series. *International Journal of Remote Sensing*, **21**(9), 1911–1917.
- Roiz, D., Neteler, M., Castellani, C., Arnoldi, D., & Rizzoli, A. 2011. Climatic Factors Driving Invasion of the Tiger Mosquito (*Aedes albopictus*) into New Areas of Trentino, Northern Italy. *PLOS ONE*, **6**(4), e14800.
- Ruiz, M.O., Chaves, L.F., Hamer, G.L., Sun, T., Brown, W.M., Walker, E.D., Haramis, L., Goldberg, T.L., & Kitron, U.D. 2010. Local impact of temperature and precipitation on West Nile virus infection in *Culex* species mosquitoes in northeast Illinois, USA. *Parasites & Vectors*, **3**(1), 19.
- Ruybal, J.E., Kramer, L.D., & Kilpatrick, A.M. 2016. Geographic variation in the response of *Culex pipiens* life history traits to temperature. *Parasites & Vectors*, **9**, 116.
- Sambri, V., Capobianchi, M., Charrel, R., Fyodorova, M., Gaibani, P., Gould, E., Niedrig, M., Papa, A., Pierro, A., Rossini, G., Varani, S., Vocale, C., & Landin, M.P. 2013. West Nile virus in Europe: emergence, epidemiology, diagnosis, treatment and prevention. *Clinical Microbiology and Infection*, **19**(8), 699–704.

- Schaffner, F., Medlock, J.M., & Van Bortel, W. 2013. Public health significance of invasive mosquitoes in Europe. *Clinical Microbiology and Infection*, **19**(8), 685–692.
- Severini, F., Toma, L., Di Luca, M., & Romi, R. 2009. LE ZANZARE ITALIANE: GENERALITÀ E IDENTIFICAZIONE DEGLI ADULTI (DIPTERA, CULICIDAE). *Fragmenta Entomologica*, **41**(2), 213.
- Simpson, J.E., Folsom-O’Keefe, C.M., Childs, J.E., Simons, L.E., Andreadis, T.G., & Diuk-Wasser, M.A. 2009. Avian Host-Selection by *Culex pipiens* in Experimental Trials. *PLoS ONE*, **4**(11), e7861.
- Simpson, J.E., Hurtado, P.J., Medlock, J., Molaei, G., Andreadis, T.G., Galvani, A.P., & Diuk-Wasser, M.A. 2012. Vector host-feeding preferences drive transmission of multi-host pathogens: West Nile virus as a model system. *Proceeding of the Royal Society B-Biological Sciences*, **279**(1730), 925–933.
- Smithburn, K.C., Hughes, T.P., Burke, A.W., & Paul, J.H. 1940. A Neurotropic Virus Isolated from the Blood of a Native of Uganda. *American Journal of Tropical Medicine*, **20**, 471–2.
- Spiegelhalter, D.J., Best, N.G., Carlin, B.R., & van der Linde, A. 2002. Bayesian measures of model complexity and fit. *Journal of the Royal Statistical Society Series B-Statistical Methodology*, **64**, 583–616.
- Spiegelhalter, D.J., Best, N.G., Carlin, B.P., & van der Linde, A. 2014. The deviance information criterion: 12 years on. *Journal of the Royal Statistical Society: Series B (Statistical Methodology)*, **76**(3), 485–493.
- Spielman, A. 2001. Structure and seasonality of nearctic *Culex pipiens* populations. *Annals of the New York Academy of Sciences*, **951**, 220–234.
- Spielman, A., & Wong, J. 1973. Environmental Control of Ovarian Diapause in *Culex pipiens*. *Annals of the Entomological Society of America*, **66**(4), 905–907.
- Taylor, L., Cummings, R., Velten, R., Collibus, K. De, Morgan, T., Nguyen, K., & Gerry, A. 2012. Host (avian) biting preference of Southern California *Culex* mosquitoes (Diptera: Culicidae). *Journal of Medical Entomology*, **49**(3), 687–696.
- Taylor, L.H., Latham, S.M., & Woolhouse, M.E. 2001. Risk factors for human disease emergence. *Philosophical Transactions of the Royal Society of London. Series B, Biological Sciences*, **356**(1411), 983–989.
- Thiemann, T.C., Wheeler, S.S., Barker, C.M., & Reisen, W.K. 2011. Mosquito Host Selection Varies Seasonally with Host Availability and Mosquito Density. *Plos Neglected Tropical Diseases*, **5**(12).
- Tilman, D. 1982. *Resource competition and community structure*. Monographs in population biology, no. 17. Princeton University Press.
- Tran, A., L’Ambert, G., Lacour, G., Benoit, R., Demarchi, M., Cros, M., Cailly, P., Aubry-Kientz, M., Balenghien, T., & Ezanno, P. 2013. A Rainfall- and Temperature-Driven Abundance Model for *Aedes albopictus* Populations. *International Journal of Environmental Research and Public Health*, **10**(5), 1698–1719.

- Trawinski, P.R., & Mackay, D.S. 2010. Identification of environmental covariates of West Nile virus vector mosquito population abundance. *Vector borne and zoonotic diseases (Larchmont, N.Y.)*, **10**(5), 515–526.
- Turell, M.J., Guinn, M.L. Ó, Dohm, D.J., & Jones, J.W. 2001. Vector Competence of North American Mosquitoes (Diptera: Culicidae) for West Nile Virus. *Journal of Medical Entomology*, **38**, 130–134.
- Turell, M.J., Dohm, D.J., & Fonseca, D.M. 2014. Comparison of the Potential for Different Genetic Forms in the Culex Pipiens Complex in North America to Transmit Rift Valley Fever Virus. *Journal of the American Mosquito Control Association*, **30**(4), 253–259.
- United States Naval Meteorology and Oceanography Command. 2013. *Naval Oceanography Portal*. <http://www.usno.navy.mil/>. Accessed: 2015-06-23.
- Vega-Rua, A., Zouache, K., Caro, V., Diancourt, L., Delaunay, P., Grandadam, M., & Failloux, A. 2013. High Efficiency of Temperate Aedes albopictus to Transmit Chikungunya and Dengue Viruses in the Southeast of France. *PLOS ONE*, **8**(3), e59716.
- Vega-Rua, A., Zouache, K., Girod, R., Failloux, A., & Lourenco-de Oliveira, R. 2014. High Level of Vector Competence of Aedes aegypti and Aedes albopictus from Ten American Countries as a Crucial Factor in the Spread of Chikungunya Virus. *Journal of Virology*, **88**(11), 6294–6306.
- Verna, T.N. 2015. Species Composition and Seasonal Distribution of Mosquito Larvae (Diptera: Culicidae) in Southern New Jersey, Burlington County. *Journal of Medical Entomology*, **52**(5), 1165–1169.
- Vinogradova, E.B. 2011. The sex structure of the larval populations of the urban mosquito Culex pipiens pipiens f. molestus Forskal (Diptera, Culicidae) in St. Petersburg. *Entomological Review*, **91**(6), 729–734.
- Wan, Z. 2014. New refinements and validation of the collection-6 MODIS land-surface temperature/emissivity product. *Remote Sensing of Environment*, **140**, 36–45.
- Whittingham, M.J., Stephens, P.A., Bradbury, R.B., & Freckleton, R.P. 2006. Why do we still use stepwise modelling in ecology and behaviour? *Journal of Animal Ecology*, **75**(5), 1182–1189.
- Winters, A.M., Bolling, B.G., Beaty, B.J., Blair, C.D., Eisen, R.J., Meyer, A.M., Pape, W.J., Moore, C.G., & Eisen, L. 2008. Combining mosquito vector and human disease data for improved assessment of spatial West Nile virus disease risk. *The American Journal of Tropical Medicine and Hygiene*, **78**(4), 654–665.
- Wong, P.J., Li, M.I., Chong, C., Ng, L., & Tan, C. 2013. Aedes (Stegomyia) albopictus (Skuse): a potential vector of Zika virus in Singapore. *PLoS neglected tropical diseases*, **7**(8), e2348.
- World Health Organization. 2016. *Mortality and global health estimates 2013*. <http://apps.who.int/gho/data/node.main.686?lang=en>. Accessed: 2016-12-06.
- Xiao, X., Boles, S., Liu, J., Zhuang, D., & Liu, M. 2002. Characterization of forest types in Northeastern China, using multi-temporal SPOT-4 VEGETATION sensor data. *Remote Sensing of Environment*, **82**(2), 335–348.

- Yamana, T.K., & Eltahir, E.A.B. 2013. Incorporating the effects of humidity in a mechanistic model of *Anopheles gambiae* mosquito population dynamics in the Sahel region of Africa. *Parasites & Vectors*, **6**, 235.
- Yang, G., Brook, B. W., & Bradshaw, C.J.A. 2009. Predicting the Timing and Magnitude of Tropical Mosquito Population Peaks for Maximizing Control Efficiency. *PLoS Neglected Tropical Diseases*, **3**(2), e385.
- Zeller, H.G., & Schuffenecker, I. 2004. West Nile virus: An overview of its spread in Europe and the Mediterranean Basin in contrast to its spread in the Americas. *European Journal of Clinical Microbiology & Infectious Diseases*, **23**(3), 147–156.